UNIVERSITY OF AGDER

Theoretical and experimental study of friction emulation and compensation

By
Tore Bakka
Johannes Bächer

Thesis submitted in Partial Fulfillment of the Requirements for the Degree Master of Science in Mechatronics

Faculty of Engineering and Science
University of Agder

Grimstad
May 2010

Abstract

This project deals with hydraulics, mechanics, electronics, dynamic modeling and control theory. The focus is on constructing a test rigg in order to to emulate desired friction and compensate for this with a control loop. The rigg is modeled in matlab/simulink and at last compared to the physical rigg. The rigg reads sensor values and control the servo valves via a CompactRIO. The controllers that are made and implemented in the matlab/simulink model are PI and LQR tracking with integral action.

Preface

Special thanks is made to our supervisors Professor Michael Hansen and Morten Ottestad. And also thanks to Eivind Johansen for helping us assembling the test stand.

Contents

List of Figures

List of Tables

Chapter 1

Introduction

1.1 Motivation

The master thesis is a continuation of a mini project held in the course Product development (MAS503) at the University of Agder. In the mini project the project group was given a used test stand which was modified to meet some design criteria. The test stand consists of two cylinders coupled in series, i.e. they are mounted together in the middle by means of a load cell. One cylinder will emulate a desirable friction and the other will compensate for this irregular heave movement and simultaneously try to obtain a sinusoid reference. This sinusoid reference is playing the role of a wave influencing a floating vessel which is trying to hold some fixed earthly reference coordinate. The mini project mainly consisted of the design and dimensioning of the parts lacking from the original test stand. The thesis problem formulation is given by Aker Solutions. Aker Solutions is one of the largest manufacturer of offshore floating drillriggs in the world. They are interested in a test stand where different friction models can be tested against different kinds of control strategies.

1.2 Goal

A test stand will be made for testing of different control strategies for compensation of an unexpected/expected heave motion. The friction emulator can easily be switched/changed to a user defined friction model.

1.3 Project description

The designed test stand from the pre project will be taken into use. The purpose of the master project is to have a test stand where disturbance-friction can be emulated and to have a control system to compensate for this movement. The main topics of the project will be modeling, friction, control strategies and to control a hydraulic system by means of a CompacRIO.

1.4 Contributions

The main contribution from the project is that a hydromechanical test stand for friction emulation and compensation is produced. It could come in handy in relation to future student assignments/labs where the objectives can be everything from Labview exercises, friction modeling, basic hydraulic understanding to control theory in practice.

1.5 Report outline / Thesis Organization

The thesis starts with a presentation of the different hydraulic components in the system as well as the electric wiring for the sensors and servo valves. Also the software interface between the user and the test stand is presented. Before the

dynamic model is presented at the end of chapter 3, some necessary theory is covered. The theory consists of an introduction to the governing differential and algebraic equations describing the dynamic model. Next follows chapter 4 where the system model is compared with the test stand based on a various set of parameters obtained from the rigg. Chapter 5 discusses the friction models which are considered in this thesis. Chapter 6 gives a short presentation of where active heave compensation is used and by which methods this is achieved. The chosen control strategies will be presented here. Chapter 7 contains a summary of results. Chapter 8 presents the conclusion of the thesis and discusses the work done and the future work.

1.6 Project overview

- Test stand assembly, involving everything from the hydromechanical assembly to the the electrical couplings to the sensors to the CompactRIO.
- A dynamic model describing the dynamic behavior will be made. The model will be tried made in the graphical programming software SimulationX.
- Develop suitable friction models which is to be tested with the rigg at the end of the project period. Do a literature search and find out what excises.
- A literature search will be made and on the basis of these a careful selection of control strategies will be selected. The control strategies will be tested on the rigg once it is finished. There will be needed control loops for both the friction emulator and the compensator. The courses Control Theory 1 and 2 at the University of Agder deals only with linear controllers. This is why only linear controllers will be considered.
- Experimentations with different friction models and control strategies. Find limitations to those who work and which do not work.

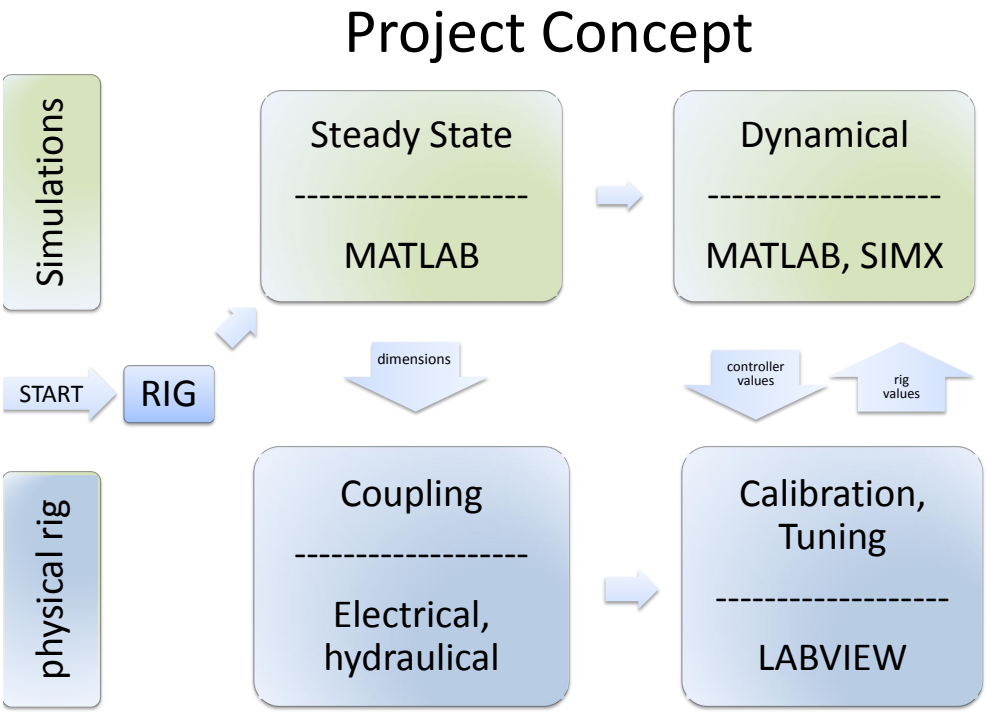

Figure 1.1: Project concept

Chapter 2

Test stand

2.1 Overview

The purpose of the test stand is to carry out hardware-in-the-loop (HIL) simulations. The hydromechanical part of the simulations canbe replaced by the physical test stand in order to carry out hardware-in-the-loop (HIL) simulations.
The test stand consists of two cylinders connected at their piston rods such that they have a common movement. The hydraulic scheme is shown in fig. 2.1.

2.2 Hydraulics

The two cylinders used are given equipment that had to be dealt with. They have different piston radius, $50mm$ and $40mm$. The oil used in this system is of the type: *STATOIL HYDRAWAY HMA 46* For further information see the data sheet in the appendix.

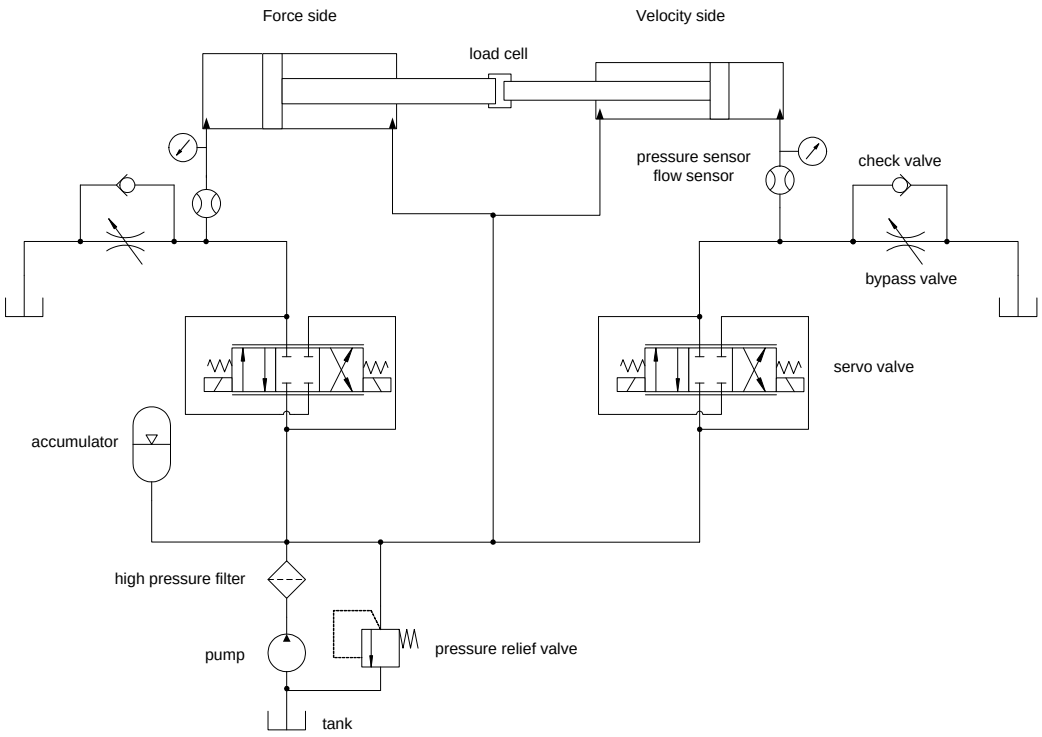

Figure 2.1: Hydraulic scheme for double flow

Specification	Value
Nominal volume	$20[l]$
Permitted operating pressure	$345[bar]$

Table 2.1: Key data for HYDAC accumulator SB330 - 20 A 1 / 112 U - 330 A 050

2.2.1 Accumulator

In order to compensate for pressure peaks a HYDAC standard bladder accumulator is added to the hydraulic system, see fig. 2.1 and specifications in tab. 2.1. The gas side accumulator is filled with nitrogen and connected to the hydraulic circuit via a check valve. A gas-proof bladder separates the oil from the gas (fig. 2.3). In case of a pressure increase or decrease, the gas will be compressed or will expand, respectively, and such compensate for the high oil stiffness (fig. 2.4).

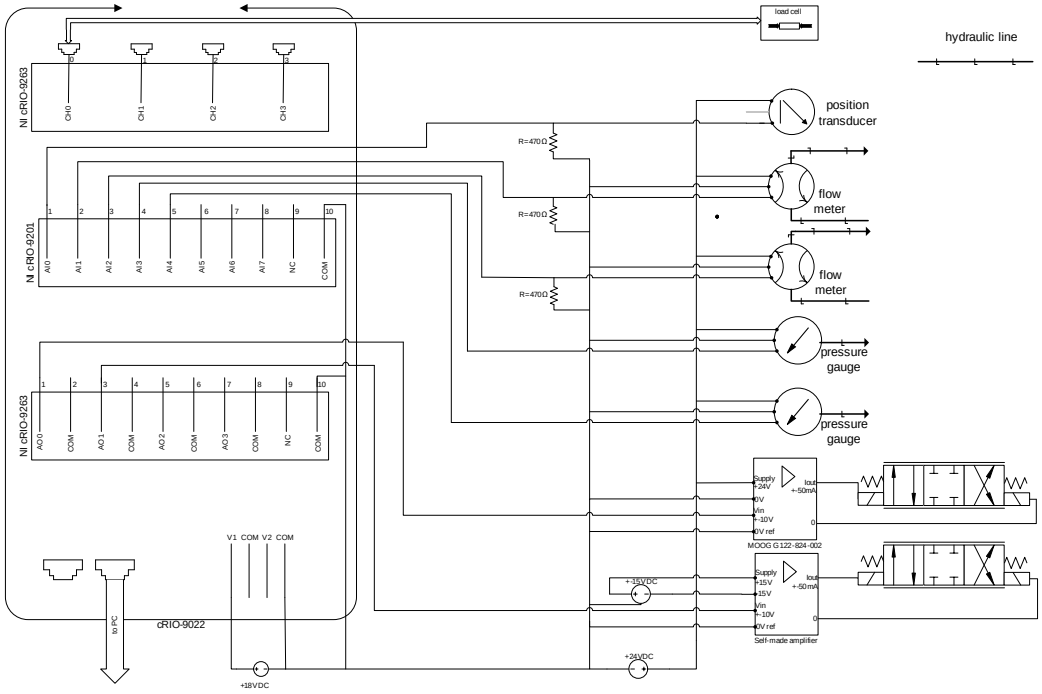

Figure 2.2: Electrical scheme

The dynamic simulations show very little pressure variations, see SimulationX results in sec. (A). The minimum system pressure is $\approx\ 160\,[]$. The disturbance force is relative small compared to the max rating (tab. (4.1)), i.e. somewhat larger variations can be expected. According to the gas equations in sec. (3.1) the pre charge pressure should be set to the minimum pressure in the system. Pre charge pressure is selected to be: $155\ [bar]$

2.2.2 Valves

Two MOOG D631 series servo valves are used with 10% overlap and $\pm 50mA$ control signal, see appendix.

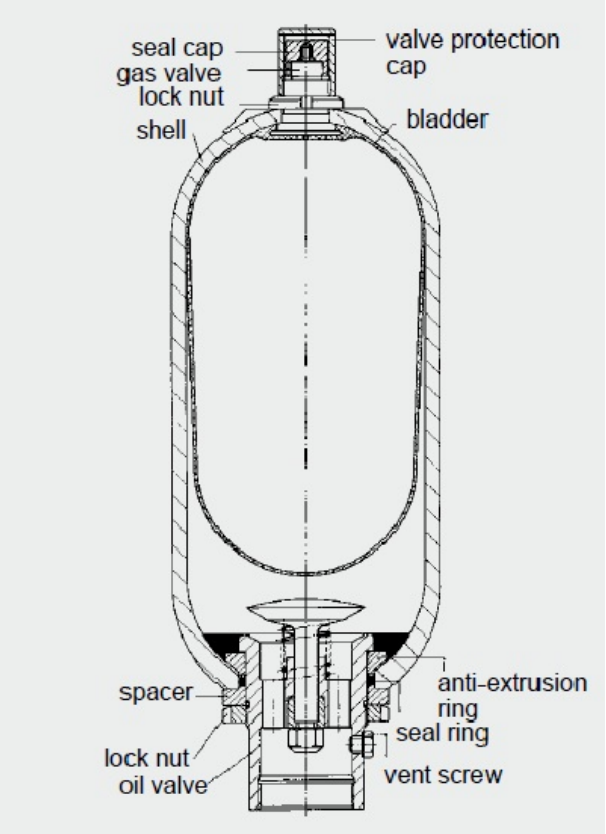

Figure 2.3: Cross-sectional view of a HYDAC standard bladder accumulator, www.hydac.de

2.3 Sensors

2.3.1 Position

The displacement sensor, shown and characterized in fig. 2.5 and tab. 2.2, respectively, is a Celesco PT1MA-50-UP-420E-M6. The electrical diagram for this sensor is shown in fig. 2.6. An application is made in LabView in order to measure the voltage drop over the resistance R. This voltage drop is proportional with the extension of the cable. Tab. 2.3 shows the calibration data and fig. 2.7 shows

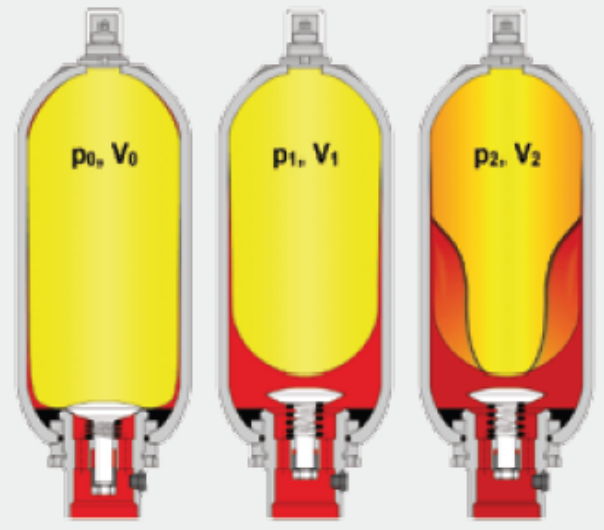

Figure 2.4: Cross-sectional view of a HYDAC standard bladder accumulator at different volume and pressure levels, www.hydac.de

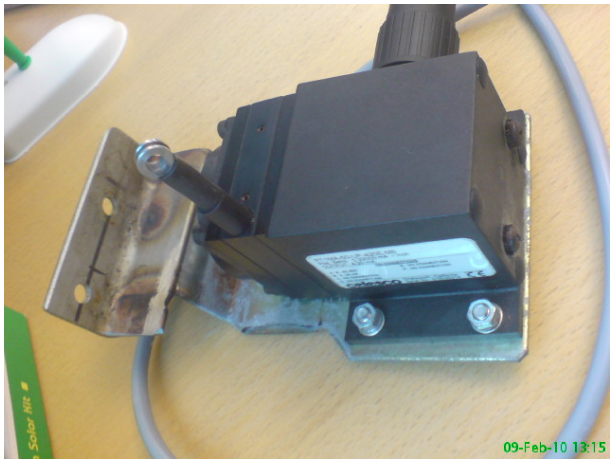

Figure 2.5: Celesco PT1MA-50-UP-420E-M6

a graph based upon these data.

Table 2.2: Celesco displacement transducer - data

min. full stroke range [mm]	1270
accuracy [mm]	1.905
input [VDC]	$8 - 40$
output [mA]	$4 - 20$
accuracy [$\%range$]	0.15
cable tension (20) [oz.]	5
max. cable acceleration (3G) [m/s]	29.43

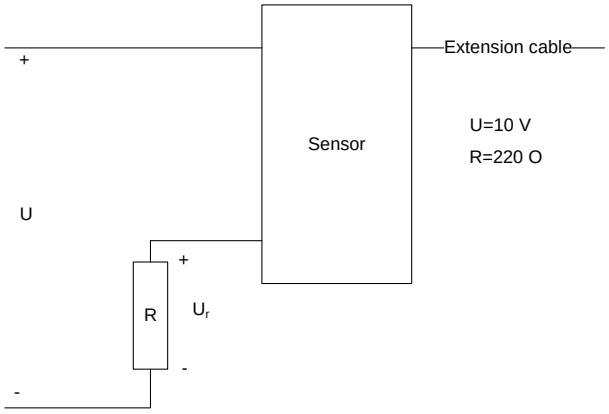

Figure 2.6: Electrical coupling

2.3.2 Force

In order to emulate the desired disturbing force, a load cell is made using strain gauges connected in a full bridge for temperature compensation. This sensor also serves as a connecting casing of the cylinder rods. Installation, placement of strain gauges and the load cell itself are shown in fig. (2.9)). The load cell is calibrated using LABVIEW with a NI CompactDAQ and a calibrated tension test machine. The voltage output from the Wheatstone bridge $V_{measured}$ is found to be proportional to the force applied, which confirms a linear strain - stress behavior. The

Extension $[cm]$	**Voltage drop** $[V]$
0	0.88
6	1.046
16	1.324
26	1.601
36	1.876
46	2.154
56	2.433
66	2.725
76	2.987
86	3.254
96	3.412

Table 2.3: Calibration data for position sensor

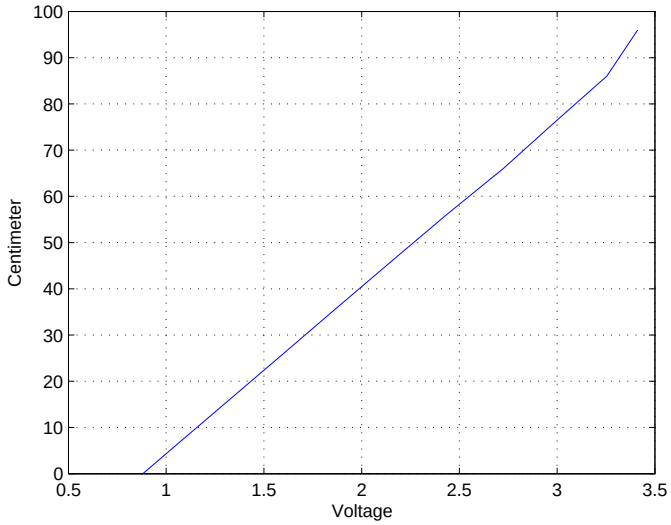

Figure 2.7: Calibration curve for position sensor, extension vs. voltage drop

acting force can therefore be calculated by

$$F \;=\; F_0 + k\, V_{measured}. \tag{2.1}$$

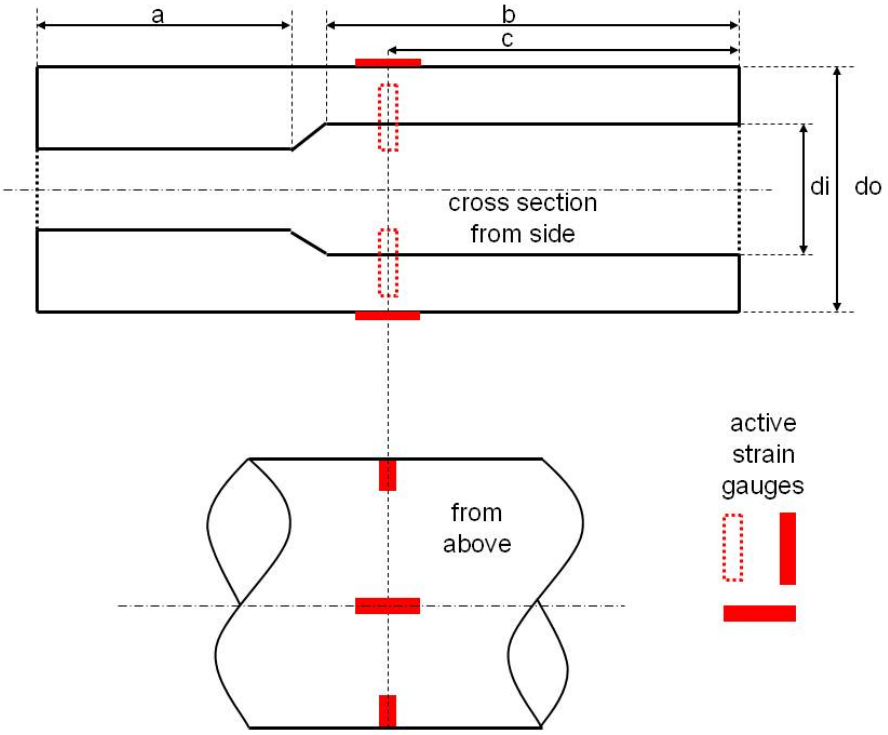

Figure 2.8: Load cell, cross-sectional view

Fig. (2.10) shows that eq.(2.1) gives accurate force values for the calibrated range up to $30kN$.

2.4 National Instruments components

The user interface is a NI compactRIO 9022. Since this device has turned out be sensitive to high work load on the target level and kept disconnecting, a very simple labview programm was made to read and convert the signals and the give out the desired signal to the servo valves.

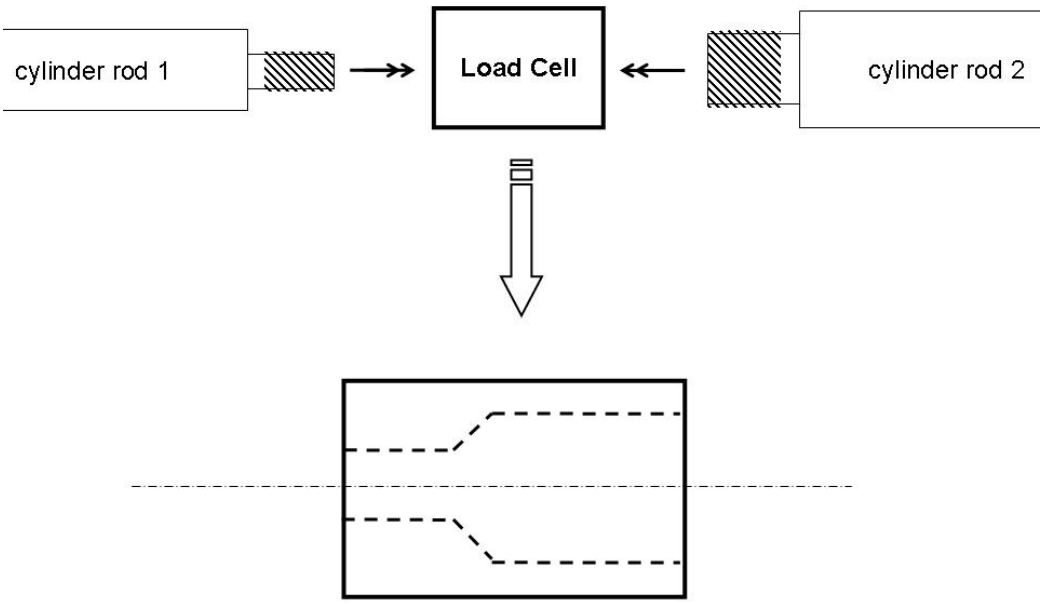

Figure 2.9: Load cell, installation

2.5 Range of Operation

The distance in between the two cylinders is about $S_L = 0.5\,[m]$, and the zero point is at the middle. The max velocity of the cylinder is calculated in the pre project and is found to be $v_{max} = 0.01\left[\frac{m}{s}\right]$. Underneath follows a calculation to

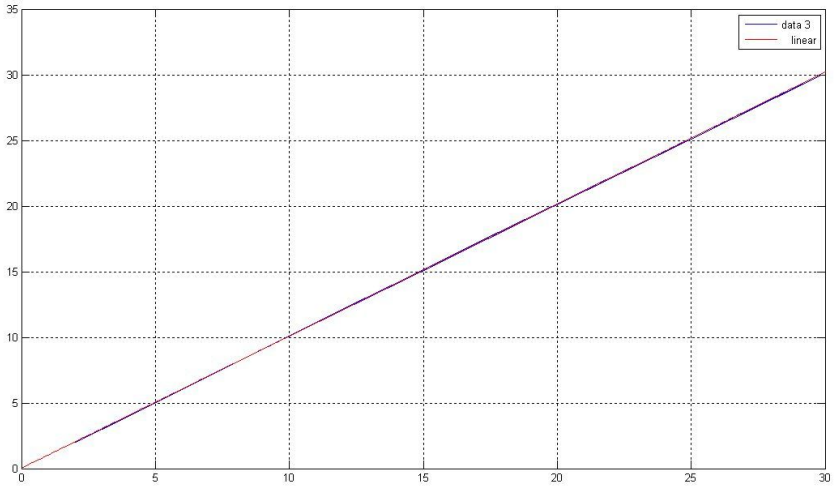

Figure 2.10: Load cell, $F_{measured}$ vs. $F_{applied}$

find what frequency is needed to utilize the whole space between the cylinders.

$$\begin{aligned} v(t) &= v_{max} sin(\omega t) \\ x(t) &= \int v(t)\ dt = \int v_{max} sin(\omega t)\ dt \\ &= -\frac{v_{max}}{\omega} cos(\omega t) \\ &\Rightarrow \frac{v_{max}}{\omega} = \frac{S_L}{2} \Rightarrow \omega = \frac{2v_{max}}{S_L} = 0.04 \left[\frac{rad}{s}\right] \end{aligned} \tag{2.2}$$

This will give a period of:

$$T = \frac{1}{f} = \frac{2\pi}{\omega} = 157.08\,[s] \tag{2.3}$$

Chapter 3

Dynamic model

Dynamic simulation is an important part of the hydraulic design process. The main purpose of the dynamic simulation is a more detailed picture of the transient system behavior. Initially a steady state simulation was carried out by solving a set of algebraic equations. Based on these results the different hydraulic components were selected. The steady state simulations is not time dependent, i.e the accelerations of the mechanical components and the pressure gradients are not take into consideration. The pressure gradient appear when the fluid compressibility is considered. In the dynamic simulation the system is described with a mixed set of differential and algebraic equations. This examination will partly be done in SimulationX and in Matlab/Simulink. SimulationX is a graphical software, which therefor means the different differential and algebraic equations will not be coded in manually but they are included via the different components. In Matlab/Simulink however, these different equations needs to be derived and coded manually. This chapter gives an introduction to some of these governing equations, and next two dynamic models of the considered system are presented. One nonlinear and one linear. The nonlinear model is made in SimulationX. When it comes to controlling the system, only linear controllers will be considered. This is why a linear model is needed. The model is made by linearizing these govern-

ing equations. Since there were some delay between the model making and the test stand assembly, the linearization points were obtained from the SimulationX model. Trusting in this model the linearized model could be ”checked” before the test stand was ready for use. These results are not included in the report, the main goal is not to have a model representing SimulationX, but rather a model that represent the test rigg in a realistic way. When the test stand was assembled and connected with necessary sensor the new and more realistic linearization points were obtained.

3.1 Dynamic equations

The acceleration of a body is described by Newton‘s second law.

$$\sum F \; = \; m\ddot{x} \tag{3.1}$$

Where

- $\sum F$ is the resulting force on the body
- m is the mass of the object
- $\ddot{x}$ is the acceleration of the mass center of the body

The consequence of the oil compressibility is described by means of the mass balance of a volume (eq. 3.2). An example of where oil can be compressed is when it enters a chamber in the hydraulic cylinder, see fig. (3.1). The change in pressure, i.e the pressure gradient is derived in equation (3.5).

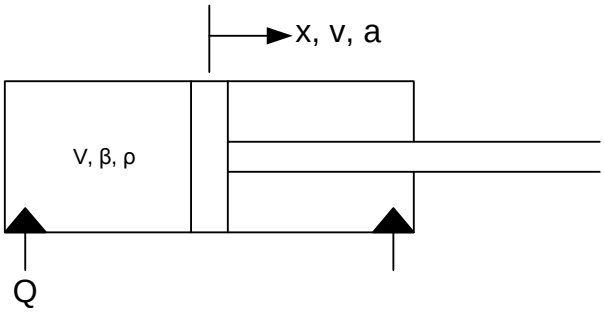

Figure 3.1: Hydraulic cylinder

$$\begin{aligned} m &= \rho V \\ \frac{d}{dt}(m) &= \frac{d}{dt}(V\rho) \\ Q\rho &= \frac{d}{dt}(V\rho) \\ Q\rho &= \dot{\rho}V + \rho\dot{V} \end{aligned} \tag{3.2}$$

The Bulk modulus (oil stiffness) β is defined in eq. (3.3). It has the same units as pressure and describes the correlation between pressure and volume variations, and in this case a volume of fluid. If a fluid has a high bulk modulus then it is less compressible than a fluid with a low bulk modulus.

$$\beta = \frac{\rho}{\frac{d\rho}{dp}} \tag{3.3}$$

Eq. (3.3) may be rearranged to:

$$\begin{aligned} \beta d\rho &= \rho dp \\ \beta\dot{\rho} &= \rho\dot{p} \\ \dot{\rho} &= \frac{\rho}{\beta}\dot{p} \end{aligned} \tag{3.4}$$

Inserting this in the mass balance (eq. 3.2) gives the pressure gradient.

$$\begin{aligned} \frac{V}{\beta}\dot{p} + \dot{V} &= Q \\ \dot{p} &= \frac{\beta\left(Q - \dot{V}\right)}{V} \end{aligned} \tag{3.5}$$

Where

- $\dot{p}$ is the pressure gradient
- β is the bulk modulus, often referred to as the effective oil stiffness
- Q is the net flow into the volume, positive if the net flow is into the volume and negative if the net flow is out of the volume
- V is the volume of fluid
- $\dot{V}$ is the change in volume, $\dot{V} = A\dot{x}$, for a cylinder with area A and velocity $\dot{x}$, see fig. (3.1)

The motivation for installing an accumulator (fig. 3.2) into the system is its ability to store energy and keep the system pressure as close to constant as possible. The compression and expansion of gas in the accumulator is assumed to be adiabatic. An adiabatic process means that little or no heat is transferred into or out of the volume (accumulator). The equation for this process is stated underneath.

$$pV_g^n = p_0 V_0^n \tag{3.6}$$

Where

- p is the pressure in the accumulator
- V_g is the gas volume

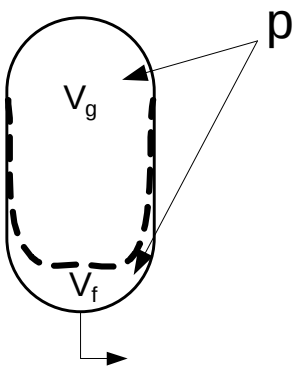

Figure 3.2: Accumulator

- p_0 is the minimum working pressure of the accumulator, i.e. when the gas inhabits approximately 90 % of the entire accumulator $V_g = V_0 = 0,9 \cdot V_a$
- V_0 is the gas volume @ p_0
- n for diatomic gas such as nitrogen is 1.4

Differentiating equation (3.6) the rate of change in the gas volume is found.

$$\begin{aligned} \frac{d}{dt}\left(pV_g^n\right) &= \frac{d}{dt}\left(p_0 V_0^n\right) \\ \dot{p}V_g^n + pnV_g^{n-1}\dot{V}_g &= 0 \\ \dot{V}_g &= -\frac{\dot{p}}{pnV_g^{n-1}}V_g^n \\ \dot{V}_g &= -\frac{\dot{p}}{pn}V_g \end{aligned} \tag{3.7}$$

The total volume in the accumulator V_a is constant.

$$V_g + V_f = V_a \implies \dot{V}_g + \dot{V}_f = 0 \tag{3.8}$$

Combining equations (3.7) and (3.8) the rate of change of the fluid volume is found.

$$\dot{V}_f = \frac{\dot{p}}{np} V_g \tag{3.9}$$

The gas volume can be found from eq. (3.6) and the fluid volume can be found by combining eq. (3.6) and (3.8). Reference is made to [8].

$$V_g = \left(\frac{p_0}{p}\right)^{\frac{1}{n}} V_0 \tag{3.10}$$

$$V_f = V_a - \left(\frac{p_0}{p}\right)^{\frac{1}{n}} V_0 \tag{3.11}$$

Two things are important to keep in mind when dimensioning an accumulator. The first one is that the accumulator should never run out of fluid, and the second one is that the pressure of the gas should never become less then the minimum pressure in the system. The dimensioning of the accumulator will be based on these criteria and carried out using the dynamic simulation.

3.2 Simulation parameters

Before the modeling can start it is necessary sort out what the different valve coefficients and what the servo valve dynamics are.

3.2.1 Bypass valves

The hydraulic system contains two bypass valves, one on the velocity control side and one on the force control side. They were dimensioned in the steady state calculation part of the project (pre-project). The valve dimensions, that were found, are formulated as the amount of flow at $1\,[bar]$ pressure drop.

- Velocity control: $0.7\left[\frac{l}{min}\right]$ @ $1\,[bar]$ pressure drop
- Force control: $0.9\left[\frac{l}{min}\right]$ @ $1\,[bar]$ pressure drop

The flow through this kind of valve is typically turbulent. The turbulent flow equation is stated underneath.

$$Q = C_d A\sqrt{\frac{2}{\rho}\Delta p} \tag{3.12}$$

Where

- Q is the flow through the orifice
- C_d is an orifice constant
- A is the area of the orifice
- ρ is the density of the fluid
- Δp is the pressure drop across the orifice

To be able to simulate these valves in SimulationX the values of C_d and A for both valves needs to be calculated. All constant values are assembled in a valve constant, $K_{bp} = C_d A\sqrt{\frac{2}{\rho}}$
Velocity control:

$$\begin{aligned} Q_2 = K_{bp1}\sqrt{\Delta p} \quad ; \quad K_{bp2} &= \frac{0.7\left[\frac{l}{min}\right]}{\sqrt{1}\,[bar]} \\ K_{bp2} &= \frac{0.7\cdot\frac{1}{60000}\left[\frac{m^3}{s}\right]}{\sqrt{10^5\,[Pa]}} \\ K_{bp2} &= 3.68932\cdot 10^{-8}\left[\frac{\frac{m^3}{s}}{Pa}\right] \end{aligned} \tag{3.13}$$

Rewriting eq. (3.12) the expression for $C_d A_1$ is found. From this, C_d and the orifice diameter d is extracted.

$$\begin{aligned} C_d A_2 &= \frac{K_{bp1}}{\sqrt{\frac{2}{\rho}}} \\ C_d A_2 &= \frac{3.68932 \cdot 10^{-8} \left[\frac{\frac{m^3}{s}}{Pa}\right]}{\sqrt{\frac{2}{875\left[\frac{Kg}{m^3}\right]}}} = 7.7167 \cdot 10^{-7} \left[m^3\right] \end{aligned} \tag{3.14}$$

For simplicity the orifice constant C_d is set as 1, normally this value lies around 0.6. Once this value is set, the diameter d is easily found. The calculations underneath accounts for the by pass valve on the velocity side.

$$A_2 = \frac{\pi}{4} d_2^2 \rightarrow d_2 = \sqrt{\frac{4A_2}{\pi}} = \sqrt{\frac{4 \cdot 7.7167 \cdot 10^{-7} \left[m^3\right]}{\pi}} = 9.91 \cdot 10^{-4} \left[m\right] \tag{3.15}$$

The same procedure is done for the force control bypass valve. The SimulationX parameters is presented in table. (3.1).

	$\mathbf{C_d}$	$\mathbf{d\,[m]}$
Velocity control bypass valve	1	$9.91 \cdot 10^{-4}$
Force control bypass valve	1	$1.124 \cdot 10^{-3}$

Table 3.1: SimulationX parameters for bypass valves

3.2.2 Servo control valve

The performance of the servo valve is stated in its datasheet (appendix). There are especially two things that are important to determine regarding the performance of the servo valve. The first one is the flow rate and the second is the valve eigenfrequency and damping ratio. All these values are necessary inputs to SimulationX

in order to make a proper dynamic model.

The rated flow is the flow through the valve (one way) at a given pressure drop,

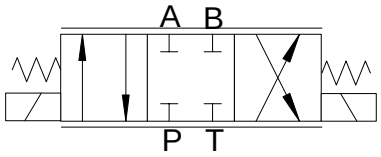

Figure 3.3: Servo valve sketch

this value is found from the datasheet, $10\left[\frac{l}{min}\right]$ @ $35\,[bar]$. In the datasheet the manufacturer suggest a way to calculate the valve flow:

$$Q \;=\; Q_N\sqrt{\frac{\Delta p}{\Delta p_N}}u \tag{3.16}$$

Where Q_N is the rated flow, Δp_N is the rated pressure drop, Δp is the actual pressure drop and u is the valve signal (range$[-1:1]$). The valve is symmetrical, i.e. all flows P$\rightarrow$A, P$\rightarrow$B, A$\rightarrow$T and B$\rightarrow$T can be modeled in a similar manner, see fig. (3.3). SimulationX calculates the flow using eq. (3.17). The only way it differs form eq. (3.12) is that the variable u is introduced. This value can vary in the range [-1,1], i.e. this is the signal that is sent to the valve form the controller. SimulationX assumes a linear dependency between flow and valve opening.

$$Q_{sv} \;=\; C_d A u\sqrt{\frac{2}{\rho}\Delta p} \tag{3.17}$$

From the datasheet the valves performance curves is found, see figs. (3.4) and (3.6). Fig. (3.4) tells us in which range of frequency this servo valve is suitable for operation, fig. ((3.6)) tells us how fast it can respond. It can be seen from the plot that the higher the system pressure is the faster is the responds. Based

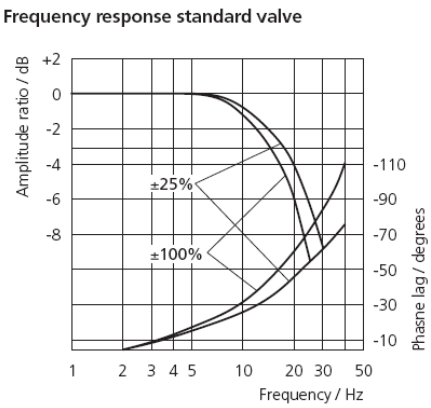

Figure 3.4: Bode plot for the servo control valve (from datasheet)

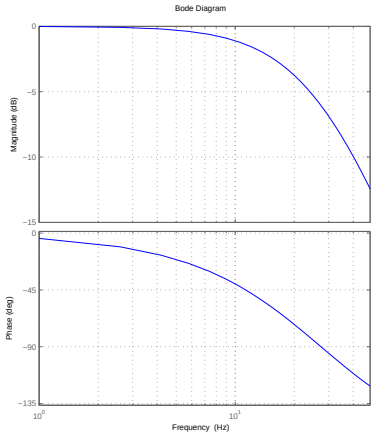

Figure 3.5: Bode plot for the servo control valve (from Simulink)

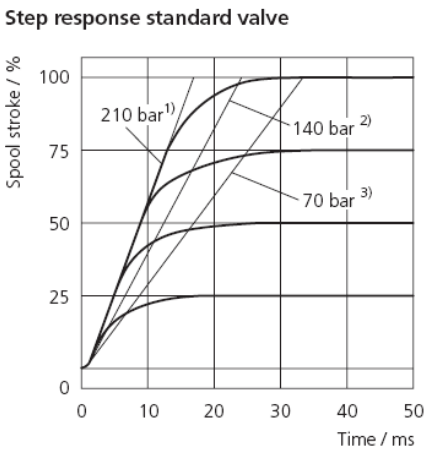

Figure 3.6: Step response for the servo control valve (from datasheet)

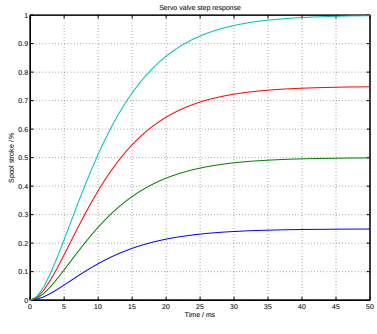

Figure 3.7: Step response for the servo control valve (from Simulink)

on figs. (3.4) and (3.6) a transfer function that fits these two performance curves should be developed. The transfer function is assumed to be of second order. The reason is that experience show that this can be an acceptable way of modeling the

valve dynamics and this is also the model that SimulationX accommodates. The standard form of a second order transfer function (Closed loop) is:

$$H(s) = \frac{\omega_n^2}{s^2 + 2\zeta\omega_n s + \omega_n^2} \tag{3.18}$$

In order to find two poles that satisfy the servo valve performance curves, a small Matlab program is made (appendix). The poles are found by trial and error. First guess on two pole values and then compare its bode plots with fig. (3.4). See eq. (3.19) for the poles that are found to be most suitable.

$$g_{sv}(s) = \frac{1}{\left(\frac{s}{25\cdot 2\cdot \pi} + 1\right)\left(\frac{s}{30\cdot 2\cdot \pi} + 1\right)} \tag{3.19}$$

In order to extract the eigenfrequency and the damping ratio the closed loop transfer function needs to be found and presented on its standard form (eq. 3.18). This is shown in eq. (3.20).

$$\begin{aligned} g_{sv}(s) &= \frac{1}{\left(\frac{s}{25\cdot 2\cdot \pi} + 1\right)\left(\frac{s}{30\cdot 2\cdot \pi} + 1\right)} \\ &= \frac{1}{3.377 \cdot 10^{-5} s^2 + 0.01167 s + 1} \\ &= \frac{\frac{1}{3.377\cdot 10^{-5}}}{s^2 + \frac{0.01167}{3.377\cdot 10^{-5}} s + \frac{1}{3.377\cdot 10^{-5}}} \end{aligned} \tag{3.20}$$

The eigenfrequency ω_n and the damping ratio ζ can now be calculated.

$$\omega_n = \sqrt{\frac{1}{3.377 \cdot 10^{-5}}} = 172.082 \left[\frac{rad}{s}\right] = 27.39\,[Hz] \tag{3.21}$$

$$\zeta = \frac{\frac{1}{3.377\cdot 10^{-5}}}{2\omega_n} = \frac{\frac{1}{3.377\cdot 10^{-5}}}{2 \cdot 172.082} = 1 \tag{3.22}$$

ζ is equal to one, this indicate that the system is critical damped, i.e. no overshoot. This can also be seen on the step response plot fig. (3.7).

For Matlab/Simulink simulation eq. (3.19) can not be used directly, the reason is that it is not possible to implement initial conditions in the transfer function block. The solution is to rewrite the transfer function into a mass-spring-damper (msd) system. The transfer function for this msd - system is shown in eq. (3.23) and its corresponding block diagram in fig. (3.8). Now it is possible to implement the initial conditions for the servo valve.

$$G_{msd} = \frac{1}{m_{sv}s^2 + Ds + K} = \frac{1}{3.377 \cdot 10^5 s^2 + 0.0117s + 1} \tag{3.23}$$

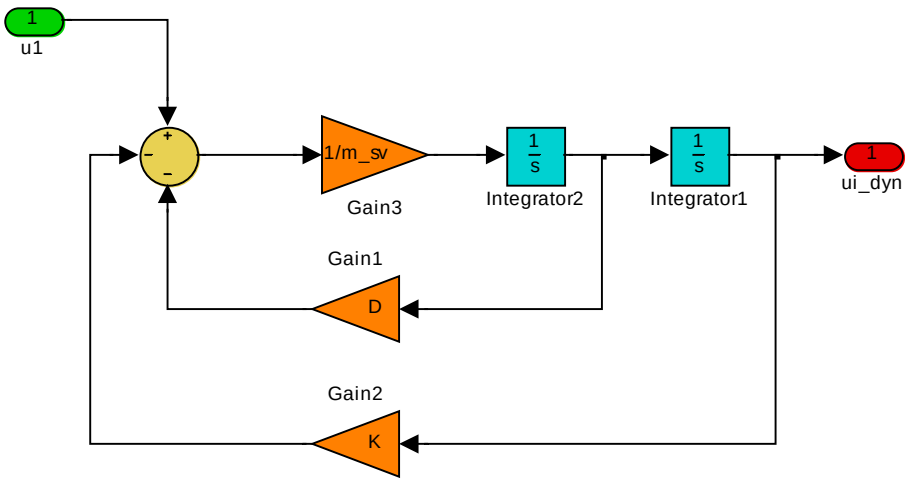

Figure 3.8: Mass-spring-damper system for servo valve

3.3 Nonlinear model

The considered system is nonlinear due to the turbulent flow trough the different valves, also the friction that will be emulated is nonlinear. Step one in the model making is to make a nonlinear model. For this SimulationX is used. In this graphical simulation tool the hydraulic system is modeled by connecting the components in a manner similar to the hydraulic diagram (fig. 3.9). The nonlinear model is useful for verification of the dynamic performance of the system as well as for the tuning of the valve controllers. In the figure there are two PI controllers, input for the controller on the velocity side is the deviation between the reference velocity and the actual velocity of the mass. The input to the second controller is the deviation between the reference disturbance force and the actual cylinder force. The control parameters are found by trial and error. In order to get as smooth transient response as possible, some volumes are added into the system. Another thing that contributes to the transient behavior is the values of the different initial values of the pressures. $160\ [bar]$ is set on the pump side, and on the piston side of the cylinder the pressure that gives equilibrium state is set. Since the area ratio is the same for both cylinders the initial pressures are the same, $127.6\ [bar]$.
This model will be used to check that the system works dynamically. Prior to this only the steady state situation is considered. The results from this will also give the values needed calculation of the preset pressure in the accumulator.

3.4 Linear model

As mentioned in the beginning of this chapter, the dynamic model will be used for testing the systems transient behavior and a linearized model will be made and used for controller design. A linear model is required because the controllers that will be tested are all linear. To make this linear model the initial idea was to use a

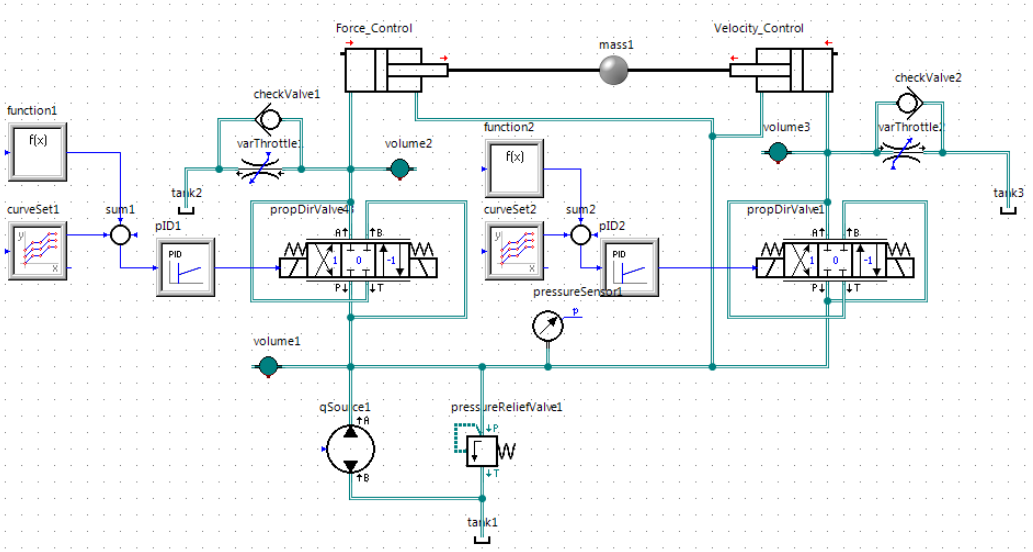

Figure 3.9: SimulationX model

tool in SimulationX which gives out the state space representation of the system. The state space model could then be transformed to a transfer function. But for some reason this tool did not seem to work properly. As a consequence the system model has to be made manually with the different differential and algebraic equations. The linearization is done around a given point of steady state velocity. These steady state values will be extracted via the sensors on the test stand. The values are piston side pressures and servo valve opening. Tank and pump pressure are assumed constant.
Underneath follows the nonlinear equations in the system. The linear expressions of these equations are the first order term of its Taylor expansions.

Velocity control side:

Turbulent flow over the servo valve.

$$Q_{v2} = K_v u_2 \sqrt{p_s - p_2} \tag{3.24}$$

The Taylor expansion ([9]) of this expression is:

$$\Delta Q_{v2} \;=\; \left.\frac{\partial Q_{v2}}{\partial u_2}\right|_{\overline{p_2}} \Delta u_2 + \left.\frac{\partial Q_{v2}}{\partial p_2}\right|_{\overline{u_2},\overline{p_2}} \Delta p_2 \tag{3.25}$$

The Δ-values are deviation values from its linearization point $\overline{u_2}$ and $\overline{p_2}$.

$$\frac{\partial Q_{v2}}{\partial u_2} \;=\; K_v\sqrt{p_s - \overline{p_2}} \;=\; K_{sv2,u2} \tag{3.26}$$

$$\frac{\partial Q_{v2}}{\partial p_2} \;=\; -\frac{K_v\overline{u_2}}{2\sqrt{p_s - \overline{p_2}}} \;=\; -K_{sv2,p2} \tag{3.27}$$

The turbulent flow over the bypass valve:

$$Q_{bp2} \;=\; K_{bp2}\sqrt{p_2 - p_t} \tag{3.28}$$

The Taylor expansion for the bypass valve:

$$\Delta Q_{bp2} \;=\; \left.\frac{\partial Q_{bp2}}{\partial p_2}\right|_{\overline{p_2}} \Delta p_2 \tag{3.29}$$

$$\frac{\partial Q_{bp2}}{\partial p_2} \;=\; \frac{K_{bp2}}{2\sqrt{\overline{p_2} - p_t}} \;=\; K_{bp2,p2} \tag{3.30}$$

Force control side:

The linearized equations for the force control side are quite similar:
Servo valve:

$$\frac{\partial Q_{v1}}{\partial u_1} \;=\; K_v\sqrt{p_s - \overline{p_1}} \;=\; K_{sv1,u1} \tag{3.31}$$

$$\frac{\partial Q_{v1}}{\partial p_1} \;=\; -\frac{K_v\overline{u_1}}{2\sqrt{p_s - \overline{p_1}}} \;=\; -K_{sv1,p1} \tag{3.32}$$

Bypass valve:

$$\frac{\partial Q_{bp1}}{\partial p_1} = \frac{K_{bp1}}{2\sqrt{p_1 - p_t}} = K_{bp1,p1} \tag{3.33}$$

Now, once the linearization is done, the modeling based on algebraic and differential equations can begin.

3.5 Matlab model

It was at the beginning a bit unclear how to model this system. But after some considerations and consulting with the supervisors it became more clear. The model is divided into two parts, velocity side and force side. The two models will be made separately. The inputs and outputs of the models are described in tab. (3.2). Underneath follows the derivation of the two models.

Velocity side		**Force side**	
Input	Output	Input	Output
Servo valve signal	Velocity of cylinder	Servo valve signal	Cylinder force
Disturbance force		Velocity of cylinder	

Table 3.2: Model input - output

3.5.1 Velocity side

The model is based on two equations, the force balance of the cylinder and its pressure gradient. The pressure gradient is dependent of the flow into or out of the cylinder. The force balance is given in eq. (3.34). First the transfer function from servo valve position to cylinder velocity will be found. The servo valve needs voltage as input, so afterwards the transfer function from servo valve voltage to

cylinder velocity will be found.

$$\begin{aligned} \sum F &= m\dot{v} \\ &= p_2 A_2 - p_s \phi A_2 - F_{dis} \end{aligned} \tag{3.34}$$

Applying the Laplace transformation on eq. (3.34) gives:

$$ms\Delta v = \Delta p_2 A_2 - \Delta F_{dis} \tag{3.35}$$

Combining eq. (3.5) and the linearized flows over the servo valve and the bypass valve the expression for the pressure gradient is found.

$$\begin{aligned} \Delta\dot{p}_2 &= \frac{\beta}{V_2}\left(Q - \dot{V}\right) \\ &= \frac{1}{C_2}\left(K_{sv2,u2}\Delta u_2 - K_{sv2,p2}\Delta p_2 - K_{bp2,p2}\Delta p_2 - A_2\Delta v\right) \\ &= \frac{1}{C_2}\left(K_{sv2,u2}\Delta u_2 - K_{p2}\Delta p_2 - A_2\Delta v\right) \end{aligned} \tag{3.36}$$

Applying the Laplace transformation on eq. (3.36) and solving for Δp_2 gives:

$$\begin{aligned} s\Delta p_2 &= \frac{1}{C_2}\left(K_{sv2,u2}\Delta u_2 - K_{p2}\Delta p_2 - A_2\Delta v\right) \\ \Delta p_2 &= \frac{K_{sv2,u2}\Delta u_2 - A_2\Delta v}{C_2 s + K_{p2}} \end{aligned} \tag{3.37}$$

Combining the two equations (3.35) and (3.37).

$$\Delta v\left(mC_2 s^2 + mK_{p2}s + A_2^2\right) = A_2 K_{sv2,u2}\Delta u_2 - \Delta F_{dis}\left(C_2 s + K_{p2}\right) \tag{3.38}$$

The velocity side has two inputs and one output, and in order to find its transfer function the principle of superposition has to be utilized. First the disturbance is set to zero, and the transfer function from valve signal to velocity is found. Afterwards the same is done when the valve signal is set to zero. The velocity

sides total transfer function $G_{vel}(s)$ is at last found by adding these to functions together (without valve dynamics).

$$\begin{aligned} G_{vel}(s) &= \frac{\Delta v}{\Delta u_2} + \frac{\Delta v}{\Delta F_{dis}} \\ &= \frac{\frac{A_2}{C_2 m} K_{sv2,u2}}{s^2 + \frac{K_{p2}}{C_2} s + \frac{A_2^2}{C_2 m}} - \frac{\frac{1}{m} s + \frac{k_{p2}}{C_2 m}}{s^2 + \frac{K_{p2}}{C_2} s + \frac{A_2^2}{C_2 m}} \end{aligned} \tag{3.39}$$

Fig. (3.10) shows the block diagram of what the dynamics are from servo valve voltage in to position out. Its transfer function is:

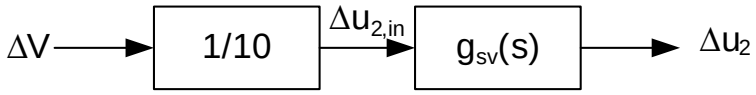

Figure 3.10: Bode plot of velocity side model

$$\Delta u_2 = \Delta V \frac{1}{10} g_{sv}(s) \tag{3.40}$$

Eq. (3.41) states the total transfer function including the valve dynamics.

$$G_{vel}(s) = \frac{1}{10} \frac{g_{sv}(s) \frac{A_2}{C_2 m} K_{sv2,u2}}{s^2 + \frac{K_{p2}}{C_2} s + \frac{A_2^2}{C_2 m}} - \frac{\frac{1}{m} s + \frac{k_{p2}}{C_2 m}}{s^2 + \frac{K_{p2}}{C_2} s + \frac{A_2^2}{C_2 m}} \tag{3.41}$$

The transfer functions bode plot is shown in fig. (3.11). The figure shows that for low frequencies the magnitude is negative, this means the amplitude of the output is less then the amplitude of the input. Knowing the maximum servo valve signal is 1 and the velocity of the cylinder lies around $0.01 - 0.02 \left[\frac{m}{s}\right]$, then this makes sense. The magnitude is more or less constant until $80 \left[\frac{rad}{s}\right]$, as mentioned the frequency of operation is quite small. The phase is also unaffected at low frequencies, low frequencies in this context are $\omega < 10 \left[\frac{rad}{s}\right]$. Since the bode plot has a slope of zero at low frequencies, the system is of type zero. Eq. (3.42) shows

an example of a transfer function of this type.

$$g(s) = \frac{1}{s^0 \left(as^2 + bs + c\right)} \tag{3.42}$$

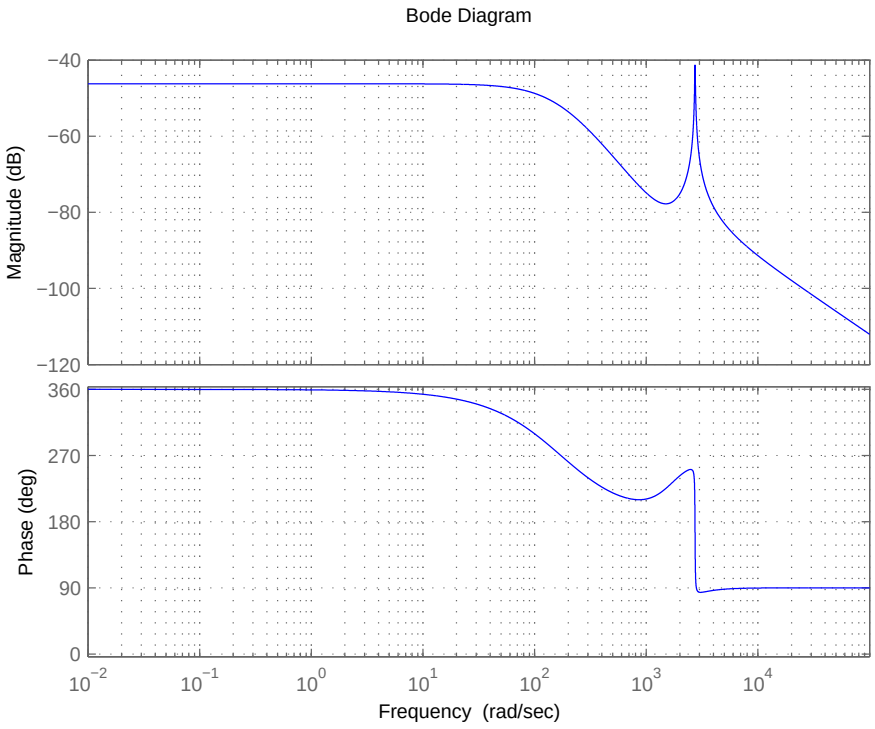

Figure 3.11: Bode plot of velocity side model

The corresponding block diagram for eq. (3.35) and eq. (3.37) is shown in fig. (3.12)

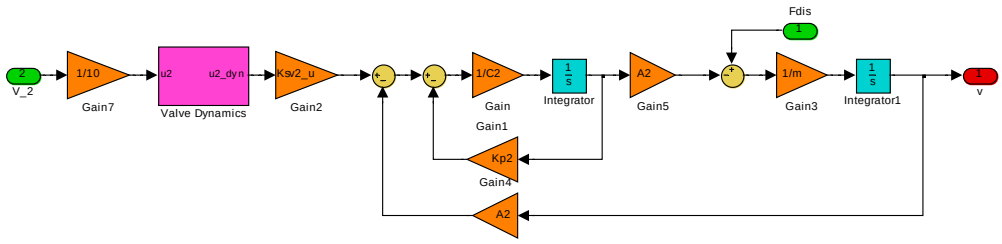

Figure 3.12: Block diagram of velocity side model

Stability

The Nyquist criterion is used to check the stability of the system. By using the frequency response of the open loop system one can find in which range of gain the closed loop system is stable. Step one is to find the open loop zeros and poles, tab. (3.3). The calculations are done for $K = 1$. Reference is made to [17].

The table shows there are only stabile open loop poles in the system, but there

Open loop poles and zeros	
Poles	Zeros
$-16.2 + 1933.1i$	1654.5
$-16.2 - 1933.1i$	$-1016.3 + 1539.8i$
$-16.2 + 1933.1i$	$-1016.3 - 1539.8i$
$-16.2 - 1933.1i$	$-16.229 + 1933.1i$
-188.5	$-16.229 - 1933.1i$
-157.1	-

Table 3.3: Open loop poles and zeros, velocity side

is one unstable zero. The effect of the right half plane (RHP) zero is that as the gain increase it will 'pull' the poles towards the RHP. The Nyquist criterion says $Z = P - N$, where P is unstable poles and N is the number of encirclements around -1. Clockwise crossings are negative and counterclockwise are positive. From the zero crossing of the imaginary axis on fig. (3.13) one can calculate how large K are when $|G(j\omega)| = 1$.

$$\frac{1}{k} = 3.51 \cdot 10^{-3} \Longrightarrow K = 285 \tag{3.43}$$

This implies that for values $K > 285$ two clockwise encirclements around -1 will occur, $Z = 0 - (-2) = 2$. The system will have two closed loop in the RHP, and the system is unstable. This is only valid when there is a disturbance force influencing the system.

Stability check is also done for the no disturbance situation. Now the root lo-

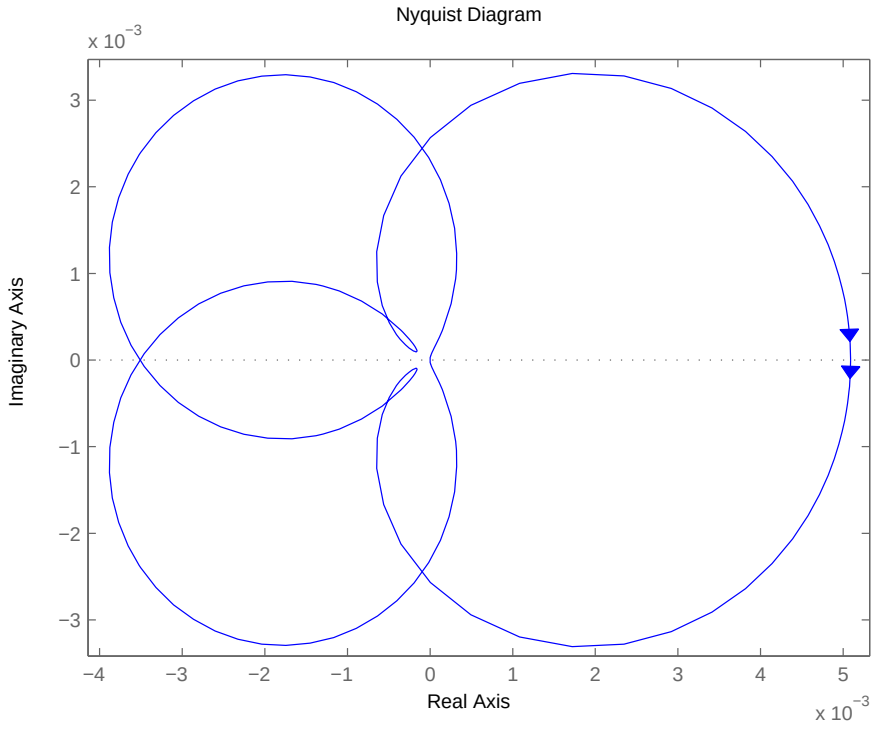

Figure 3.13: Nyquist plot of velocity side model, with disturbance

cus technique is used. Also here the open loop transfer function is the starting point, and the result gives a plot where one can see how the closed loop poles travel. Fig. (3.14) shows this plot. System has two RHP poles for $K > 1750$

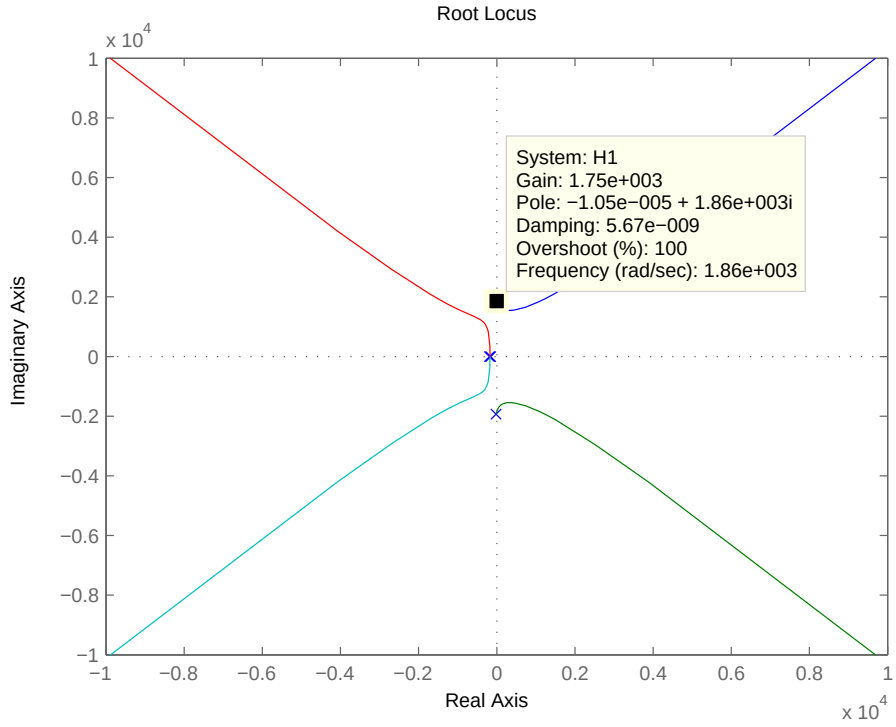

Figure 3.14: Root locus plot of velocity side model, with no disturbance

3.5.2 Force side

The model of the force side is built up quite similar compared to the velocity side model. The staring point is also here the equations describing the force balance and pressure gradient. The transfer function of the model including the servo valve dynamics is stated in eq. (3.44). The corresponding bode plot and block diagram is shown in fig. (3.15) and fig. (3.16).

$$\begin{aligned} G_{dis}(s) &= \frac{\Delta F_{dis}}{\Delta V_1} + \frac{\Delta F_{dis}}{\Delta v} \\ &= \frac{1}{10}\frac{g_{sv}(s)\frac{A_1}{C_1}K_{sv1,u1}}{s+\frac{K_{p1}}{C_1}} - \frac{\frac{A_1^2}{C_1}}{s+\frac{K_{p1}}{C_1}} \end{aligned} \tag{3.44}$$

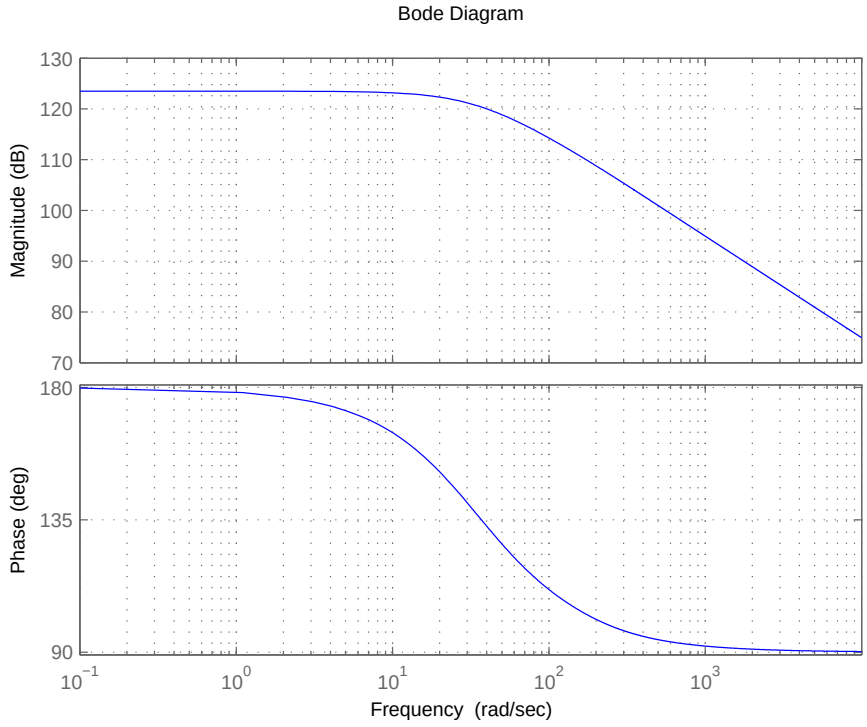

Figure 3.15: Bode plot of force side model

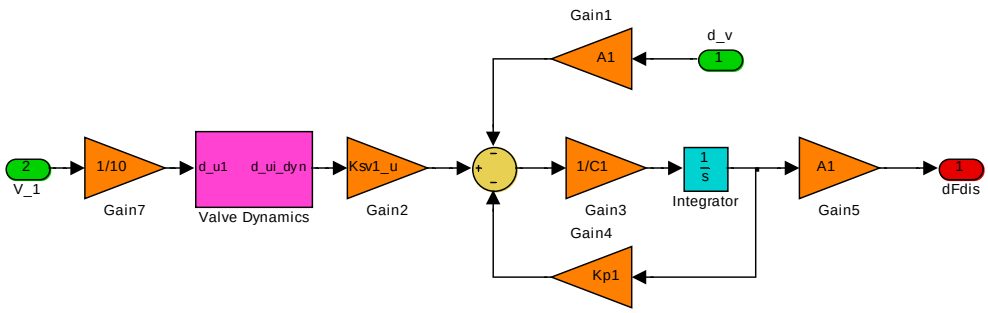

Figure 3.16: Block diagram of force side model

Stability

Tab. (3.4) shows the placement of the open loop poles. Fig. (3.17) shows there

Open loop poles and zeros	
Poles	Zeros
-188.4956	-190.7307
-157.0796	-154.8445
-25.4855	-25.4855
-25.4855	$-$

Table 3.4: Open loop poles and zeros, force side

is one encirclement around -1, which implies one closed loop pole in the RHP. Using the zero crossing of the imaginary axis, the range of stability can be found.

$$\frac{1}{k} \;=\; 2.2854 \cdot 10^{6} \Longrightarrow K \;=\; 4.34 \cdot 10^{-7} \tag{3.45}$$

This means system is stabile for $K < 4.34 \cdot 10^{-7}$

Root locus for the open loop system with no disturbance: This shows system with no disturbance is stable for $K < 3.16 \cdot 10^{-3}$

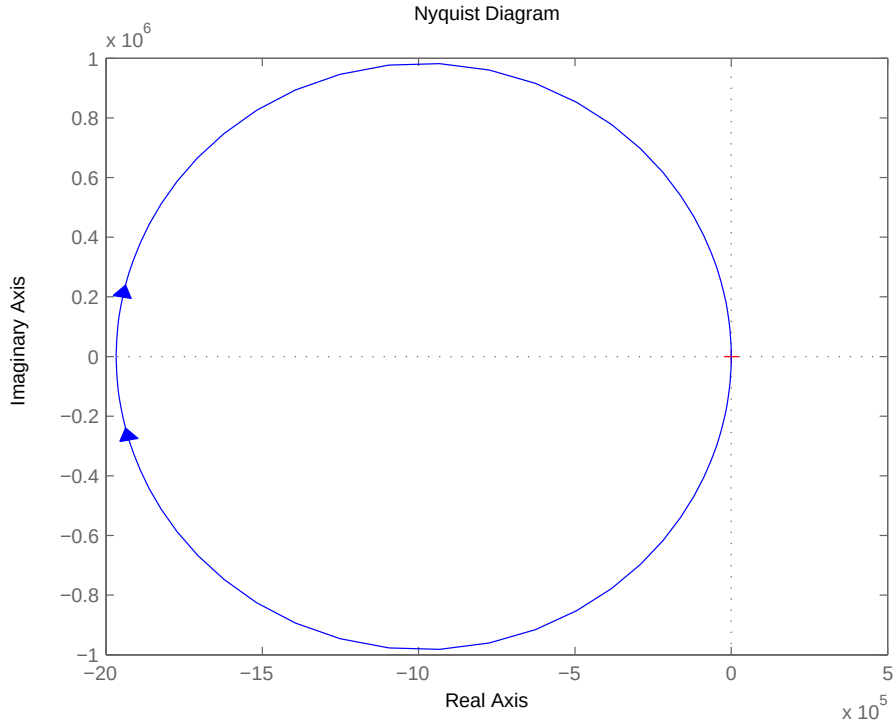

Figure 3.17: Nyquist plot of force side model, with disturbance

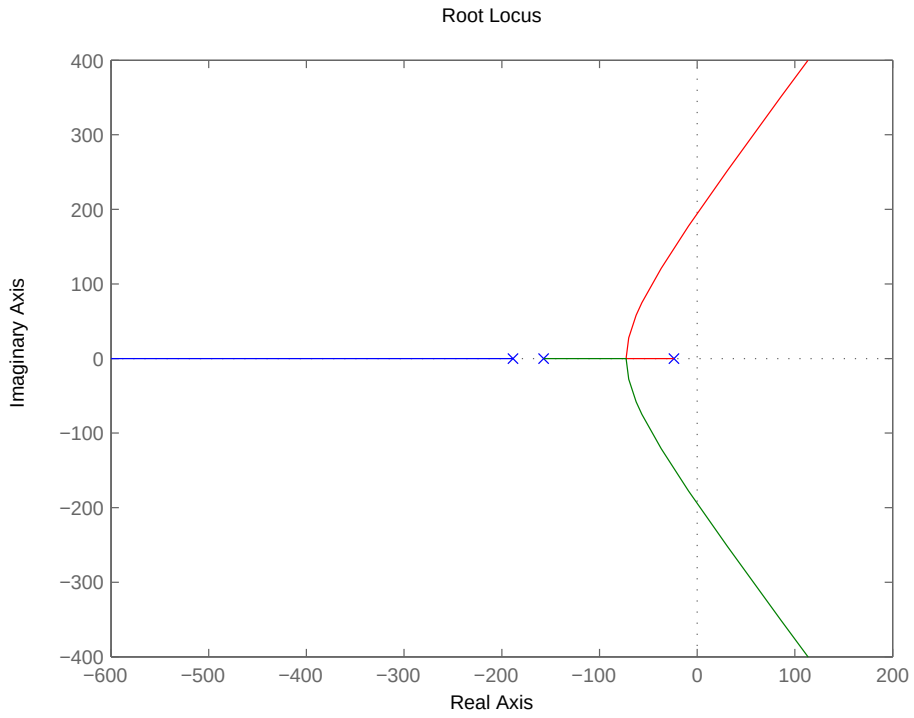

Figure 3.18: Root locus plot of force side model, with no disturbance

3.6 State space model

State space model is only made for the velocity side. The reason is manly due to time limitations and partly because it is not that straight forward as for the velocity side. The model is therefor left as further work to be done.

3.6.1 Velocity side

In order to obtain a suitable state space system the Simulink model needs to be modified, fig. (3.19). The consequence of the disturbance force is that it tries to change the piston side pressure. Knowing this the disturbance force can be changed to a disturbance pressure on the piston side, only by dividing the force on the piston side area. This will now give a system with two inputs and two outputs, i.e. multiple input multiple output (MIMO) system. The states are described in eq. (3.46).

$$x = \begin{bmatrix} cylinder\ velocity \\ piston\ side\ pressure \\ servo\ valve\ position \\ servo\ valve\ velocity \end{bmatrix} \tag{3.46}$$

The general representation of a state space system is presented in eq. (3.47).

$$\begin{aligned} \dot{x} &= Ax + Bu \\ y &= Cx + Du \end{aligned} \tag{3.47}$$

The state space model is made using the linmod() - function in matlab. The input to the function is a Simulink model, where the two inputs and the output are

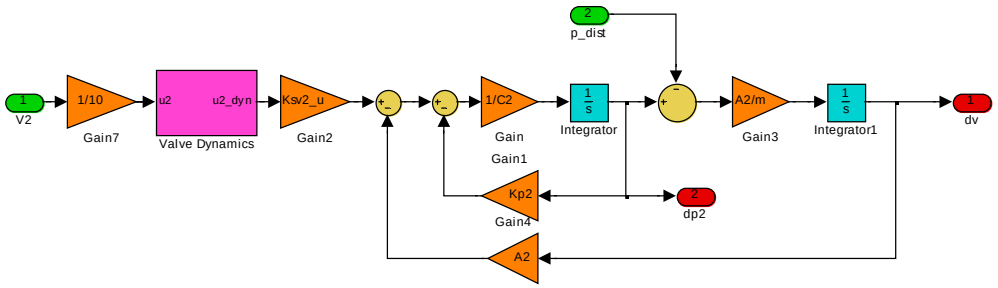

Figure 3.19: Modified block diagram for velocity side

selected.

$$\dot{x} = \begin{bmatrix} 0 & 5.0265 \cdot 10^{-4} & 0 & 0 \\ -7.4345 \cdot 10^{9} & 32.4577 & 3.7847 \cdot 10^{8} & 0 \\ 0 & 0 & 0 & 1 \\ 0 & 0 & -2.9609 \cdot 10^{4} & -345.5752 \end{bmatrix} x$$
$$+ \begin{bmatrix} 0 & -0.1000 \\ 0 & 0 \\ 0 & 0 \\ 2.9609 \cdot 10^{3} & 0 \end{bmatrix} u \tag{3.48}$$

$$y = \begin{bmatrix} 1 & 0 & 0 & 0 \\ 0 & 1 & 0 & 0 \end{bmatrix} x \tag{3.49}$$

Whether the system is controllable or not is checked via the controllability matrix. As stated in [17] p. 735: *If an input to a system can be found that takes every state variable from a desired initial state to a desired final state, the system is said to*

be controllable: otherwise, the system is uncontrollable. Controllability matrix:

$$C_M = \left[\begin{array}{ccccc} A & AB & A^2B & ... & A^{n-1}B \end{array} \right] = 4 \tag{3.50}$$

If the system is of full rank, i.e. the rank has the same value as the order of the system, then the system is controllable.

Chapter 4

Verification of Model

This chapter describes the procedures used for verifying the models by finding system constants and analyzing system behavior. The found values are then used to adjust the simulation models such that control strategies can be tried out. The tests are done for each cylinder separately. First, a step from zero to full opening and back to zero is applied. Since the aim is to have the controlled cylinder go in a harmonic motion, different sine signals are sent to the valve as a second test. At the end of the chapter is the corresponding plots done in matlab/simulink. The following equations are used for a critical analysis of the analyzed velocity (v), pressures (p_s,p_2,p_t), and flows (Q_{sv},Q_{bp},Q_2), which are defined in fig. (4.1):

$$Q_{sv} = u\, K_{sv} \sqrt{\Delta p_{sv}} \tag{4.1}$$

$$K_{sv} = C_{d,sv}\, A_{sv} \sqrt{\frac{2}{\rho}} \tag{4.2}$$

$$\Delta p_{sv} = p_s - p_2 \tag{4.3}$$

$$Q_{bp} = K_{bp}\sqrt{\Delta p_{bp}} \tag{4.4}$$

$$K_{bp} = C_{d,bp}\, A_{bp}\sqrt{\frac{2}{\rho}} \tag{4.5}$$

$$\Delta p_{bp} = p_2 - p_t \tag{4.6}$$

$$v = Q_2/A_{cyl} \tag{4.7}$$

The force $F_a = m\ddot{x}$ needed to accelerate the mass of the piston and the piston rod is relatively small compared to the forces delivered by the cylinders, because the maximum velocities reached are low and the mass small. It is therefore neglected, which gives the following equation for force equilibrium according to fig. (4.1):

$$p_2 A = p_s A\phi + sign(v)F_f \tag{4.8}$$

$$\Rightarrow F_f = A\Delta p \tag{4.9}$$

The tank pressure p_t is assumed to be constant at $0.5[bar]$. The following steps are taken:

1. Identify the servo valve constant K_{sv}. Bypass valve closed.
2. Choose the bypass valve opening. With respect to the control task, the opening is chosen to yield $v_{max,stroke-in} = -v_{max,stroke-out}$.
3. Identify the bypass valve constant K_{bp} at the chosen opening.
4. Take measurements of p_2, Q_2, x; calculate all other system variables; evaluate the found values. Repeat this step for different valve signals.

For evaluating the signals with respect to range, noise, and accuracy, it must be remembered that only p_2, Q_2, and x are measured directly; the others are obtained from a calculation or derivation. The circumstances for each measurement or calculation are chosen such that there are fewest possible system variables and

that numbers are rather calculated from pressure than from flow due to accuracy. The resulting constants and values of the this chapter are summarized in tab. (4.1).

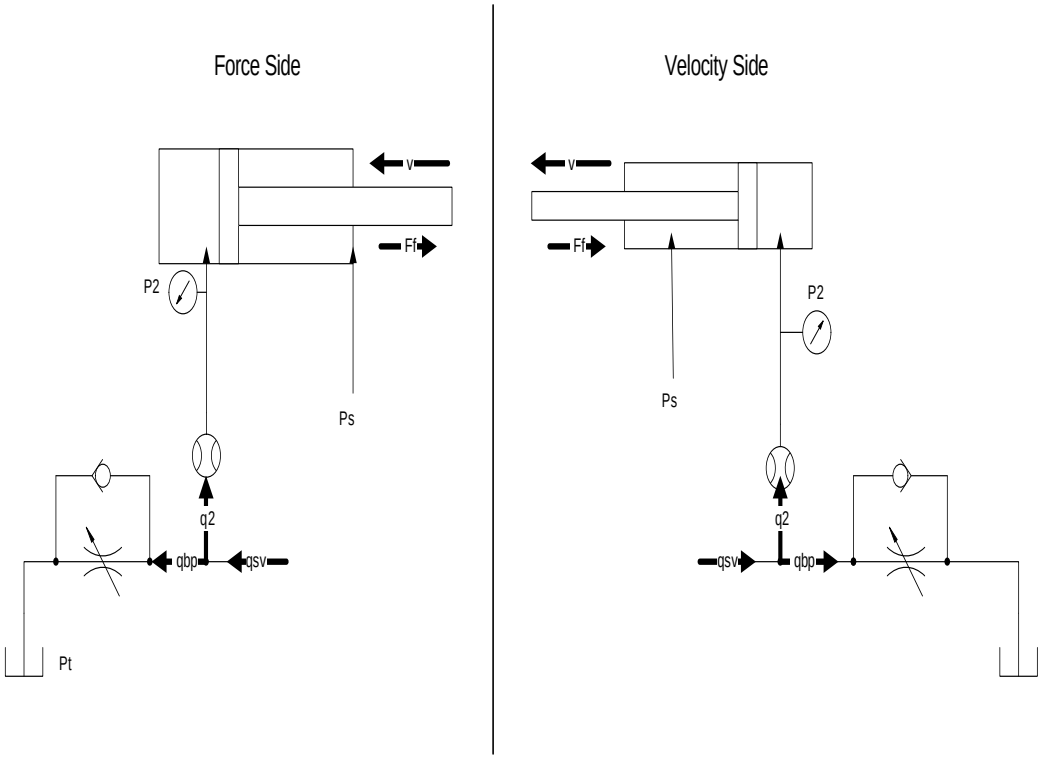

Figure 4.1: Definition of system variables

4.1 Velocity Side

Valve Constants

If the bypass valve is completely closed, all servo valve flow Q_{sv} will go through the flow sensor. At the measured pressure p_2 the servo valve constant can then be calculated using eq. (4.1):

$$K_{sv} = \frac{Q_2}{u\sqrt{p_s - p_2}} = 1.41 \cdot 10^{-7} \tag{4.10}$$

K_{sv} should be independent of the valve signal u. Measurements (see appendix (C)) show that there is some drift in the values, especially for a small u. It is therefore chosen to approximate K_{sv} by an average of the values found for openings from 40% to 100%, because Matlab simulations show that the valves are never completely closed for the desired piston movement. K_{sv} refers to the whole valve, i.e. to both slots together.

The bypass valves are adjustable; they are tuned such that the cylinder has the same constant maximum velocity when it travels in as it has when it travels out. For the found bypass valve position, the valve constant can be determined from eq. (4.4), if the relevant flow and pressure are known. There are two feasible situations: First, when the piston has reached its maximum stroke and the valve is fully opened, and secondly, when the cylinder is moving in and the valve is closed. In order to avoid uncertainties due to leakage flow, the first possibility is chosen and K_{bp} is found according to eq. (4.4):

$$K_{bp} \;=\; \frac{Q_{sv}}{\sqrt{p_2 - p_t}} \;= 3.43 \cdot 10^{-8} \tag{4.11}$$

Steady State Analysis

For adjusted bypass valve and found parameters K_{sv} and K_{bp}, values are measured for maximum and minimum velocity cylinder movement, i.e. for the valve fully opened ($u = 1$) and fully closed ($u = 0$), respectively. In the case of ideal conditions with no internal friction, the ring side pressure p_2 is expected to be

$$p_{2,ideal} \;=\; \phi p_t \;=\; 127.6[bar]. \tag{4.12}$$

Is is observed in fig. (4.2) that p_2 varies from $127.8[bar]$ stroking out to $127.3[bar]$ stroking in (averaged over $10[s]$). Assuming friction F_f is equally large in both directions, p_2 becomes $127.55 \pm 0.25[bar]$, i.e. eq. (4.8) yields a friction force of $F_f = 250000[Pa] \cdot 0.04^2[m^2]\pi = 125[N]$. Equivalently the pressure peaks at change of direction give $\Delta p \approx 6[bar] \equiv 3000[N]$.

Leakage flow at operating pressure is not given accurately in the documentation of the valve and can be up to several bar. The measured pressures for $u = 0$ lie around $6.5[bar]$ which is equivalent to $Q_2 = 1.60 \left[\frac{l}{min}\right]$ (eq. (4.1)) and therefore a realistic value. Together with the values found above, the pressure measurements seem to be very reasonable.

A critical situation is when the cylinder has reached its final position and the servo valve is still fully opened: All the servo flow must now go through the bypass valve, where higher flow means higher pressure drop. An increased p_2 is measured, which implies less flow through the servo valve, such that a equilibrium situation is reached where $Q_{sv} = Qbp$. This is not observed in the plot; there is a $1.1 \left[\frac{l}{min}\right]$ gap, that no reason can be identified for. The same gap appears at the stroking out situation, where Q_2 and Q_{bp} should add up to Q_{sv}. A possible error source might be the flow sensor or/and inaccuracies in the determined system constants.

Dynamic Analysis

The purpose of the dynamic analysis is to obtain measurements for a reasonable range of the valve signal V and the frequency f. The later is chosen at $f = 0.1[Hz]$, higher than the frequency that shall be used for the simulation, in order to see more of the dynamic behavior. For the adjusted bypass valve the servo valve signal for $v = 0[m/s]$ is found to be $-4.4[V]$, such that an amplitude of $4.4[V]$ can be used:

$$V = -4.4 + 4.4 \sin(0.2\pi)[V] \tag{4.13}$$

The velocity derived from position follows a sine function with amplitude $A \approx 2.25 \left[\frac{cm}{s}\right]$. This appears a reasonable value, regarding the found steady-state values and the fact that the maximum values $+6.49 \left[\frac{l}{min}\right]$ and $-7.87 \left[\frac{l}{min}\right]$ in cylinder flow Q_2 yield piston velocities of $2.15 \left[\frac{cm}{s}\right]$ and $-2.6 \left[\frac{cm}{s}\right]$, respectively.

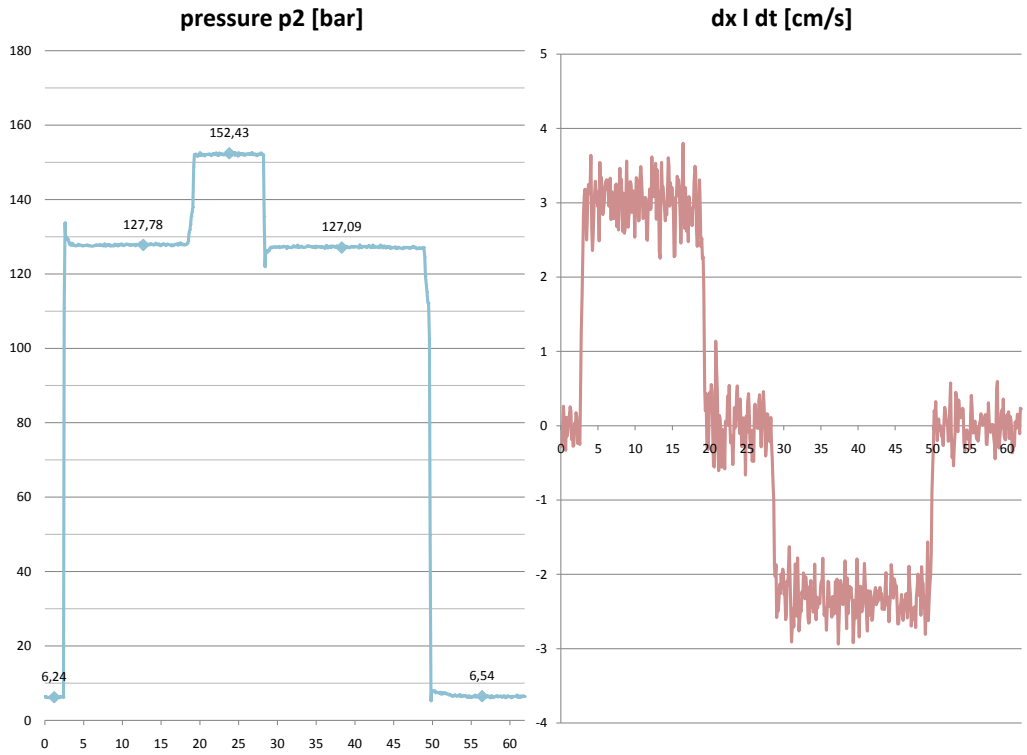

Figure 4.2: Results A for $0[V]$ and $-10[V]$ valve signal, velocity side

At almost constant bypass flow, the cylinder flow describes a sine function, which has an offset slightly under the bypass flow. This explains why the cylinder position experiences drift in negative x-direction. When the cylinder flow sinks under the time axis, it remains around $0\left[\frac{l}{min}\right]$ for about $0.4[s]$ before undergoes a relatively high acceleration for about the same time. Having a look at the force F_a needed to accelerate the mass, using the values $m_{pisten+rod} \approx 5[kg]$ and $\ddot{x} \approx \frac{(0.025-(-)0.025)[m/s]}{5[s]} = 0.01\left[\frac{m}{s^2}\right]$, a value of $F_a = 5[N]$ is found. Trusting the flow sensor it can therefore be concluded that the delay in cylinder movement is only due to static friction acting on the piston rod at very low velocities (see chapter "Friction Models"). This statement is stressed by that fact that once stopped,

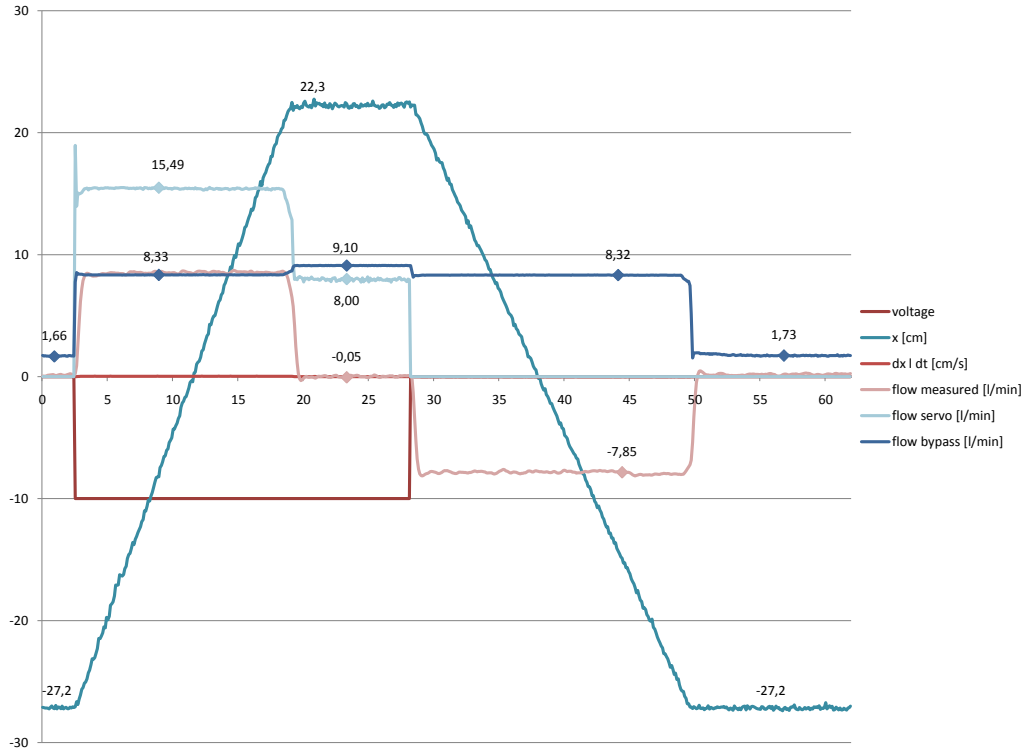

Figure 4.3: Results B for $0[V]$ and $-10[V]$ valve signal, velocity side

the flow will not start increasing again before the valve opening has changed further such that a change in pressure p_2 causes the piston to start moving again.
A delay of $\approx 0.3[s]$ can be observed between flow Q_{sv} through servo valve and both valve signal and flow Q_2 into the cylinder.
At the minimum value $Q_2 = -7.87 \left[\frac{l}{min}\right]$ the cylinder flow stays constant for about $1.5[s]$. This effect can be explained with the ± 10 overlap the valve has. The signal does however not start flattening before it reaches an area of much less then 10 valve opening. Considering that leakage flow through the servo valve comes into the picture at the latest when the valve is in a theoretically closed position, this behavior is according to theory. At the maximum value ($Q_2 = +6.49 \left[\frac{l}{min}\right]$) this effect in the cylinder flow curve can not be observed, because leakage flow

is not a relevant value at large openings. A similar effect can be expected, if the valve signal exceeds the saturation point of $-10[V]$; however, this is prevented programmatically.

Fig. (4.6,4.7,4.8) shows the plots from Simulink. The same input signal is used as input.

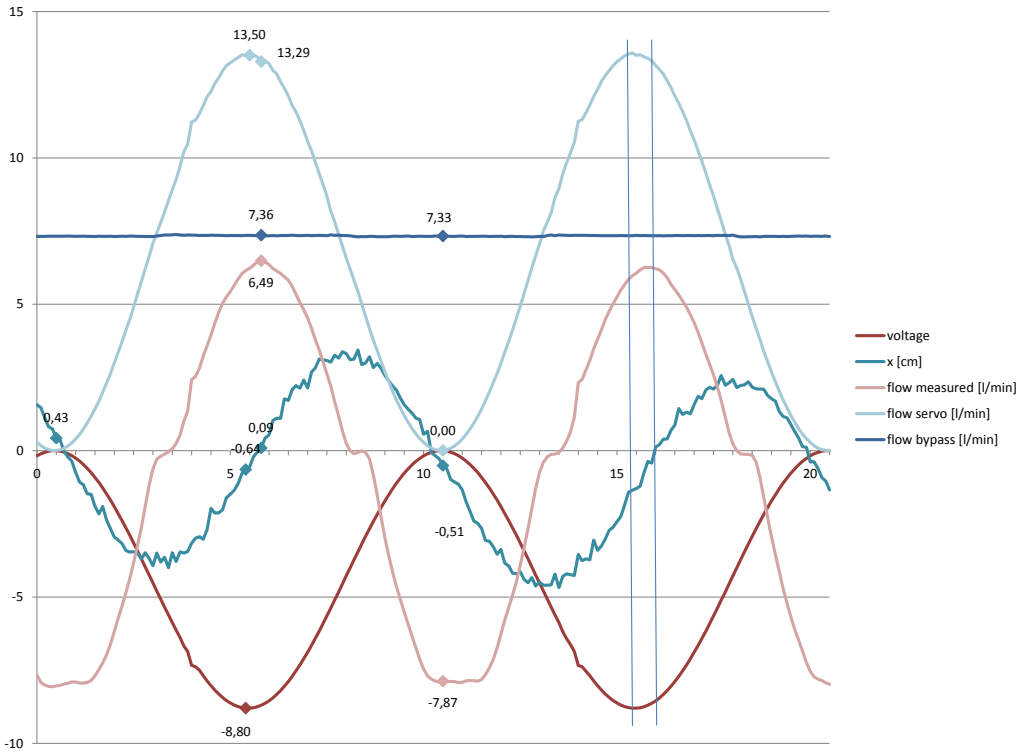

Figure 4.4: Results A for sine signal to valve, velocity side

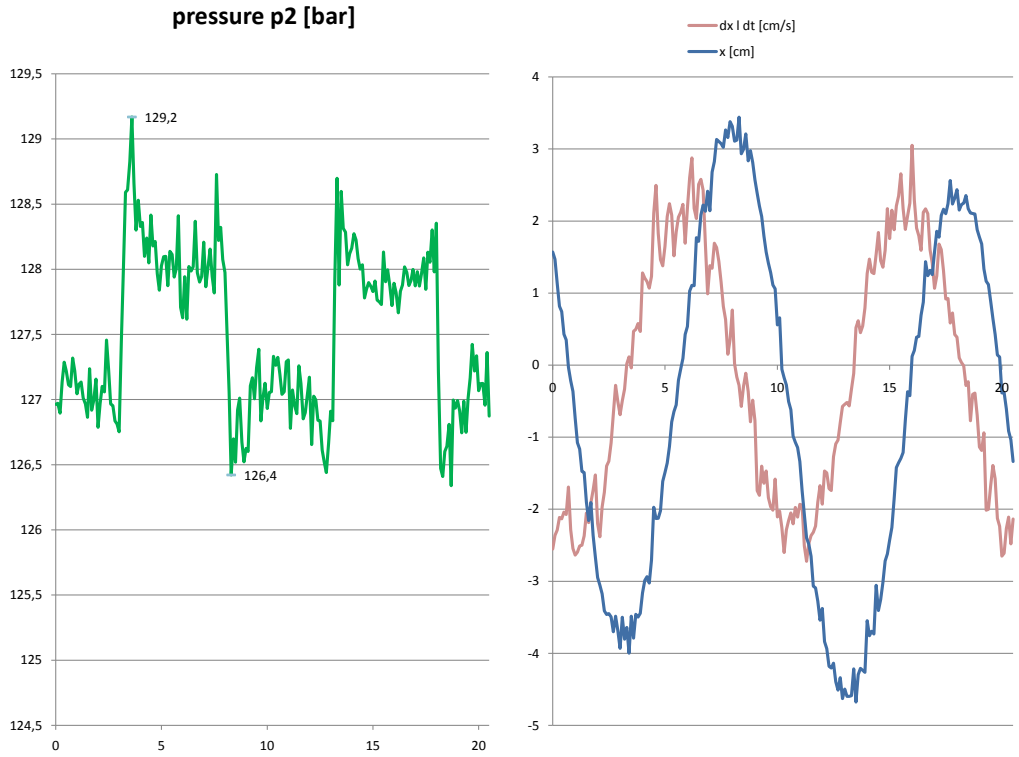

Figure 4.5: Results B for sine signal to valve, velocity side

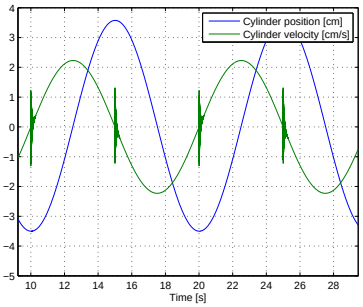

Figure 4.6: Simulink plots of position and velocity

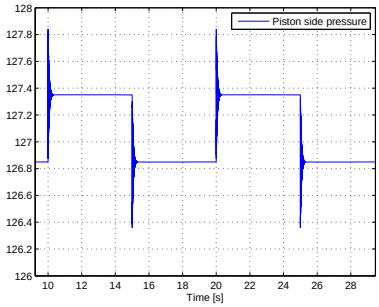

Figure 4.7: Simulink plot of piston side pressure

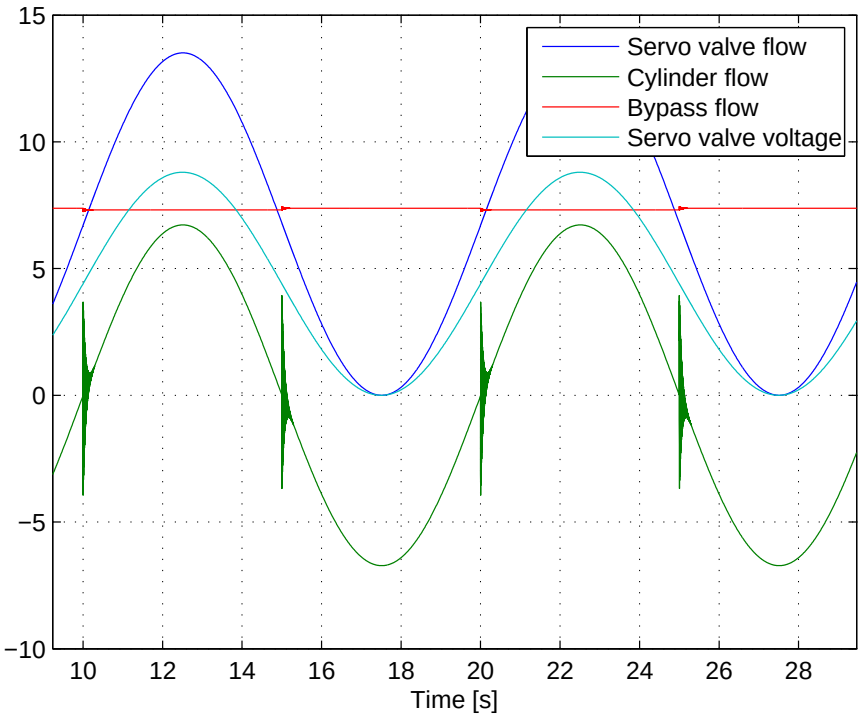

Figure 4.8: Corresponding Simulink plot for results A

	Force side	**Velocity side**
K_{sv}, Theoretical value (Datasheet)	$1.78 \cdot 10^{-7}$	$1.78 \cdot 10^{-7}$
K_{sv}, Real value (Test rig)	$1.36 \cdot 10^{-7}$	$1.41 \cdot 10^{-7}$
K_{bp}	$2.75 \cdot 10^{-8}$	$3.43 \cdot 10^{-8}$
$Q_{2,max,out}$	$6.1[l/min]$	$8.3[l/min]$
$Q_{2,min,in}$	$-6.6[l/min]$	$-7.8[l/min]$
p_f, friction loss	$\pm 8.55[bar]$	$\pm 0.3[bar]$
F_f	$\pm 6700[N]$	$\pm 125[N]$

Table 4.1: Summary: key values

4.2 Force Side

The analysis of the force side is equivalent to the velocity side. The results are summarized in tab.(4.1). The only difference between the force side and the velocity side is the size of the cylinders. It was however found that the larger cylinder has significantly higher internal friction: averagely stroking out for $t = 15...30[s]$: $p_2 = 136.4[bar]$, stroking in for $t = 75...90[s]$: $p_2 = 119.3[bar]$. $17.1[bar]$ difference are equivalent to a friction force of about $6.7[kN]$. The plots fig. (4.9) and fig. (4.10) show in addition that the internal friction is not constant over the full stroke length. In the area of maximum stroke length the pressure p_2 goes down and the cylinder flow goes up, indication less friction.

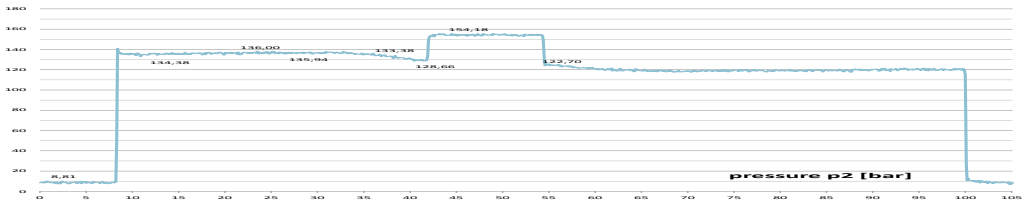

Figure 4.9: Results A for $0[V]$ and $-5[V]$ valve signal, force side

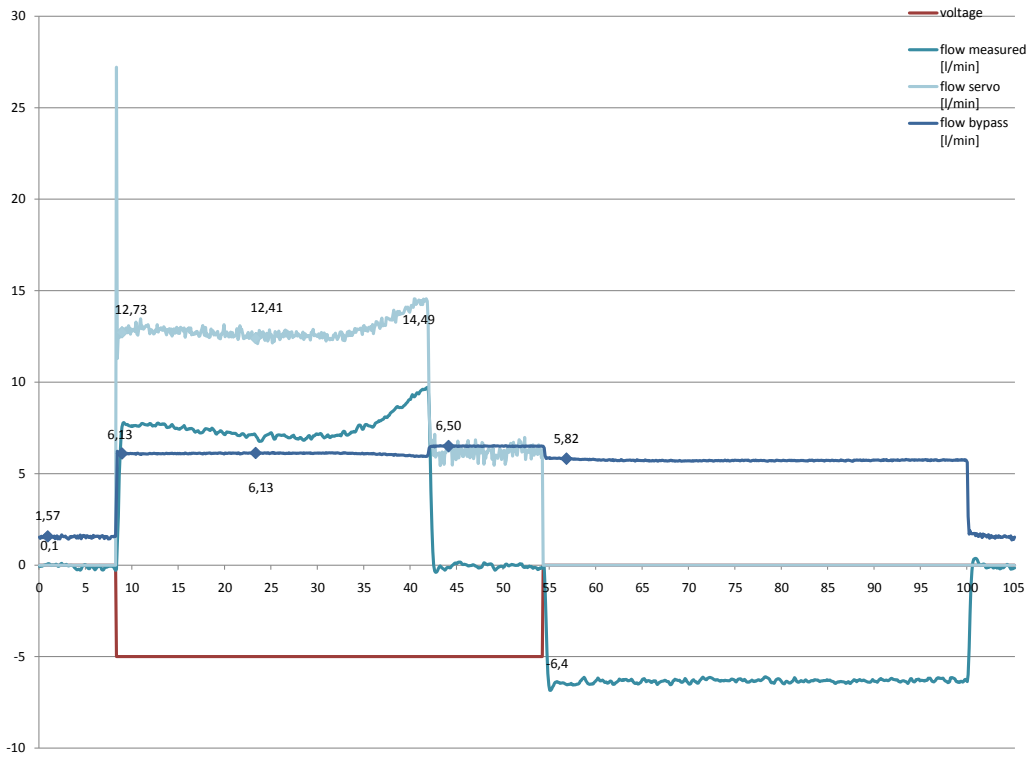

Figure 4.10: Results B for $0[V]$ and $-5[V]$ valve signal, force side

Chapter 5

Friction Models

The aim of the project is to try out different control strategies for friction compensation, while the friction itself is simulated, i.e. the emulator test stand can be used for testing friction control loops for any given system, if its friction characteristics are known, under the following circumstances

- Friction can be simulated up to the maximum values that the cylinder can deliver / tolerance of the load cell
- Friction can be simulated down to the resolution of the load cell and the hydraulic system
- Friction can be simulated for systems operating within the velocity range of the test rig
- Friction can be simulated for systems operating within the bandwidth of the test rig

The following known and commonly used friction models (i.e. [2]) are the starting point for the friction emulator and the motivation for the force-side-controller

design. They are therefore listed with respect to simplicity of implementation and controlling.

5.1 Coulomb Friction

Coulomb Friction is the most basic disturbance considered. A constant friction K_c is working against the direction of motion, i.e. decelerating it. When the velocity crosses zero, i.e. the motion changes direction, the Coulomb Friction will jump instantly from K_c to $-K_c$ and the other way round:

$$F_c \;=\; \text{sign}(v) K_c \tag{5.1}$$

Modification: For first tests of control strategies it might be desirable to avoid infinity-slope jumps in the friction force and rather have a smooth transition between areas of positive and negative friction. Therefore it is suggested to start with an arcus tangent approximation and let the slope go towards infinity by increasing m, as illustrated in fig. (5.1)and(5.2):

$$F_c \;=\; K_c \, \arctan(mt) \tag{5.2}$$

5.2 Viscous Friction

The part of the friction that is proportional to velocity is called Viscous Friction and depends on no other variables:

$$F_v \;=\; K_v \, v \tag{5.3}$$

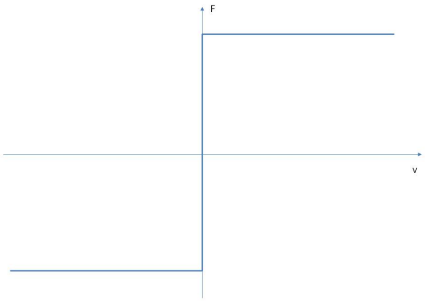

Figure 5.1: Coulomb friction model

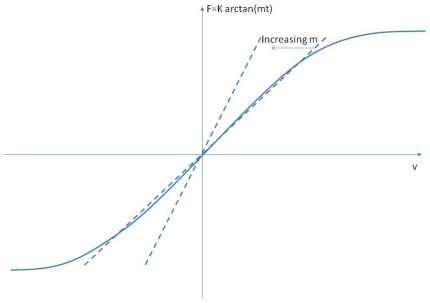

Figure 5.2: approximation with arcus tangent

Further discussion considers friction phenomena added to the previous ones.

5.3 Stiction

Having a closer look at what is happening at deceleration when the velocity curve passes a low critical value $v = v_{stic} > 0$, one can find the motion appearing to be suddenly blocked, i.e. the mechanical part is "sticking" to the supporting structure. With continuing velocity decrease the considered object will not start moving in opposite direction before it passes the respective negative value $v = -v_{stic} < 0$. This means that two impulse-like peaks are added in the zero-velocity area of the friction curve, as seen in fig. (5.3). In order for an object to start moving, the accelerating force must therefore be higher than this peak value. After the peak muss less force is needed to maintain the desired motion.

5.3.1 Stick-Slip Effect

Considering a situation where an acceleration force has just about overcome the friction peak from stiction, the friction will suddenly drop and the force difference

will result in an instant acceleration (”slipping”) to and over a velocity equilibrium point, i.e. over a point where the velocity is constant because of an equilibrium between accelerating and friction force. A resulting deceleration due to the higher friction causes then the velocity to drop below the equilibrium point v_{eq}, where acceleration occurs again. If the velocity stays around $|v| \approx v_{stic}$, the moving object will continue in a stick-slip-motion, as illustrated in fig. (5.4).

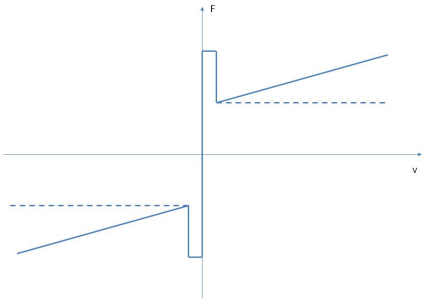

Figure 5.3: Coulomb+viscous+stiction

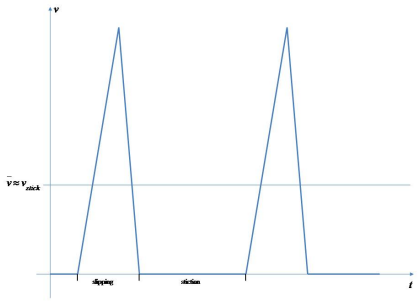

Figure 5.4: Stic-Slipp Effect

5.4 Stribeck Effect

The Stribeck Curve is a traditional way of modeling the transition from static to viscous friction [20]. In stead of an impulse-like peak, the Stribeck model uses an exponential function with negative exponent, yielding an easy analytic description for static friction with smooth transitions to the linear area.

$$F_s \;=\; K_s \, e^{\left(-\frac{v}{v_s}\right)} \tag{5.4}$$

5.5 Summary the Models

The models considered in this chapter are a good starting point for friction modeling, because they can be implemented simply implemented and build the base for a other models. A more advanced model that introduces micro-deflections as an additional degree of freedom is the LuGre Model. The reactions between the surfaces are here modeled with springs and dampers. The LuGre model is over the scope of this project, but might be very interesting to implement, if all of the simpler models have been tried out. Another aspect that none of the models above consider is lubrication, as suggested by [10].

Chapter 6

Control strategies/design

Over the last ten to fifteen years a lot of research attention has been given to problems dealing with dynamic positioning systems for floating vessels, i.e. systems that compensate for movement in the horizontal direction. References can be made to [4, 6, 7, 19]. While the systems that compensate for the heave motion, due to waves, have been given much less research attention. In 1998 Korde [13] proposed a control system that utilized classical control theory and it showed to be efficient within the bounds of linearity. In 2008 Do and Pan [5] presents a method to design a nonlinear controller. The controller design is based on Lyapunov‘s direct method and the making of disturbance observers. In 2009 Li and Lui [14] propose a Linear-Quadratic-Regulator based on dynamic vibration absorbers. Over the last couple of years some papers dealing with heave compensated cranes have been published, e.g. [18, 11, 15, 16]. The main attention here is the critical phase when the crane lowers the payload into the water, also refereed to as the splash zone. Some of the control methods they are dealing with are for example impedance control, feedforward control, feedback control and heave motion prediction. The content in the papers that are cited here acts as inspiration on how to address the control problem in this thesis.

The rest of this chapter will describe the different control strategies and the design of the controllers.

6.1 Frequency domain technique

The controller is designed after some performance criteria. Closed loop at low frequencies the magnitude should be $\approx 0\,[dB]$ and the phase $\approx 0\,[degrees]$. PI controllers are chosen for this design.

6.1.1 Velocity side

Fig. (6.1) shows the control scheme for a standard feedback system. The standard PI - controller will be considered and will be designed by inspection of the closed loop magnitude and phase at a selected range of frequencies. These values can be found from the systems closed loop bode plot. If a PI controller is implemented

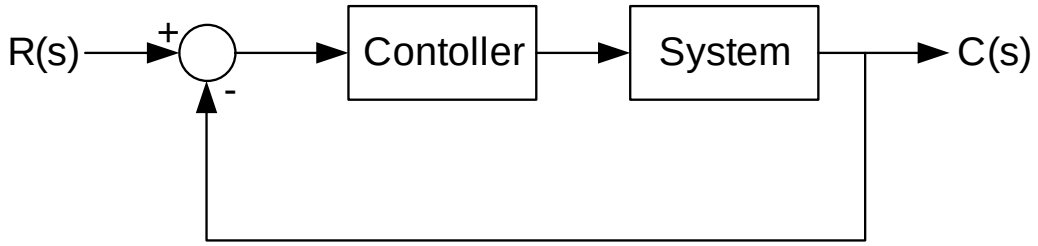

Figure 6.1: Scheme for feedback control

in a system of type 0 and is subjected to a step input, then the error signal will eventually converge to zero. The considered system is of type 0. The Laplace transform of a step input is $\frac{1}{s}$, this structure can also be found in the PI controller. This implies, in order to achieve zero error the structure of the input needs to be included in the controller. The reference signal to be tracked is a sinusoid. The Laplace transform of a sin() function is $\frac{A\omega}{\omega^2+s^2}$, and this structure is not part of the

PI controller. I.e. the system will always have a periodic error signal, but as the plots will show the steady state error is $\approx 0.12\%$ of the reference signal.
The transfer function for the PI controller is stated in eq. (6.1).

$$G_{PI}(s) = K\left(1 + \frac{1}{T_i s}\right) \tag{6.1}$$

There are no straight forward ways to do this. The way it is done here is first to try with $K = 1$, let T_i vary in a specified range and plot what the response is on the magnitude and phase. Next iteration will be with another K. The iterations will stop when the above criteria are reached. Fig. (6.2) shows how the different values vary as K and T_i change. Blue line is for $K = 1$, the purple one is for $K = 50$ and the others are for values in between. The plot shows that as long as

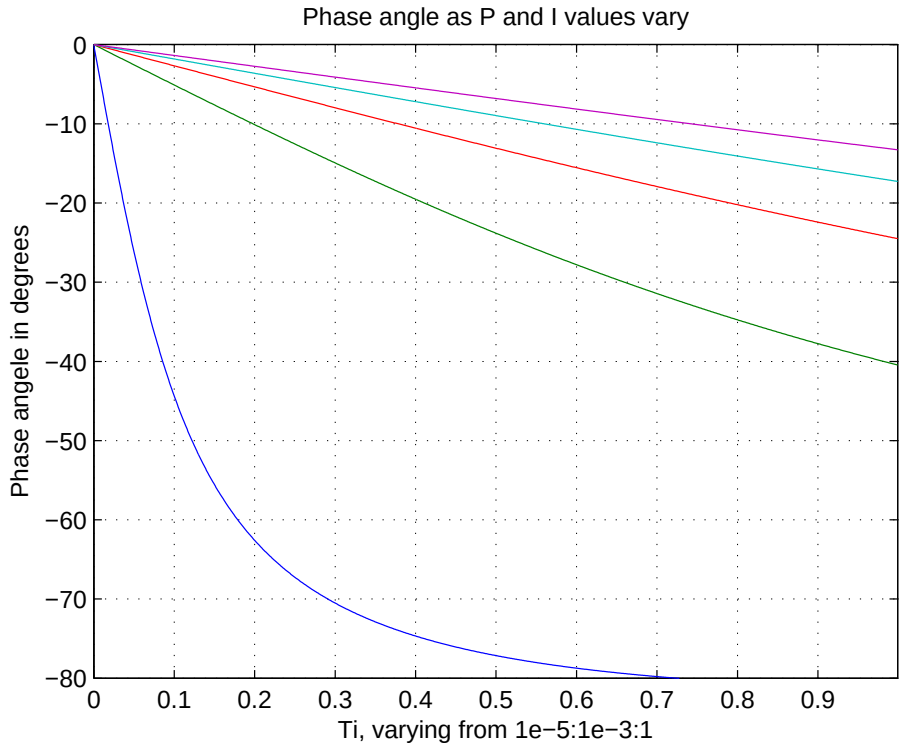

Figure 6.2: Phase angle as K and T_i vary

the T_i is small, the phase criteria is fulfilled. Choosing $K = 10$ and $T_i = 10^{-3}$, underneath follows a calculation to check what the phase and magnitude will be with these controller gains. $H(s)$ referees to closed loop transfer function.

$$|H(s)| = 1 = 0\,dB \tag{6.2}$$

$$\angle H(s) = -0.0563^{\circ} \tag{6.3}$$

Simulation with no disturbance

Here follows the simulation results from the above discoursed PI controller. Note that the offset for the linearized values are added. The reference signal is of the form:

$$r(t) = 0.01sin(0.05t) \tag{6.4}$$

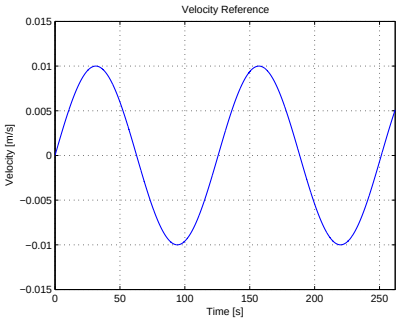

Figure 6.3: Reference Velocity

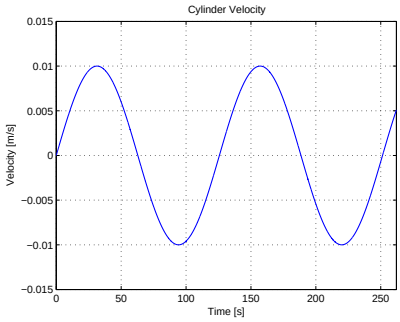

Figure 6.4: Velocity output

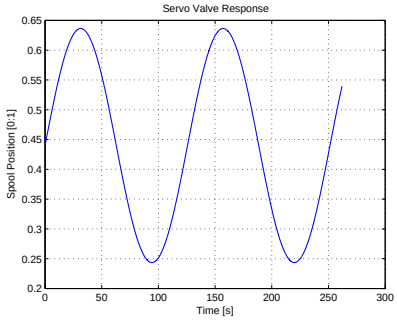

Figure 6.5: Servo valve position

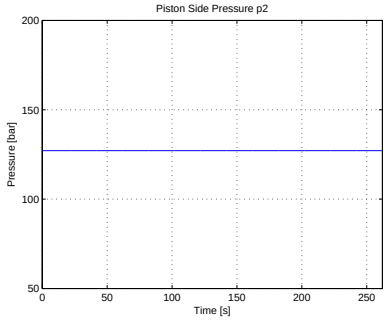

Figure 6.6: Piston side pressure

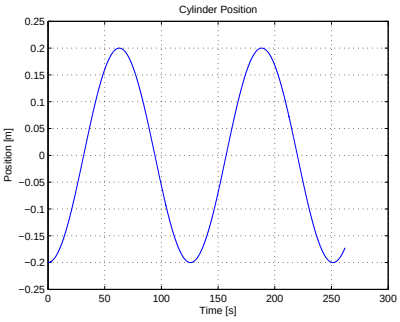

Figure 6.7: Cylinder position

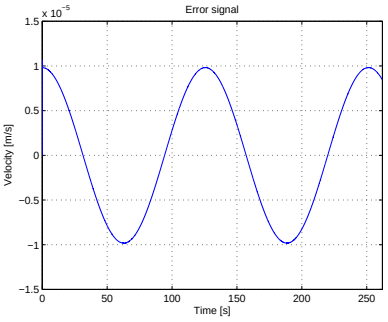

Figure 6.8: Error signal

Simulation with disturbance

The disturbance force implemented here is simplified in comparison to reality. The force is set to be negative when the velocity is positive, and vice versa. The force is set to to $\pm 15\ 000\,[N]$. There are some effects on the cylinder velocity due to the disturbance. The effect has its peaks when the force changes signs. The slope of the curve as it changes signs is infinitely steep, in reality this is not true. The servo valve shows the valve needing some rapid changes in position, it needs to change from $0.18 - 0.68$ in $0.15\,[s]$. From the step response plot of the servo valve, fig. (3.7), it is shown that the valve can reach full opening in $50\,[ms]$. i.e. the valve should handle this position change. Limits are included to the position integrator to prohibit the position to exceed lower limit 0 and upper limit 1.

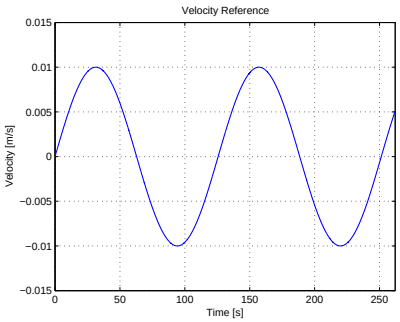

Figure 6.9: Reference Velocity

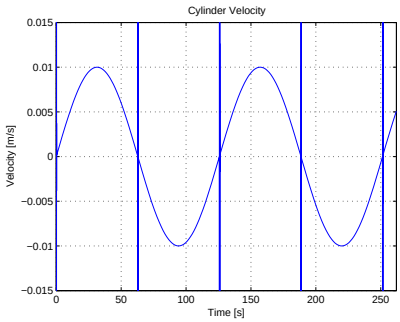

Figure 6.10: Velocity output

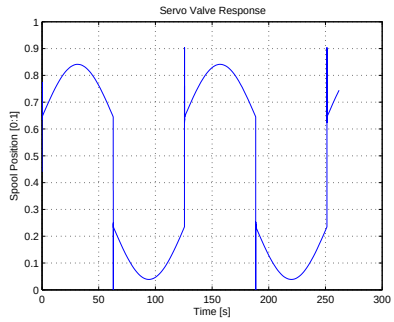

Figure 6.11: Servo valve position

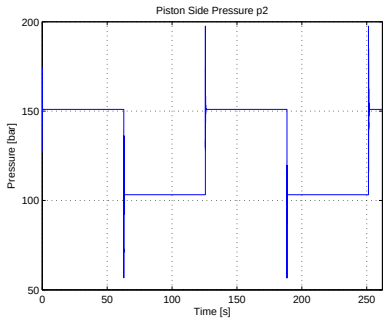

Figure 6.12: Piston side pressure

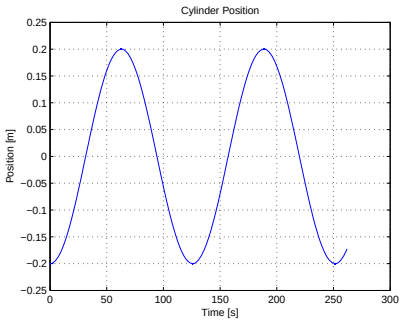

Figure 6.13: Cylinder position

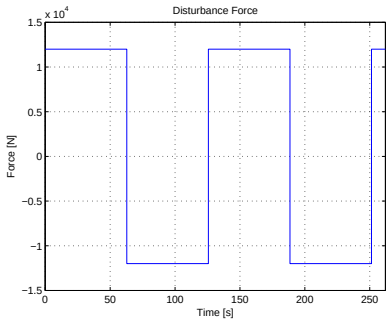

Figure 6.14: Disturbance force

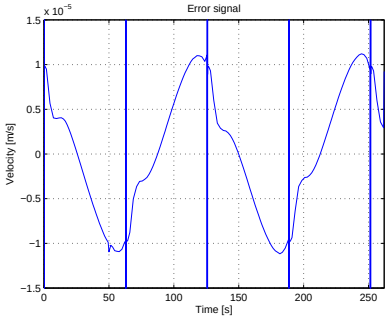

Figure 6.15: Error signal

6.1.2 Force Side

The plot show that the design criteria are achieved as long as the P-gain and I-gain are small.

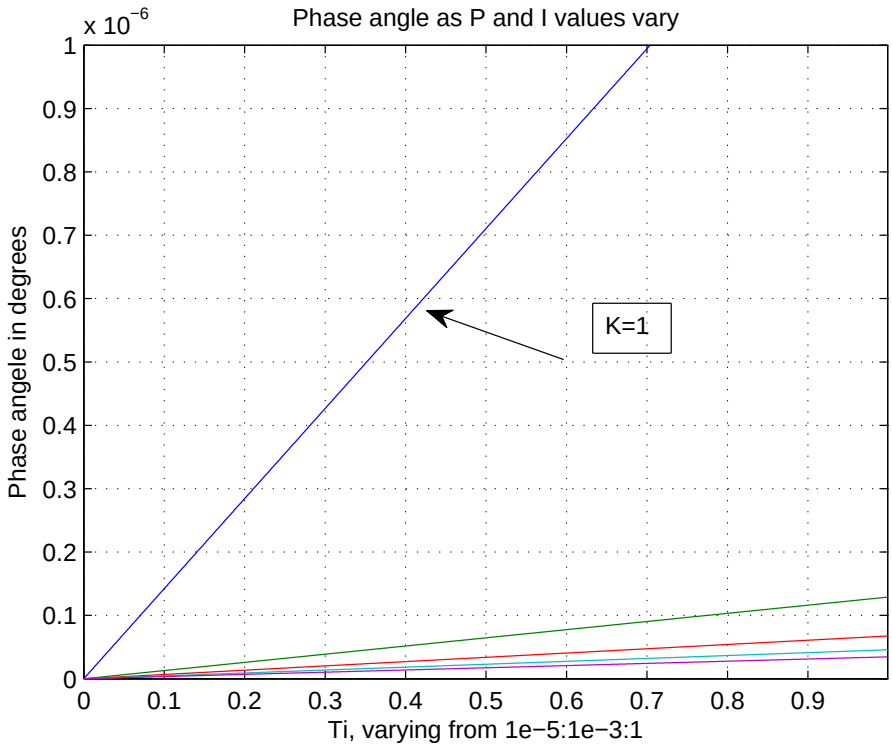

Figure 6.16: Phase angle as K and T_i vary

6.2 Tracking optimal control with integral action

If the requirements of the controller is expressed as a minimization or maximization of some performance index, then the controller is an optimal one. In this case it is desirable that the deviation between the reference signal and the output

is minimal, see fig. (6.17). This kind of controller is called Linear-Quadratic-Regulator (LQR). Some of the benefits the controller has are infinite gain margin and a phase margin of $60°$. This means the system is always stabile. A drawback of the controller is that it requires full state feedback. i.e. all the states needs to be measured and fed back. Integral action or integral control is introduced to the system by adding an extra state to the state variables, this extra state is the derivative of the tracking error. The tracking error is defined with the differential equation in eq. (6.5). For this method of integral action and the calculations of the controller gains, reference is made to [3] and [12]. The input signal given to the considered system in a sinusoid. The method used in this section obtains zero error signal only with constant reference signals. But as the plots will show, this error is $\approx 0.075\%$. Simulation with constant reference signal is shown in appendix B.

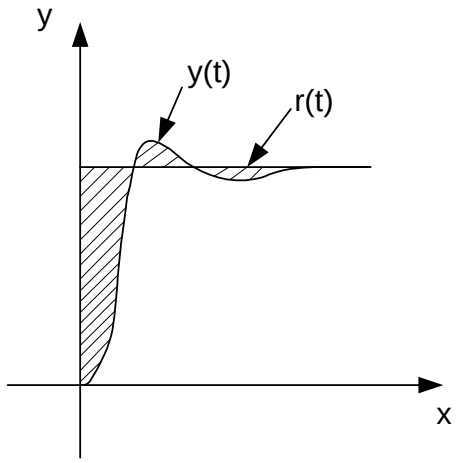

Figure 6.17: Typical transient response

$$\dot{w}(t) \;=\; r(t) - y(t) \;=\; r(t) - Cx(t) \tag{6.5}$$

New state vector:

$$\hat{x} \;=\; \begin{bmatrix} x \\ w \end{bmatrix} \tag{6.6}$$

When this new state is introduced some manipulations of the original state space system is required.

$$\dot{\hat{x}}(t) = \underbrace{\begin{bmatrix} A & 0 \\ -C & 0 \end{bmatrix}}_{\hat{A}} \hat{x} + \underbrace{\begin{bmatrix} B \\ 0 \end{bmatrix}}_{\hat{B}} u + \underbrace{\begin{bmatrix} 0 \\ r \end{bmatrix}}_{d} \tag{6.7}$$

$$y = \underbrace{\begin{bmatrix} C & 0 \end{bmatrix}}_{\hat{C}} \hat{x} \tag{6.8}$$

A suitable performance index would be:

$$\begin{aligned} J &= \frac{1}{2}\left(y\left(t_f\right) - r\left(t_f\right)\right)^T P_y \left(y\left(t_f\right) - r\left(t_f\right)\right) \\ &+ \frac{1}{2} w\left(t_f\right)^T P_w w\left(t_f\right) \\ &+ \frac{1}{2}\int_0^{t_f} \left((y-r)^T Q_y (y-r) + w^T Q_w w + u^T R u \right) dt \end{aligned} \tag{6.9}$$

Where $Q_y \geq 0,\ Q_w > 0,\ P_y \geq 0,\ R > 0$. If $t_f \longrightarrow \infty$ and the reference signal r is constant, this can be rewritten as:

$$J = \frac{1}{2}\int_0^{\infty} \left(\hat{x}^T Q \hat{x} + u^T R u \right) dt \tag{6.10}$$

Where Q is given by:

$$Q = \begin{bmatrix} C^T Q_y C & 0 \\ 0 & Q_w \end{bmatrix} \tag{6.11}$$

Q needs to be positive semidefinite, i.e. $\hat{x}^T X \hat{x} \geq 0$. R needs to be positive definite, i.e. $u^T R u > 0$. The speed of the system is dependent of the values of these weighting matrices. If $Q >> R$ the system will tend to respond fast, but the consequence is a high control signal. In the opposite case $R >> Q$ the control signal remains low and the system response is limited.

The optimal control law for the performance index in eq. (6.10):

$$\begin{aligned} u(t) &= \hat{K}(t)\,\hat{x}(t) + K_r r \\ \hat{K}(t) &= R^{-1}\hat{B}^T\hat{S}(t) \end{aligned} \tag{6.12}$$

$\hat{S}(t)$ is the solution to the matrix algebraic Riccati equation (MARE).

$$0 = \hat{Q} + \hat{A}^T\hat{S} + \hat{S}\hat{A} - \hat{S}\hat{B}R^{-1}\hat{B}^T\hat{S} \tag{6.13}$$

$\hat{K}$ contains the gains for both x and w and can be written as:

$$\hat{K} = \begin{bmatrix} K_x & K_w \end{bmatrix} \tag{6.14}$$

In order to find the gain for the input r some additional matrices needs to be found.

$$\begin{aligned} W &= R^{-1}\hat{B}^T\left[\left(\hat{A} - \hat{B}\hat{K}\right)^T\right]^{-1} \\ &= \begin{bmatrix} W_1 & W_2 \end{bmatrix} \end{aligned} \tag{6.15}$$

$$\begin{aligned} G &= R^{-1}\hat{B}^T\left[\left(\hat{A} - \hat{B}\hat{K}\right)^T\right]^{-1}\hat{S} \\ &= \begin{bmatrix} G_1 & G_2 \end{bmatrix} \end{aligned} \tag{6.16}$$

The gain K_r is then:

$$K_r = \left(G_2 - W_1 C^T Q_y\right) \tag{6.17}$$

With these gains calculated the optimal control law is as follows:

$$u = -K_x x - K_w w + K_r r \tag{6.18}$$

Fig. (6.18) shows the block diagram of the considered system.
The speed of the system is found from the location of the closed loop poles. The

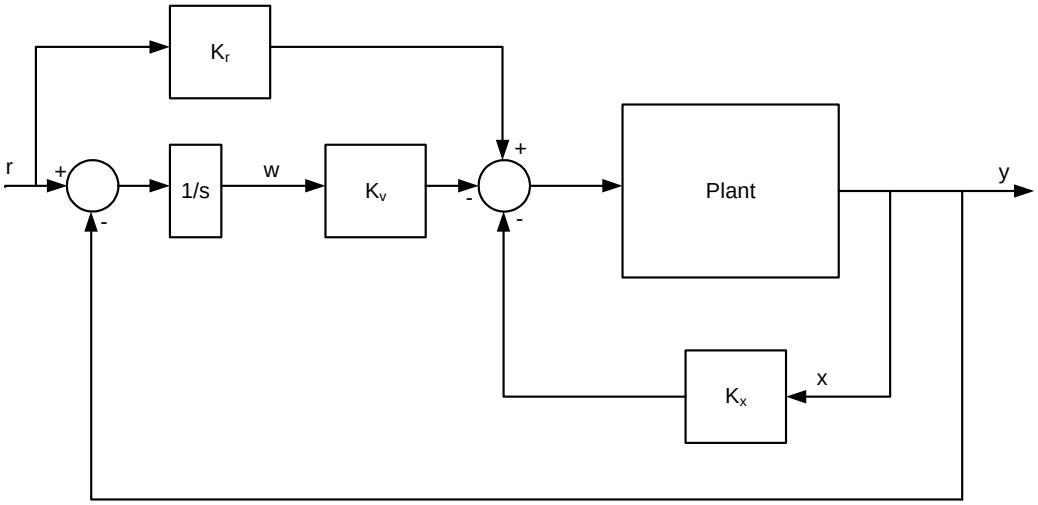

Figure 6.18: Linear quadratic tracking controller with integral action

closed loop system is stated in eq. (6.19)

$$\begin{aligned} \dot{x}(t) &= Ax(t) + B\left(K_x x(t) - K_w w(t) + K_r r\right) \\ &= Ax(t) + BK_x x(t) - BK_w w(t) + BK_r r \\ &= \left(A - BK_x\right) x(t) - BK_w w(t) + BK_r r \end{aligned} \tag{6.19}$$

The eigenvalues of the expression: $(A - BK_x)$ gives the location of the closed loop poles.

Simulation result

After implementing the above equations in matlab the following gains K_x, K_w, K_r are calculated.

$$
\begin{aligned}
u = & - \begin{bmatrix} -1.2724 \cdot 10^3 & -83335 & 64.7730 & 0.1228 \\ -25.4970 & 5.4752 \cdot 10^8 & 1.2050 & 2.1601 \cdot 10^4 \end{bmatrix} \begin{bmatrix} x_1 \\ x_2 \\ x_3 \\ x_4 \end{bmatrix} \\
& - \begin{bmatrix} -9.999 \cdot 10^4 & -9.2479 \cdot 10^6 \\ 9.2479 \cdot 10^6 & -9.9996 \cdot 10^4 \end{bmatrix} \begin{bmatrix} w_1 \\ w_2 \end{bmatrix} \\
& + \begin{bmatrix} 196.4280 & -8.2694 \cdot 10^4 \\ -1.8267 & 1 \end{bmatrix} \begin{bmatrix} r_1 \\ r_2 \end{bmatrix}
\end{aligned}
$$

When these gains are calculated and implemented in the Simulink model, the weighting matrices needs to be found. There are no straight forward way to do this other then trial and error. In this way the LQR controller design is an iterative process. Try with different combinations of Q and R and evaluate wether the result meet the design goals.
Chosen matrices are:

$$
Q = \begin{bmatrix} 10^{-2} & 0 & 0 & 0 & 0 & 0 \\ 0 & 10^{-2} & 0 & 0 & 0 & 0 \\ 0 & 0 & 0 & 0 & 0 & 0 \\ 0 & 0 & 0 & 0 & 0 & 0 \\ 0 & 0 & 0 & 0 & 10^{-2} & 0 \\ 0 & 0 & 0 & 0 & 0 & 10^{-2} \end{bmatrix}, \quad R = \begin{bmatrix} 10^4 & 0 \\ 0 & 10^4 \end{bmatrix} \tag{6.20}
$$

The closed loop poles is presented in tab. (6.1). The systems response is dependent of these poles. The system is only as fast as its slowest pole, i.e. its distance from the imaginary axis. The table shows a complex conjugate pole pair, its distance from the real axis indicate the damping of the system.

Closed loop poles	
1	$-1.4226 \cdot 10^2 + 1.9483 \cdot 10^3 i$
2	$-1.4226 \cdot 10^2 - 1.9483 \cdot 10^3 i$
2	-364.0675
4	-79.6342

Table 6.1: Location of the closed loop poles

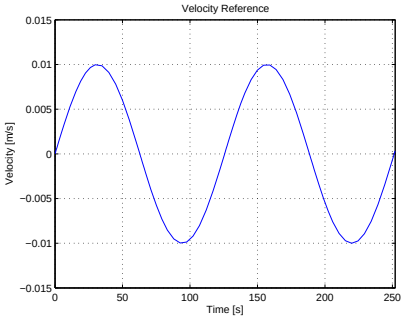

Figure 6.19: Reference Velocity

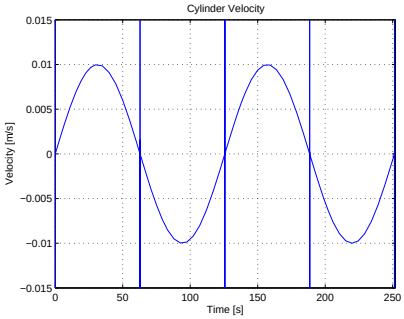

Figure 6.20: Velocity output

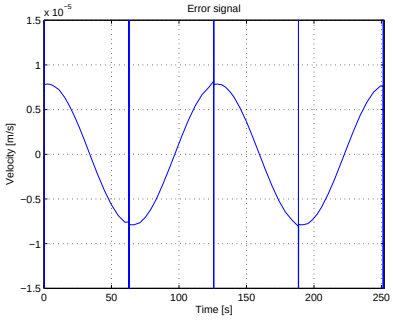

Figure 6.21: Error signal

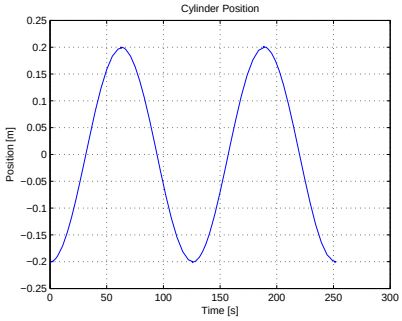

Figure 6.22: Cylinder position

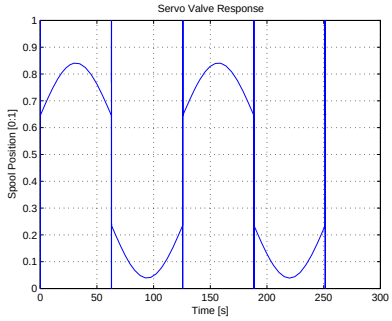

Figure 6.23: Servo valve position

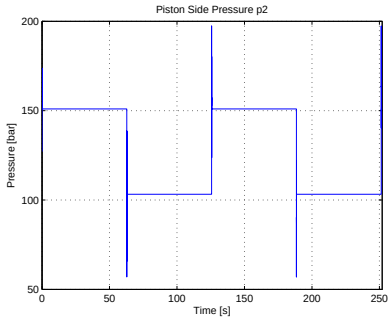

Figure 6.24: Piston side pressure

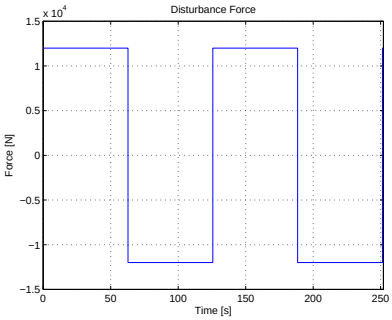

Figure 6.25: Disturbance force

Chapter 7

Experiments and Results

The result from the previous chapters shows that the model which is made in matlab/simulink is a good estimation of the test stand. The model only contain physical values, no tuning was needed for the comparison. This is judged by the comparison of the different sensor values and the corresponding plots from matlab/simulink. Only the velocity side is included in the report. The models are made in the same way, therefor it is assumed if the velocity is accurate, then the force side is accurate. Also in the force side cylinder some strange frictions occurred, and this is hard to imitate in matlab/simulink.
Controllers for both sides are made are made, and the closed loop bode plot are examined to reach the preset design goals.
The optimal control system works slightly better than the one designed from frequency domain. This is judged by the error signal.
There was no time to verify the controllers on the test rig, this will be left for further work.

Chapter 8

Conclusion and further work

8.1 Summary of Results

The goal of the project was to set up a test stand for friction emulation and compensation. During the project new challenges occurred rapidly, this led to less attention to some parts and more to others. Underneath is a followup list to the one stated in the introduction.

- The hydromechanical part of the test stand assembly finished according to schedule. The time that was devoted to the establishment of communication between actuators/sensors and laptop was a bit optimistic. The ability to programme the CompactRIO demands some fundamental knowledge about Labview, this takes time to gain.
- The considered system is nonlinear and the system shall be controlled by linear controllers. Due to this a linear model is made in matlab/simulink. The model is linearized about a constant velocity, by means of Taylor series expansion. The dynamic model was originally set out to be made in SimulationX, but due to some problems explained in the next section, sim-

ulation tool was changed. The upside when modeling in this way is that one gets more familiar with how the system works, the theoretical meaning of the algebraic and differential equations is easily lost when programming in SimulationX.

- The development of friction models is very limited
- Some literature review is done regarding the control strategies for heave motions. A short summary is presented of where heave motion compensation is a necessity and with which techniques this is accomplished. This was also a natural motivator to find out how this compensation problem would be addressed.
- The experimental testing of friction models and control strategies is not carried out to the extent of that was first set out to do. Also the part where the model was to de verified took up much more time than was expected.

8.2 Problems

- The initial plan was to make a nonlinear model in SimulationX and then convert this to state space or transfer function with a tool exciting in the software. This did not turn out as planned, for some reason it worked for a simplified model but gave some strange results for our system. But the chance of a human mistake along the way is not ruled out. As a consequence the differential and algebraic equations of the system was linearized and modeled in matlab/simulink.
- One of the MOOG servo amplifiers was suddenly broken. The problem was sufficiently solved by a self-made amplifier.

8.3 Further Work

- In order to implement the LQR with integral action, we might also need a Kalman filter to estimate some of the states. The system only have measuring for servo valve position, cylinder position and pressure. The LQR require feedback from all states, i.e. the time derivative of the measured position of the valve and the cylinder needs to be applied. This is not always a good practice. Especially when the original measurement contains noise, then the derivative of it will experience even more noise.

- It would also be desirable to eliminate the error in the control loop. Some work was started, but due to time limitations it was not finished. As explained in sec. (6.2) and showed in appendix B this tracking system and controller achieves zero error for constant reference signal. The idea was then to rewrite the tracking system in such a way that the reference signal is of constant value, but the system tracks a sinusoid curve. In [1] exosystem is discoursed, the input to this system is a constant value of frequency and the output is a sinusoid signal.

$$\dot{r} = \begin{bmatrix} 0 & \omega \\ -\omega & 0 \end{bmatrix} r \tag{8.1}$$

  If such a system was included in front of where the input signal enters the loop ,fig. (6.18). This could lead to solving the non zero error problem, but as mentioned was not finished. This also require the adding of another state.

- Include the model in the Labview program, in this way one would easily see how the model behaves in relation to the test stand.

- The linearization is only done for the case of zero velocity. When sufficient disturbance in influencing the system the piston side pressures will vary, this means the linearization might not hold. To which extent the linearization holds has not been tested.

- There was no time to test the controllers implemented in physical rigg.

Bibliography

[1] J. Abedor, K. Nagpal, P. Khargonekar, and K. Poolla, "Robust regulation in the presence of norm-bounded uncertainty," *IEEE Transactions on Automatic Control*, vol. 40, pp. 147–152, 1995.

[2] B. Armstrong-Hélouvry, P. Dupont, and C. Canudas De Wit, "A survey of models, analysis tools and compensation methods for the control of machines with friction," *Automatica*, vol. 30, pp. 1083–1138, 1994.

[3] V. Becerra, "Optimal control (course cy3h2), lecture 5: More LQ tracking plus LQG optimal control," 2008.

[4] K. Do, Z. Jiang, and J. Pan, "Universal controllers for stabilization and tracking underactuated ships," *Systems and Control Letters*, vol. 47, pp. 299–317, 2002.

[5] K. Do and J. Pan, "Nonlinear contgrol of an active heace compensation system," *Ocean Engineering*, vol. 35, pp. 558–571, 2008.

[6] T. Fossen and J. Strand, "Nonlinear passive weather optimal positioning control (wopc) for ships and rigs: experimental results," *Automatica*, vol. 37, pp. 701–715, 2001.

[7] M. Gimble, R. Patton, and D. Wise, *Optimal Control and Application Methods 1*. Wiley, 1980, ch. The design of dynamic positioning control systems using stochastic optimal control theory, pp. 167–202.

[8] M. Hansen and T. Andersen, "Hydraulic components and systems (course mas402) ,lecture notes," 2009.

[9] J. Haugan, *Formler of tabeller*. NKI Forlaget, 2007, ch. Rekker, p. 27.

[10] H. Hideki and Y. Sekikawa, "Modeling of dynamic behaviors of friction," *Mechatronics*, vol. 18, pp. 300–339, 2008.

[11] T. Johansen, T. Fossen, S. Sagatun, and F. Nielsen, "Wave synchronizing crane control during water entry in offshore moonpool operations–experimental results," *IEEE Jurnal of Oceanic Engeneering*, vol. 08, pp. 720–728, 2003.

[12] H. Karimi, "Control theory 2 (course mas501), lecture notes," 2009.

[13] U. Korde, "Active heave compensation on drill-ships in irregular waves," *Ocean Engineering*, vol. 25, pp. 541–561, 1998.

[14] L. Li and S. Lui, "Modeling and simulation of active-controlled heave compensation system of deep-sea mining based on dynamic vibration absorber," *International Conference on Mechatronics and Automation*, 2009.

[15] C. Messineo, F. Celani, and O. Egeland, "Crane feedback control in offshore moonpool operations," *Control Engineerig Practice*, vol. 16, pp. 356–364, 2008.

[16] J. Neupert, T. Mahl, H. Bertrand, O. Sawodny, and K. Schneider, "A heave compensation approach for offshore cranes," *American Control Conference*, 2008.

[17] N. Nise, *Control Systems Engineering*. John Wiley & Sons, INC., 2004.

[18] S. Sagatun, "Active control of underwater installation," *IEEE Transactions on Control Systems Technology*, vol. 10, pp. 743–748, 2002.

[19] A. Sorensen, "Structural issues in the design and operation of marine control systems," *Annual Reviews in Control*, vol. 29, pp. 165–171, 2005.

[20] R. Stribeck, "The key qualities of sliding and roller bearings,," *Zeitschrift des Vereines Deutscher Ingenieure*, vol. 46(38,39), pp. 13 421 348, 14 321 437, 1902.

Appendix A

SimulationX

Velocity reference:

$$v\left(t\right) \;=\; 0.01sin\left(\frac{0.05}{2\pi}t\right) \tag{A.1}$$

Reference force:

$$F_{dis} = \begin{cases} -1000 & x \leq 0 \\ +1000 & x \geq 0 \end{cases} \tag{A.2}$$

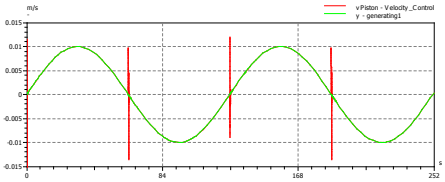

Figure A.1: Reference and output velocity

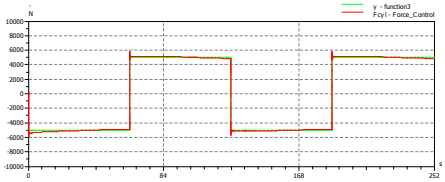

Figure A.2: Reference and output force

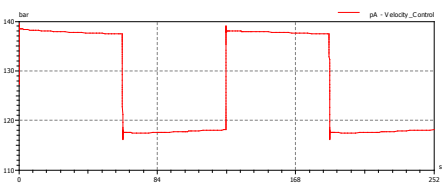

Figure A.3: Piston side pressure, force side

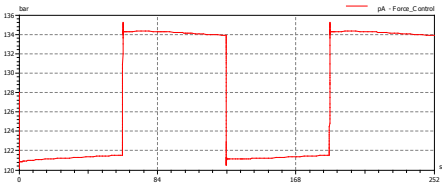

Figure A.4: Piston side pressure, velocity side

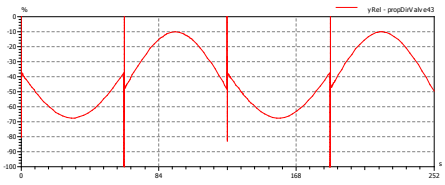

Figure A.5: Servo valve opening, velocity side

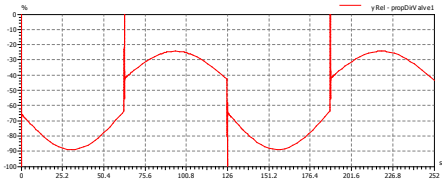

Figure A.6: Servo valve opening, force side

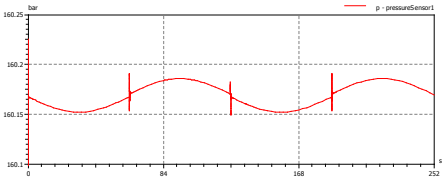

Figure A.7: System pressure

Appendix B

Optimal Control with Step Input

Simulation results for step input signal. The selected values for Q and R:

$$Q = \begin{bmatrix} 10^{-2} & 0 & 0 & 0 & 0 & 0 \\ 0 & 10^{-2} & 0 & 0 & 0 & 0 \\ 0 & 0 & 0 & 0 & 0 & 0 \\ 0 & 0 & 0 & 0 & 0 & 0 \\ 0 & 0 & 0 & 0 & 10^{-2} & 0 \\ 0 & 0 & 0 & 0 & 0 & 10^{-2} \end{bmatrix}, \quad R = \begin{bmatrix} 10^{6} & 0 \\ 0 & 10^{6} \end{bmatrix} \tag{B.1}$$

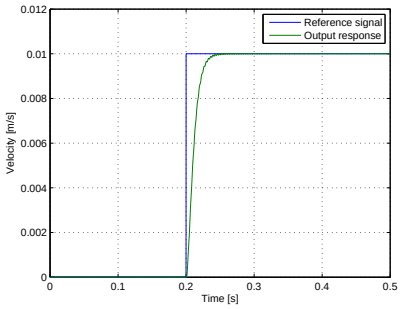

Figure B.1: Reference and output signal

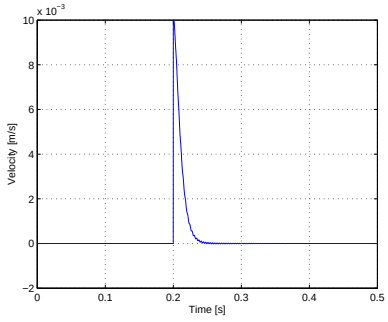

Figure B.2: Error signal

Appendix C

Measurements

not taken into account 0,007854 areal

p		q				velocity	friction
0,1	141	14100000	0,25	4,16667E-06	3,02282E-08	0,082893	10524,34
0,2	140	14000000	1,7	2,83333E-05	1,00173E-07	0,563674	9738,937
0,3	140,5	14050000	2,7	0,000045	1,07417E-07	0,895247	10131,64
0,4	139	13900000	4,1	6,83333E-05	1,17886E-07	1,359448	8953,539
0,5	139	13900000	5,5	9,16667E-05	1,26512E-07	1,82365	8953,539
0,6	139	13900000	7	0,000116667	1,34179E-07	2,32101	8953,539
0,7	138	13800000	8,5	0,000141667	1,36445E-07	2,818369	8168,141
0,8	139	13900000	10,2	0,00017	1,46639E-07	3,382043	8953,539
0,9	139	13900000	11,5	0,000191667	1,46958E-07	3,813087	8953,539
1	139	13900000	13	0,000216667	1,49514E-07	4,310446	8953,539

snitt	1,29525E-07
0,4 - 1,0	1,36876E-07

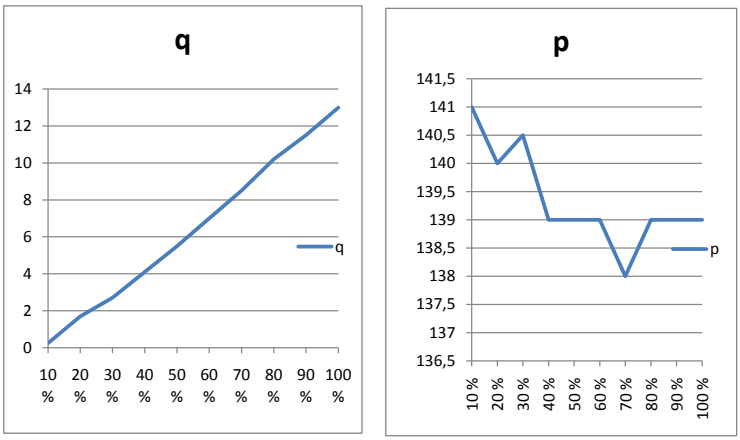

Figure C.1: Servo valve constant, velocity side

not taken into account 0,007854 areal

	p		q			velocity	friction
0,1	141	14100000	0,25	4,16667E-06	3,02282E-08	0,082893	10524,34
0,2	140	14000000	1,7	2,83333E-05	1,00173E-07	0,563674	9738,937
0,3	140,5	14050000	2,7	0,000045	1,07417E-07	0,895247	10131,64
0,4	139	13900000	4,1	6,83333E-05	1,17886E-07	1,359448	8953,539
0,5	139	13900000	5,5	9,16667E-05	1,26512E-07	1,82365	8953,539
0,6	139	13900000	7	0,000116667	1,34179E-07	2,32101	8953,539
0,7	138	13800000	8,5	0,000141667	1,36445E-07	2,818369	8168,141
0,8	139	13900000	10,2	0,00017	1,46639E-07	3,382043	8953,539
0,9	139	13900000	11,5	0,000191667	1,46958E-07	3,813087	8953,539
1	139	13900000	13	0,000216667	1,49514E-07	4,310446	8953,539

snitt	1,29525E-07
0,4 - 1,0	1,36876E-07

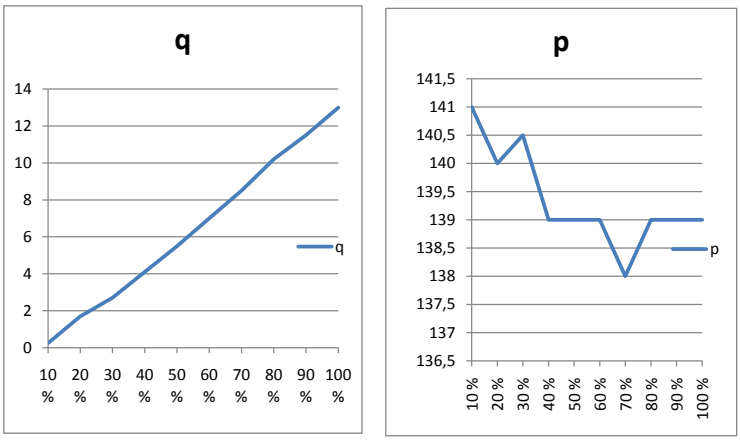

Figure C.2: Serve valve constant, force side

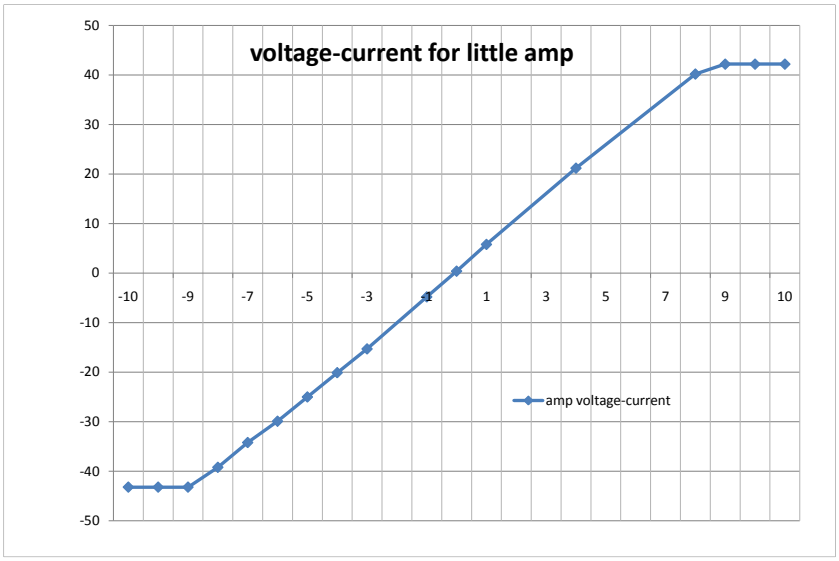

Figure C.3: Voltage-current characteristics for self made amplifier

oil temperature rise water cooled

23:xx	Δt	temp	Δtemp
12	0	24	0
19	7	24,5	0,5
24	12	40,2	16,2
33	21	44	20
37	25	44,8	20,8
51	39	46,9	22,9
54	42	47,3	23,3

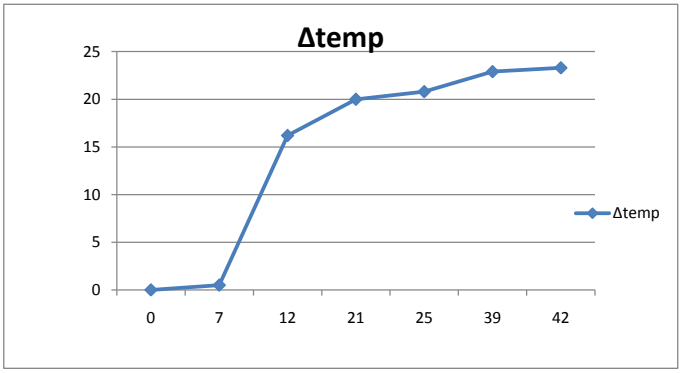

Figure C.4: Oil temperature change during operation

Appendix D

Test stand

Specification data for the two cylinders:

1 CDT3MS2/80/36/500Z10/B1CHDTWW

2 CDT3MS2100/45/600Z10/B1CHUTWW

MATERIALS

BODY	OT 58 - UNI 5705 NICKEL PLATED
NEEDLE	X 10 CR NI S 1809 - UNI 6900
O R	NITRILE
ANTIEXTRUSION RING	PTFE
KNOB	GD AL SI 12 - UNI 5706
SPRING	ABS
BALL	AISI 302
BALL GUIDE	UNI 100 C 6
GUIDA SFERA	NYLON 66 + CARBON FIBER

EXAMPLE FOR ORDERING

			ACCESSORIES ON REQUEST		
	CODE	TYPE	PANEL RING NUT	VITON SEAL	KNOB ABS
OTTONE	FT 1251/5-01	38	G	V	MP

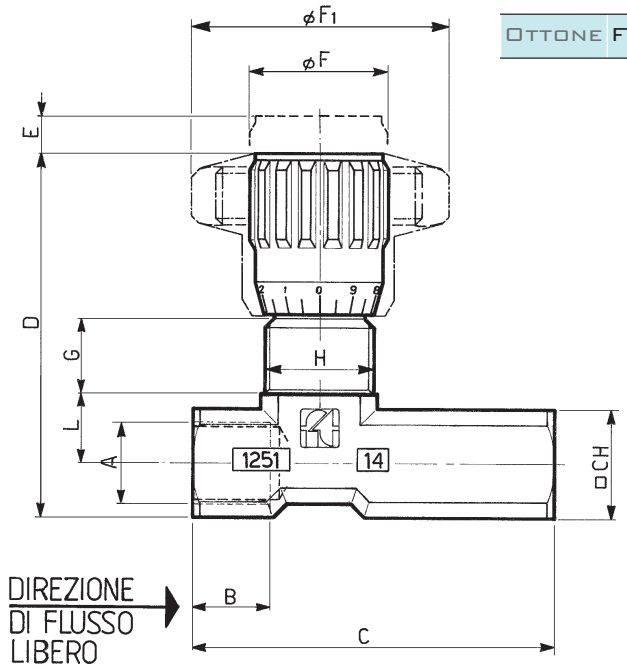

DIMENSIONS

TYPE	A UNI 338	B	C	D	E	ØF	ØF1	G	H	L	□CH	WEIGHT KG
14	1/4"G	12	56	57	4,5	22	40	11	M17x1	11,5	18	0,138
38	3/8"G	13	64,5	69	7	27	50	12,5	M20x1	15	22	0,259
12	1/2"G	16	87	82	10	33	70	13	M25x1,5	19	27	0,499
34	3/4"G	20	115	100	12	38	80	15	M30x1,5	22	34	0,975

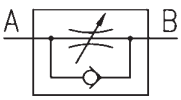

SINGLE-ACTING CONTROL VALVES FEMALE-FEMALE IN LINE

They allow regulation of flow in one direction and full free flow in opposite direction
thanks to the single-acting unit of ball type with guide cage they are equipped with.
As an alternative to FT 257/5 (suitable up to 400 bar) where the working pressure does not exceed 210 bar and where ferrous materials cannot be used.
They have the same characteristics as the FT 257 series:

- accurate flow regulation;
- efficient metallic sealing;
- simple setting of flow rates;
- secure against accidental needle withdrawal;
- secure needle position with locking screw inserted in the knob;
- provision for panel mounting, for which special lock nut (G) is supplied on request.

For use with pressure up to 210 bar

On request

- Viton (V) seals
- NPT threads
- ABS (mp)Knob
- Complete with lock nut (G)

FT 251/5-01

TECHNICAL DATA

Type	Flow sq mm²	Max working pressure bar	Working temperature °C	Filtration grade µm
14	12,57	210	-20°/+100°	25
38	19,64	210	-20°/+100°	25
12	50,27	210	-20°/+100°	25
34	78,54	210	-20°/+100°	25

FT 1251/5-01-14

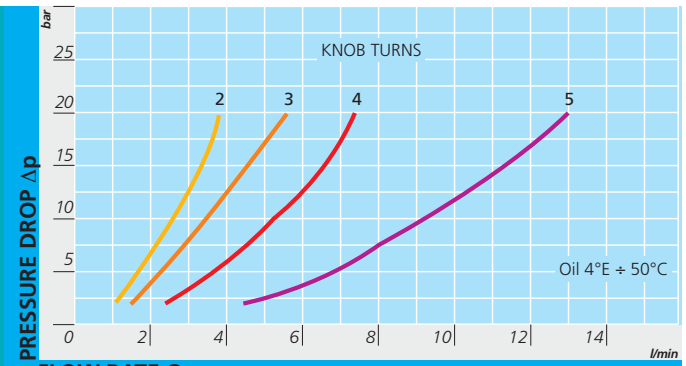

FT 1251/5-01-38

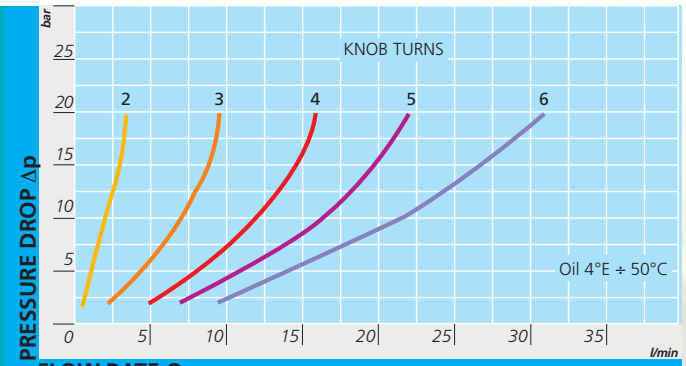

FT 1251/5-01-12

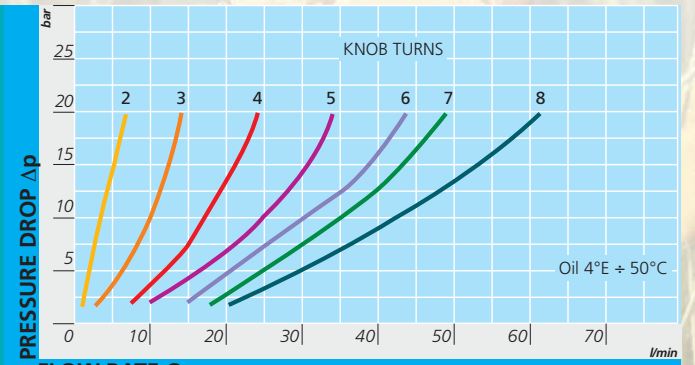

FLOW RATE CURVES

FT 1251/5-01 - 34

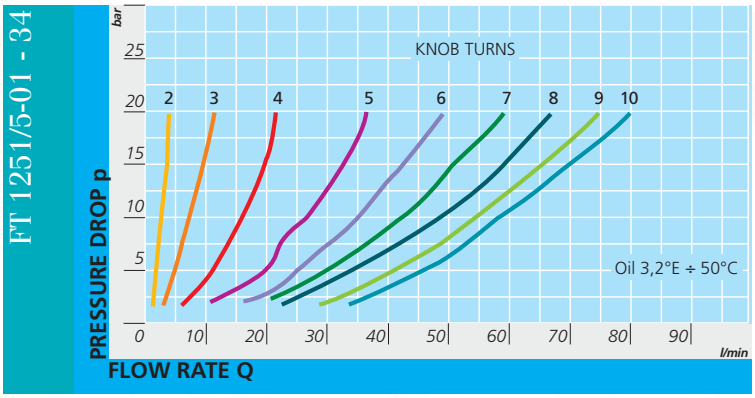

FT 1251/5-01

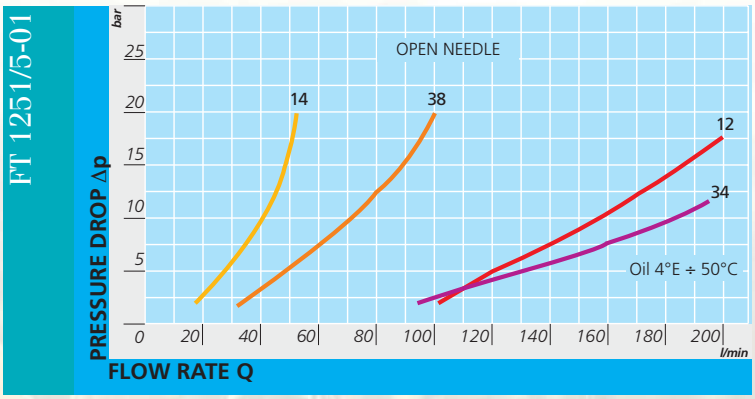

FT 1250

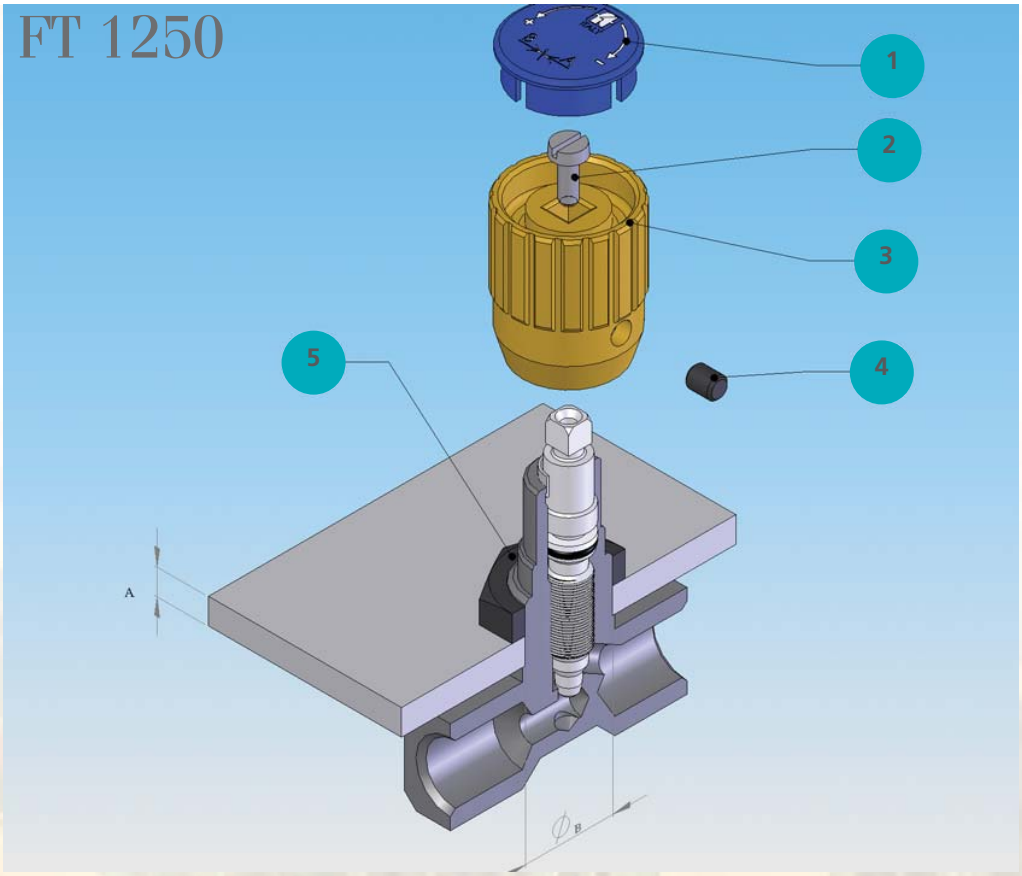

ASSEMBLY INSTRUCTION

1°	Loosen screw pressure dowel (4)
2°	Remove plug (1)
3°	Remove screw (2)
4°	Pull off knob (3)
5°	Insert ring nut (5), on request it is supplied with the valve
(A)	Max. Thickness
(B)	Panel hole Ø

Type valve	Thickness panel A max	Panel hole Ø B
1 8	5	16
1 4	5	18
3 8	5	21
1 2	6	26
3 4	6	31

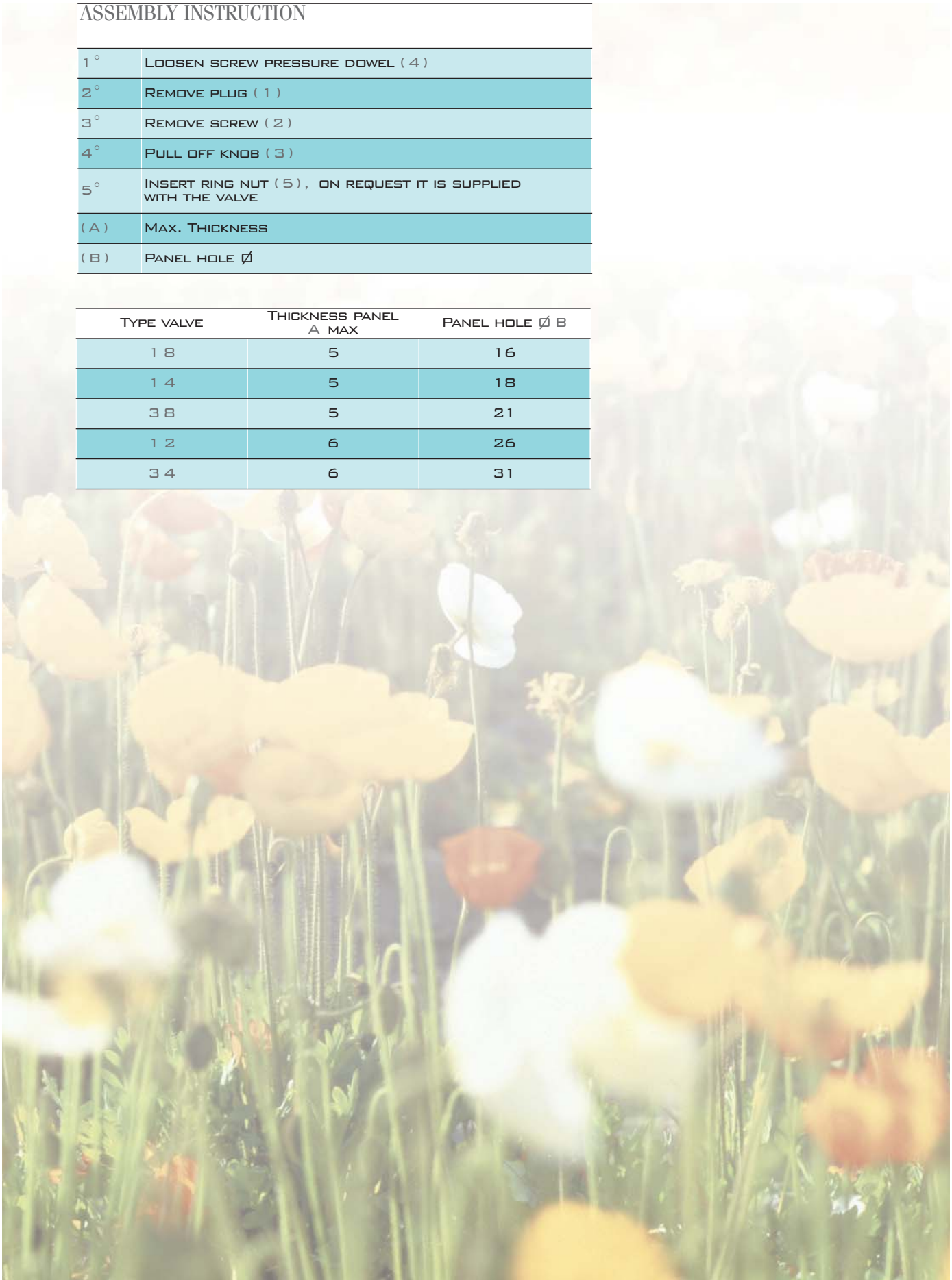

0/4...20 mA Output
Ranges: 0-2 to 0-50 inches
Compact Size • OEM Applications

PT1MA

CE

Specification Summary:

GENERAL

Full Stroke Range Options ..... 0-2 to 0-50 inches
Output Signal Options..... 4...20 mA (2-wire) and 0...20 mA (3-wire)
Accuracy..... ± 0.28% to ±0.15% full stroke *see ordering information*
Repeatability..... ± 0.05% full stroke
Resolution ..... essentially infinite
Measuring Cable ..... .019-in. dia. nylon-coated stainless steel
Enclosure Material..... glass-filled polycarbonate and black anodized aluminum
Sensor ..... plastic-hybrid precision potentiometer
Potentiometer Cycle Life ..... *see ordering information*
Maximum Retraction Acceleration..... *see ordering information*
Weight..... 1 lb. max.

ELECTRICAL

Input Voltage ..... *see ordering information*
Input Current..... 20 mA max.
Maximum Loop Resistance (Load) ..... (loop supply voltage - 8)/0.020
Circuit Protection ..... 38 mA max.
Impedance..... 100M ohms@100 VDC, min.
Output Signal Adjustment
Zero Adjustment..... from factory set zero to 50% of full stroke range
Span Adjustment..... to 50% of factory set span
Thermal Effects
Zero ..... 0.01% f.s./°F, max.
Span..... 0.01% f.s./°F, max.

ENVIRONMENTAL

Enclosure ..... NEMA 4, IP 65
Operating Temperature ..... 0° to 200°F (-17° to 90°C)
Vibration..... up to 10 G's to 2000 Hz maximum

EMC COMPLIANCE PER DIRECTIVE 89/336/EEC

Emission/Immunity EN50081-2/EN50082-2

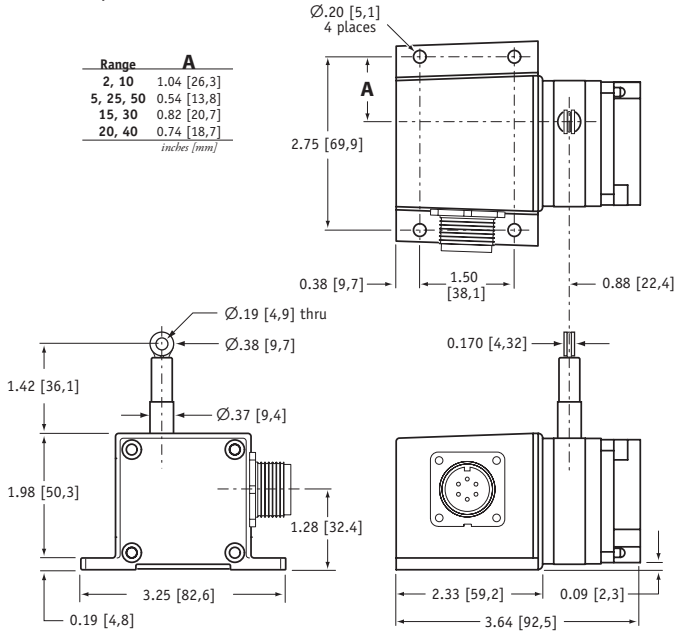

dimensions are in inches [mm], tolerances are 0.03 inches [0,8 mm]

The PT1MA adds 4...20 mA position feedback signal to Celesco's compact line of cable-extension transducers. The PT1MA is available with full stroke ranges from as little as 2 inches on up to 50 inches with adjustable zero and span settings to precisely match the full scale output to your exact measurement range.

The PT1MA offers several options including forward and reverse 0...20 and 4...20 mA output signals, alternate measuring cable exits and a couple different electrical connection options.

Output Signal

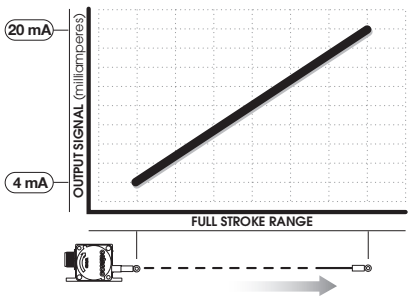

celesco
celesco.com • info@celesco.com

Celesco Transducer Products, Inc.
20630 Plummer Street • Chatsworth, CA 91311
tel: 800.423.5483 • +1.818.701.2750 • fax: +1.818.701.2799

Ordering Information:

Model Number:

PT1MA - ____ - ____ - ____ - ____ - ____
order code: Ⓡ Ⓐ Ⓑ Ⓒ Ⓓ

Sample Model Number:

PT1MA - 30 - UP - 420E - MC4 - SG

Ⓡ	range:	30 inches
Ⓐ	measuring cable exit:	up
Ⓑ	output signal:	4...20mA
Ⓒ	electrical connection:	4-pin micro connector
Ⓓ	cable guide:	spring-loaded guide

Full Stroke Range:

Ⓡ *order code:*	2	5	10	15	20	25	30	40	50
full stroke range, min:	2 in.	5 in.	10 in.	15 in.	20 in.	25 in.	30 in.	40 in.	50 in.
accuracy (% of f.s.):	0.28%		0.18%				0.15%		
potentiometer cycle life:	2,500,000 cycles		500,000 cycles				250,000 cycles		
cable tension (20%):	12 oz.	5 oz.	12 oz.	9 oz.	6 oz.	5 oz.	9 oz.	6 oz.	5 oz.
maximum cable acceleration:	11 G's	3 G's	11 G's	5 G's	4 G's	3 G's	5 G's	4 G's	3 G's

Cable Exit:

Ⓐ *order code:*	UP	DN	FR	BK
direction:	up	down	front	back

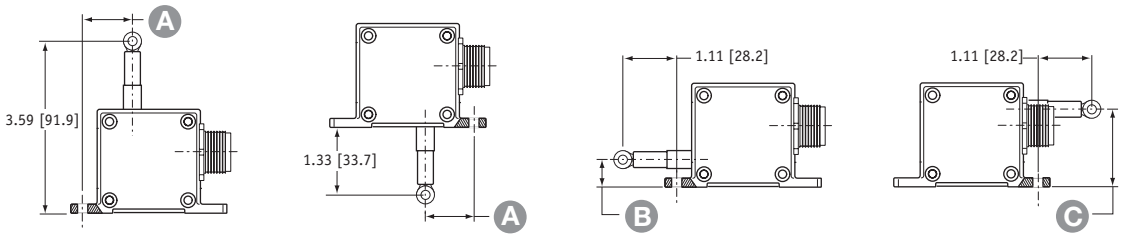

measurement range —	2	5	10	15	20	25	30	40	50
Ⓐ	1.04 in. 26,3 mm	0.54 in. 13,8 mm	1.04 in. 26,3 mm	0.82 in. 20,7 mm	0.74 in. 18,7 mm	0.54 in. 13,8 mm	0.82 in. 20,7 mm	0.74 in. 18,7 mm	0.54 in. 13,8 mm
Ⓑ	0.75 in. 19,1 mm	0.29 in. 6,1 mm	0.75 in. 19,1 mm	0.53 in. 13,5 mm	0.45 in. 11,5 mm	0.29 in. 6,1 mm	0.53 in. 13,5 mm	0.45 in. 11,5 mm	0.29 in. 6,1 mm
Ⓒ	1.43 in. 36,3 mm	1.89 in. 48,0 mm	1.43 in. 36,3 mm	1.65 in. 41,9 mm	1.73 in. 43,7 mm	1.89 in. 48,0 mm	1.65 in. 41,9 mm	1.73 in. 43,7 mm	1.89 in. 48,0 mm

Output Signals:

Ⓑ *order code:*	420E	420R	020E	020R
output signal options:	4...20 mA	20...4 mA	0...20 mA	20...0 mA
sensitivity:	16 mA/full stroke ±0.25%		20 mA/full stroke ±0.25%	
wiring configuration:	2 – wire		3 – wire	
input voltage:	8 – 40 vdc		14 – 40 vdc	

example:

ordercode = **420E** = 4...20 mA

4 mA =

20 mA =

Ordering Information (cont.)

Electrical Connection:

order code: **C**

MC4

4-pin micro-connector
with 12 ft [3.5 M] cordset

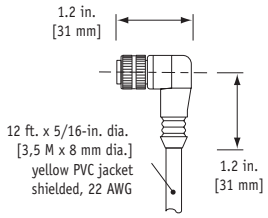

4-pin mating plug and cordset:

contact view

pin	color code	2-wire	3-wire
1	RED-BLK TR.	8...40 vdc	14...40 vdc
2	RED-WHT TR.	4...20 mA	0...20 mA
3	RED	-	common
4	GREEN	-	-

M6

6-pin plastic connector
with mating plug

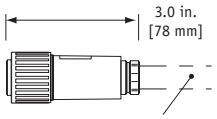

.30 – .39 in. [8 – 10 mm] cable dia.
16 AWG max conductor size
connector: MS3102E-14S-6P
mating plug: MS3106E-14S-6S

6-pin mating plug:

contact view

pin	2-wire	3-wire
A	8...40 vdc	14...40 vdc
B	4...20 mA	common
C	-	0...20 mA
D	-	-

C25

25-ft. instrumentation cable
24 AWG, shielded

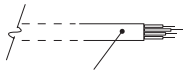

25 ft. x 0.2-in. dia.
[7,5 M x 5 mm dia.]
24 AWG, shielded

25-ft. cable:

color code	2-wire	3-wire
RED	8...40 vdc	14...40 vdc
BLACK	4...20 mA	common
WHITE	-	-
GREEN	-	0...20 mA

Cable Guide:

order code: **D**

blank

standard cable guide

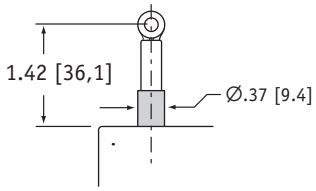

SG

spring-loaded guide

cable-guide cushions impact from accidental free release

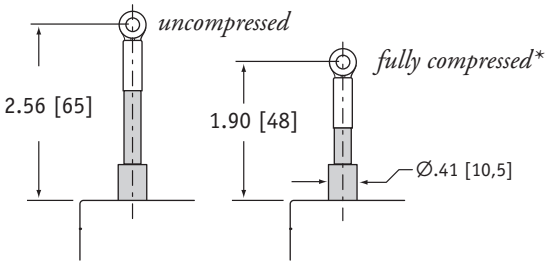

note: start of full stroke range begins at **full compression point*

Output Signal Selection:

The output signal direction can be reversed at any time by simply changing the dip-switch settings found on the internal signal board. After the settings have been changed, adjustment of the Zero and Span trimpots will be required to precisely match signal values to the beginning and end points of the stroke.

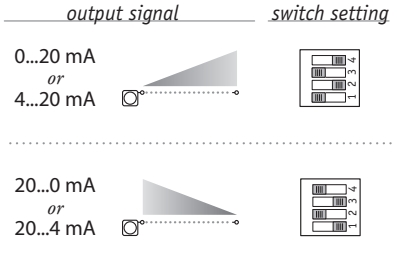

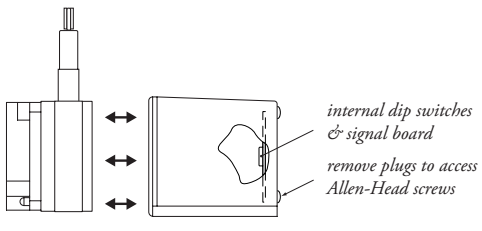

to gain access to the signal board, remove the two Allen-Head Screws and remove rear cover.

version: **4.1** last updated: **May 19, 2009**

TML STRAIN GAUGE TEST DATA

GAUGE TYPE	: FLA-10-11	TESTED ON	: SS 400
LOT NO.	: A515811	COEFFICIENT OF THERMAL EXPANSION	: 11.8 $\times 10^{-6}$/℃
GAUGE FACTOR	: 2.09 ±1%	TEMPERATURE COEFFICIENT OF G.F.	: +0.1±0.05 %/10℃
ADHESIVE	: P-2	DATA NO.	: A0588

THERMAL OUTPUT (ε app : APPARENT STRAIN)

$\varepsilon app = -2.97\times10^{1}+2.73\times T^{1}-7.23\times10^{-2}\times T^{2}+5.30\times10^{-4}\times T^{3}-1.40\times10^{-6}\times T^{4}$ (μm/m)

TOLERANCE : ±0.85 [(μm/m)/℃] , T : TEMPERATURE

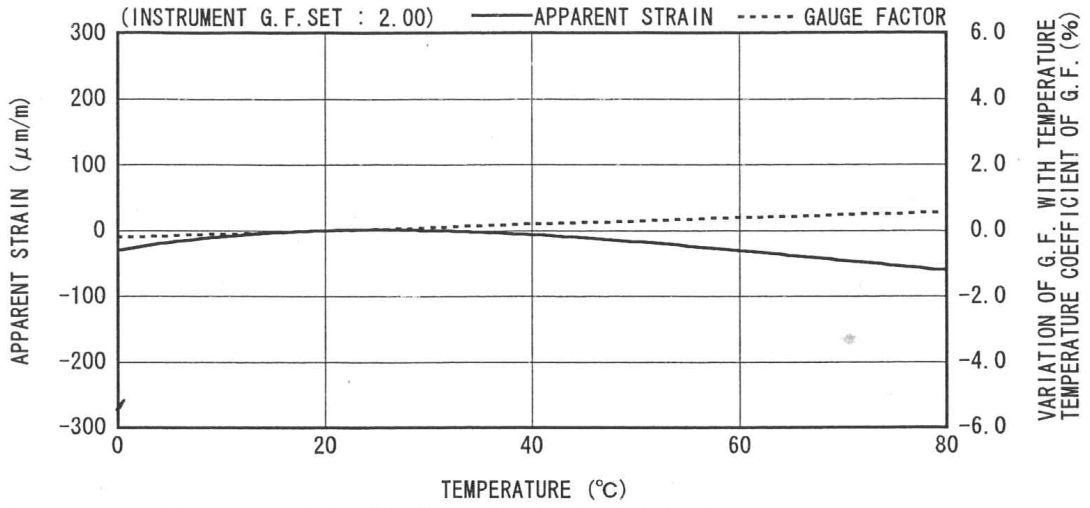

ひずみゲージ取扱いの注意事項

- ●上記の特性データは、リード線の取付けによる影響を含んでおりません。裏面記載のリード線の測定値への影響に従って補正してください。
- ●ゲージの使用温度は、接着剤の耐熱温度などにより変わります。
- ●絶縁抵抗などの点検は、印加電圧を５０Ｖ以下にしてください。
- ●ゲージリード線に無理な力を加えないでください。
- ●ゲージ裏面に接着剤を塗布して接着してください。
- ●ひずみゲージの裏面は脱脂洗浄してありますので、汚さないように取扱いしてください。
- ●ゲージの包装を開封後は、乾燥した場所で保管してください。
- ●ご使用に際してご不明な点などがございましたら、当社までお問い合わせください。

CAUTIONS ON HANDLING STRAIN GAUGES

- ● The above characteristic data do not include influence due to lead wires. Correct the data in accordance with the influence of lead wires on measured values described overleaf.
- ● The service temperature of strain gauge depends on the operating temperature of adhesive, etc.
- ● Check of insulation resistance, etc. should be made at a voltage of less than 50V.
- ● Do not apply an excessive force to the gauge leads.
- ● Apply an adhesive to the back of a strain gauge and stick the gauge to a specimen.
- ● As the back of strain gauge has been degreased and washed, do not contaminate it.
- ● After unpacking, store strain gauges in a dry place.
- ● If you have any questions on strain gauges or installation, contact TML or your local agent.

Made in Japan

TML 株式會社 東京測器研究所

〒 140-8560 東京都品川区南大井 6 - 8 - 2
TEL 03 - 3763 - 5611
FAX 03 - 3763 - 6128

Tokyo Sokki Kenkyujo Co., Ltd.

8 - 2, Minami - Ohi 6 - Chome
Shinagawa - ku, Tokyo 140-8560

TMLひずみゲージの取扱い方法

基本的な接着手順

1. **接着剤の選択** — 使用する条件に合った、ひずみゲージ用の接着剤を選びます。
2. **表面処理** — 被接着面のさび・塗料などを除去し、120～180番(ｱﾙﾐﾆｳﾑ:240～320番)のサンドペーパで軽く磨きアセトンなどで清浄して、ゲージ接着位置をけがいてください。
3. **ゲージ接着** — 接着剤の取扱説明書を参照してください。
4. **キュアリング** — 接着剤の取扱説明書を参照してください。
5. **点検** — ひずみゲージのゲージ抵抗値・絶縁抵抗値の点検を行ってください。
6. **結線** — リード線はゲージ端子を使用して、はんだ付けで接続してください。

・必要に応じて防湿処理を施してください。

リード線の測定値への影響

●リード線の温度変化による影響。
（３線式結線法では、温度影響はありません。）

$$\varepsilon l = \frac{r \cdot L \cdot \alpha \cdot \Delta T}{K\,(R + r \cdot L)} \qquad <式１>$$

εl ＝リード線の熱出力
r ＝リード線１m当たりの往復の抵抗値（Ω／m）
L ＝リード線の長さ（m）
α ＝リード線の抵抗温度係数
（銅線＝3.9×10^{-3}／℃）
ΔT ＝温度変化量
K ＝ゲージ率
R ＝ゲージ抵抗

●リード線の結線によるゲージ率の補正。
・２線式の場合

$$Ko = \frac{R}{R + r \cdot L} \cdot K \qquad <式２>$$

・３線式の場合

$$Ko = \frac{R}{R + \dfrac{r \cdot L}{2}} \cdot K \qquad <式３>$$

Ko＝補正したゲージ率

HANDLING METHOD OF TML STRAIN GAUGES

Basic Bonding Procedures

1. **Select adhesive** — Select an adhesive most suitable for test conditions.
2. **Surface treatment** — Remove grease, rust, paint, etc. from the bonding surface of a specimen, lightly polish with an abrasive paper of #120 ～ 180 (#240 ～ 320 for aluminium), wipe with acetone, etc. and mark gauge installation position.
3. **Gauge installation** — Refer to the operation manual of adhesive.
4. **Adhesive curing** — Refer to the operation manual of adhesive.
5. **Gauge installation check** — Check gauge resistance and insulation resistance.
6. **Lead wire attachment** — Solder lead wires to the strain gauges through connecting terminals.

· If necessary, apply waterproof coating.

Influence of Lead Wires on Measured Values

● **Influence of temperature variation of lead wires (3-wire system is independent of temperature.)**

$$\varepsilon l = \frac{r \cdot L \cdot \alpha \cdot \Delta T}{K\,(R + r \cdot L)} \qquad <Equation1>$$

where εl = *thermal output of lead wires*
r = *total resistance per meter of lead wires (Ω /m)*
L = *length of lead wires (m)*
α = *temperature coefficient of resistance of lead wires (copper wire = 3.9×10^{-3} / ℃)*
ΔT = *temperature variation*
K = *gauge factor*
R = *gauge resistance*

● **Gauge Factor Correction due to Lead Wire Attachment**

· **In case of 2-wire system**

$$Ko = \frac{R}{R + r \cdot L} \cdot K \qquad <Equation2>$$

· **In case of 3-wire system**

$$Ko = \frac{R}{R + \dfrac{r \cdot L}{2}} \cdot K \qquad <Equation3>$$

where Ko = *corrected gauge factor*

リード線１m当たりの往復の抵抗値
Total Resistance per Meter of Lead Wires

構成（心数／直径） Lead wires(number of cores / diameter)	ポリイミド線 polyimide	ポリイミド線 polyimide	7/0.12	10/0.12	12/0.18	20/0.18
リード線の直径または断面積 Diameter or cross sectional area of lead wires	ϕ 0.14mm	ϕ 0.18mm	0.08 mm^2	0.11 mm^2	0.3 mm^2	0.5 mm^2
1m 当たりの往復の抵抗値 Total resistance per meter	2.5 Ω/m	1.5 Ω/m	0.44 Ω/m	0.32 Ω/m	0.12 Ω/m	0.07 Ω/m

MOOG

P-I Servoamplifier
G122-824-002

Application Notes

1 Scope

These Application Notes are a guide to applying the G122-824-002 P-I Servoamplifier. The following is a summary of the process to which these Application Notes pertain:

- Determine the closed loop structure for your application.
- Select the G122-824-002 for your application. Refer also to data sheet G122-824.
- Use these Application Notes to determine your system configuration.
- Draw your wiring diagram.
- Install and commission your system.

Aspects, such as hydraulic design, actuator selection, feedback transducer selection, performance estimation etc. are not covered by this application note. The G122-202 Application Notes (part no C31015) cover some of these aspects. Moog Application Engineers can provide more detailed assistance, if required.

2 Description

The G122-824-002 is a general purpose, user configurable, P-I servoamplifier. Selector switches inside the amplifier enable either proportional control, integral control, or both to be selected. Many aspects of the amplifier's characteristics can be adjusted with front panel pots or selected with internal switches. This enables one amplifier to be used in many different applications. Refer also to data sheet G122-824.

3 Installation

3.1 Placement

A horizontal DIN rail, mounted on the vertical rear surface of an industrial steel enclosure, is the intended method of mounting. The rail release clip of the G122-824-002 should face down, so the front panel and terminal identifications are readable and so the internal electronics receive a cooling airflow.

An important consideration for the placement of the module is electro magnetic interference (EMI) from other equipment in the enclosure. For instance, VF and AC servo drives can produce high levels of EMI. Always check the EMC compliance of other equipment before placing the G122-824-002 close by.

3.2 Cooling

Vents in the top and bottom sides of the G122-824-002 case provide cooling for the electronics inside. These vents should be left clear. It is important to ensure that equipment below does not produce hot exhaust air that heats up the G122-824.

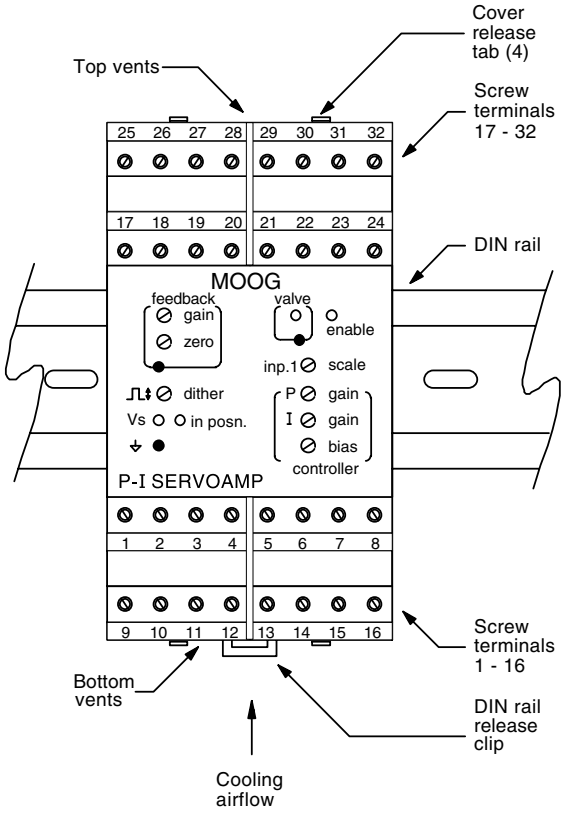

3.3 Wiring

The use of crimp "boot lace ferrules" is recommended for the screw terminals. Allow sufficient cable length so the circuit card can be withdrawn from its case with the wires still connected. This enables switch changes on the circuit card to be made while the card is still connected and operating. An extra 100mm, for cables going outside the enclosure, as well as wires connecting to adjacent DIN rail units, is adequate.

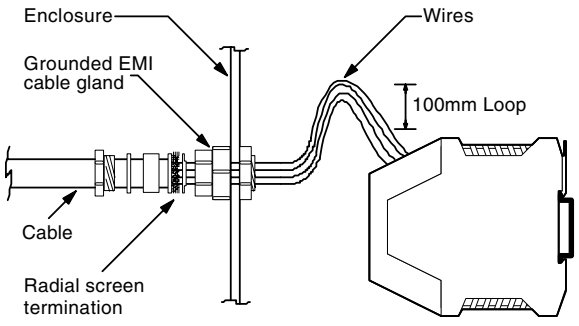

Preferred Wiring

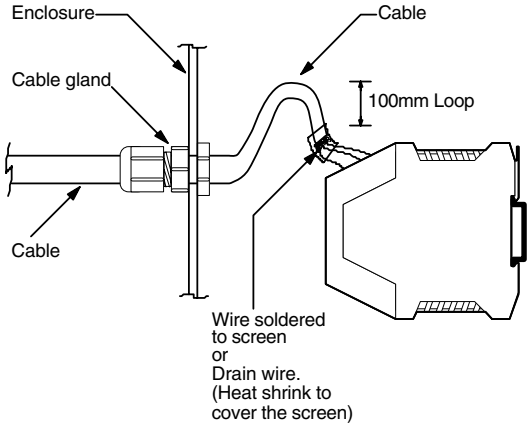

Alternative Wiring

3.4 EMC

The G122-824-002 emits radiation well below the level called for in its CE mark test. Therefore, no special precautions are required for suppression of emissions. However, immunity from external interfering radiation is dependent on careful wiring techniques. The accepted method is to use screened cables for all connections and to radially terminate the cable screens, in an appropriate grounded cable gland, at the point of entry into the industrial steel enclosure. If this is not possible, chassis ground screw terminals are provided on the G122-824-002. Exposed wires should be kept to a minimum length. Connect the screens at both ends of the cable to chassis ground.

4 Power supply

24V nominal, 22 to 28V
75mA @ 24V without a load, 200mA @ 100mA load.

If an unregulated supply is used the bottom of the ripple waveform is not to fall below 22V.

5 Set-up adjustments

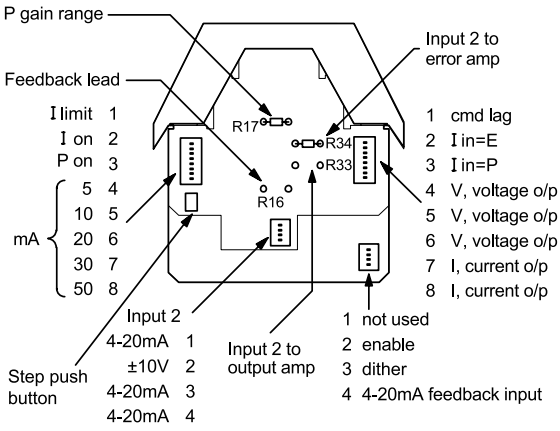

To access the circuit card switches, the circuit card must be withdrawn from the case. See paragraph 17.

The amplifier is shipped in the following default state.

- I limit switch: off
- INT (integral) switch: off
- PROP (proportional) switch: on
- mA switches: 50mA (20 + 30)
- Input 2 switches: ±10V on, 4-20mA off
- Input 1 cmd (command) lag switch: off
- I in = E switch: on
- I in = P switch: off
- V/I switches: all I (current, not integral)
- Enable switch: on
- Dither switch: off
- Feedback input switch: 4-20mA
- R17: 100k (gain range 1 to 20)
- R34: 100k (10V input)
- R33: not fitted (input 2 to output amp)
- R16: not fitted (feedback derivative)
- Feedback gain and zero pots: configured for 4-20mA input.
- Dither level pot: fully counter clockwise (FCCW)
- Scale pot: FCCW
- P gain pot: FCCW
- I gain pot: FCCW
- Bias pot: 0V

Caution

If you intend to use the feedback amplifier adjusted for 4-20mA, don't change the feedback gain or zero.

- They are already adjusted for 4-20mA
- To re-adjust for 4-20mA takes a little time, needs test equipment and is tedious to do in the field.

6 Input configuration

All three inputs can be used for feedback or command. Care needs to be taken in selecting signal polarity to achieve negative feedback for the overall closed loop. Since the input error amplifier sums the signals, the transducer feedback signal needs to be the opposite polarity of the command. This can be achieved in two ways:

- Arrange for an opposite polarity feedback transducer signal and connect it to input 1, input 2 or the positive feedback amplifier input.
- If the feedback transducer signal is the same polarity as the command, you only have one option: Connect it to the negative input of the feedback amplifier.

6.1 Feedback input

The feedback amplifier is the best choice for the feedback signal, for five reasons:

- It leaves input 1 available for command. See 6.2 below.
- It has inverting (negative) and non-inverting (positive) inputs.
- It has zero and gain adjustment pots. This enables a signal that does not go to zero volts and has less span than the command, to be scaled up to the command. While this is not essential, it helps when setting up and trouble shooting.
- There is a front panel test point for the zeroed and amplified signal. This is very convenient (essential) for setting up and trouble-shooting.
- There is the option of a plug-in resistor, R16, to give a feedback derivative (lead or D) in the output of the feedback amplifier.

Default

The feedback amplifier default set-up is 4-20mA flowing into terminal 18 and out of terminal 17, producing an output of 0 to -10V. Reversing the terminals, and hence the current flow, will not result in a 0 to +10V output. The feedback gain and zero must be adjusted for this arrangement.

6.2 Input 1

This input is ±10V non-inverting and has two important features:

- It has a scale pot on its input that enables large inputs to be scaled down to match smaller signals on other inputs. Scale range is 10 to 100%. Set fully clockwise, (FCW), an input of 100V can match a 10V signal on the other inputs.
- It has a switch selectable lag of 55mS that can be used to remove transients from the input signal that could cause unwanted rapid movement in the output.

Input 1 is well suited to be a command because of these two features. If input 1 is used for feedback, be sure the lag is switched off. Input resistance after the scale pot is 94k Ohms.

6.3 Input 2

This input is non-inverting. It is switch selectable between 4-20mA and ±10V. The 4-20mA converter produces 0 to +10V for 4 to 20mA input. R34 connects from the output of the converter to the input of the servo amp when 4-20mA is selected. Plug-in input resistor R34, of 100k Ohms, gives a nominal 0 to 10V input signal range when V rather than 4-20mA is selected. Input 2 is suitable for command or feedback. R34 can be increased to give a larger input range.

7 Output configuration

Select the output to match the input requirements of the valve. When voltage (V) is selected, ±10V is available into a minimum load of 200 Ohm. When current (I) is selected, the current level switches enable ±5 to ±100mA to be selected. The switch selections sum, so, if for instance 45mA is required, select 30,10 and 5. The output can drive all known Moog valves up to ±100mA The maximum load at I (Amp) output is:

$$\text{RL max} = \left(\frac{11\text{V}}{\text{I (Amp)}} - 39\right) \text{Ohm}$$

eg. at 50mA RL max is 181 Ohm

The output amplifier is limited to approximately 105% of the selected full scale output. If both the proportional and integrator stages are saturated, the output will not be twice the selected full scale but only 105% of full scale.

8 Step push button

The step push button injects -50% valve drive into the output. When released, the valve drive reverts to its original level. This feature is useful for closed loop gain optimisation.

9 P-I Selection

For position closed loops select only P. For pressure or velocity loops select I initially and then P. See paragraph 12 below for more detail. For a complete discussion of P and I control, see the G122-202 servoamplifier Application Notes (part no C31015).

10 Integrator input

The servoamplifier has a unity gain input error amplifier followed by two parallel stages, one a proportional amplifier and the other an integrator. The outputs of these two stages can be switched to the output power amplifier (see paragraph 7 above) which then drives the valve.

The input to the integrator stage can be switch selected from either the output of the error amplifier, I in = E, or the output of the proportional stage, I in = P. The latter arrangement is used in the G122-202. It is beyond the scope of these Application Notes to detail the benefits of each arrangement. If you have experience with the G122-202, I in = P would seem to be an easy choice.

11 P only gain

For position loops select only P control. Input a step disturbance of 50% valve current with the step push button. Adjust the P gain for the required stability, while monitoring the front panel valve test point, or the feedback signal. The gain range of the proportional amplifier can be moved by changing the plug-in resistor R17. The value loaded when shipped is 100k Ohms, which gives a 1 to 20 range. Selecting 200k Ohms will give 2 to 40. The circuit will function correctly with the value of R17 between 100k Ohms and 10M Ohms.

12 P and I gains together

If you are inexperienced with integral control the following set-up method is a good starting point.

- I in = E: Initially select only I. Press the step push button. Increase I gain until one overshoot in the feedback signal is observed.

Next select P and I together and increase the P gain to reduce the overshoot.

For the I in = E arrangement the P and I sequence could be reversed. i.e.: adjust P first, followed by I.

- I in = P: For an I in = P arrangement, only the "P followed by I" sequence of adjustment can be used.

For a more thorough discussion see G122-202 Application Notes (part number C31015).

13 I limit

The contribution from the integrator to the output amplifier can be reduced by selecting I limit on. When this switch is on the integrator contribution is reduced to approximately 15% of the level when it is off. This feature is useful in a position loop that may require integral control to achieve the required steady state accuracy. The limited integral control removes valve null error when the final position is reached.

14 Dither

The dither frequency is fixed at 200 Hz and the level is adjustable with the front panel pot to ±10% of valve drive, regardless of the type and level of valve drive selected. Dither is seldom needed in a position loop but can be beneficial in pressure or velocity loops. Increase dither until it can just be detected in the controlled variable, such as pressure or velocity. Dither can compromise valve life, so it should be kept to a minimum.

15 Enable

A relay on the circuit card needs to be energised to connect the output stage to its screw terminal and to un-clamp the integrator. The clamp prevents integrator wind-up when the loop is not operating. Supply 24V to the appropriate terminal to energise the relay. The enable switch on the circuit card can be set to permanently energise the relay and provide a permanent enable.

16 In position

When the valve drive signal falls below ±10% of the selected full scale signal, the "in position" signal goes true and provides an opto-isolated current path between the + and – terminals. This can be connected to a PLC to initiate the next step in a control sequence. Do not apply more than 40V to the + terminal and ensure the load on the – terminal is less than 20mA.

17 Withdrawing the circuit card from its case

The circuit card needs to be withdrawn from its case to set the selector switches and operate the step push button.

To do this, push one tab with a pen or screwdriver, while gently pulling on the top cover on that side. The cover will release approximately one mm. Repeat on the second tab on that side. Repeat on the other side and then withdraw the cover and circuit card until the required switches are exposed. The rigidity of the connecting wires will hold the circuit card in position while the switches are set.

18 Block-wiring diagram

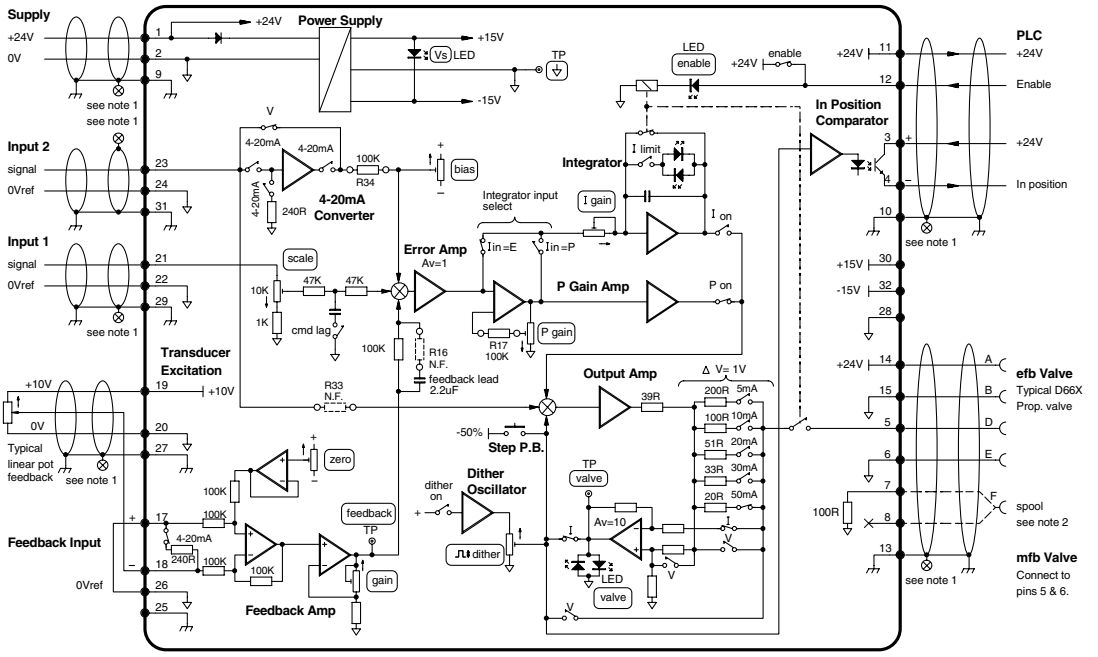

Note: 1. Connect cable screen to enclosure cable gland or chassis ground terminal on G122-824-002.

Note: 2. Connect spool (pin F) to terminal 7 if current, to terminal 8 if voltage.

Note: 3. Switches shown in default shipping mode.

Additions to -001: input2 4-20mA option, step push button.

19 Specifications

Function:	P, I, or P & I, switch selectable
Input 1:	Scaled to 95V max with switch selectable lag of 55ms.
Input 2:	4-20mA 240R load, for 0 to +10V on R34. Or 0 to ±10 direct onto R34. R34 is plug-in, 100K nominal.
Feedback input:	Differential 4-20mA or ±10V, switch selectable ±15V max. R in 100k – ±10V R in 240R – 4-20mA
Feedback amp:	Zero, ±10V. Gain, 1 to 10. Derivative (velocity) feedback via plug-in resistor and fixed capacitor.
Transducer excitation:	+10V @ 10mA max.
Error amp:	Unity gain. Bias ±1.5V.
Proportional amp gain:	1 to 20.
Integrator gain:	1 to 45 per second
Integrator input:	Switch selectable from output of unity gain error amp or proportional gain amp
Enable:	Relay, +24V @ 8mA, 17 to 32V.
Output amp:	Switch selectable voltage or current, single ended output, return to ground. V. ±10V, minimum load = 200 Ohm I. ±5, 10, 20, 30, 50mA to a maximum of ±100mA $\text{max load} = \left(\frac{11V}{I\ (Amp)} - 39\right)\ \text{Ohm}$
Step push button:	–50% valve drive.
Valve supply:	Pin 14, 300mA max.
In position:	±10% of valve drive. 20mA and 40V max.
Front panel indicators:	Vs, internal supply – green Valve drive positive – red negative – green Enable – yellow In position – green
Front panel test points:	Valve ±10V (regardless of output signal selection) Feedback amplifier output Signal 0V
Front panel trimpots:	Input 1 scale Error amp bias P gain I gain Dither level Feedback amp gain Feedback amp zero
Dither:	200 Hz fixed frequency. ±10% valve drive. Switch selectable on/off
Supply:	24V nominal, 22 to 28V 75mA @ 24V, no load, 200mA @ 100mA load
Mounting:	DIN rail IP 20
Temperature:	0 to +40ºC
Dimensions:	100W x 108H x 45D
Weight:	180g
CE mark:	EN50081.1 emission EN61000-6-2 immunity
C tick:	AS4251.1 emission

20 Internet

www.moog.com/dinmodules

MOOG

Industrial Controls Division. Moog Inc., East Aurora, NY 14052-0018. Telephone: 716/652-3000. Fax: 716/655-1803. Toll Free 1-800-272-MOOG.
Moog GmbH. Germany. Telephone: 07031-622-0. Fax: 07031-622-100.
Moog Sarl. France. Telephone: 01 45 60 70 00. Fax: 01 45 60 70 01.
Moog Australia Pty. Ltd. Telephone: 03 9561 6044. Fax: 03 9562 0246.

- Ó»¿-«®»³»²¬ °®·²½·°´» -°®·²¹ñ°·-¬±²
- Î»-°±²-» ¬·³» ìì ³-
- Ó»¿-«®»³»²¬ ·²¼»°»²¼»²¬ ±º ª·-½±-·¬§
- É·¼» ª·-½±-·¬§ ®¿²¹»
- Ý±³°¿½¬ ½±²-¬®«½¬·±²
- Ð®»--«®» ®»-·-¬¿²¬ «° ¬± ìîð ¾¿®

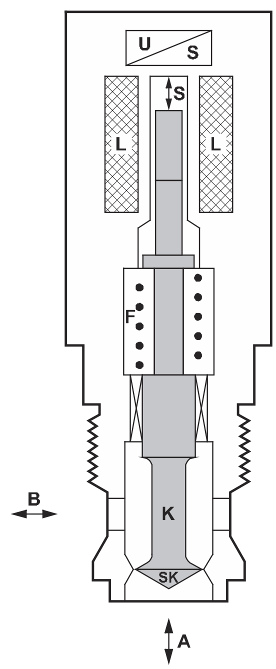

ÍÝÏ ³»¿-«®»³»²¬ °®·²½·°´»

Ú«²½¬·±²

Ì¸» °·-¬±² øÕ÷ ·- ³±ª»¼ ¾§ ¬¸» º´±© ¬¸®±«¹¸ ¬¸» ³±½¸»¬ ìØ÷ ¿²¼ ¿¹¿·²-¬ ¬¸» -°®·²¹ øÚ÷ ¿²¼ ¬¸» ³»¿-«®·²¹ ½±²» ¬± ¬¸» ®·¹¸¬ ±° ¬¸» ¼·-°´¿½»³»²¬ ±º ¬¸» ³»¿-«®»¼ ª¿´«» ©¸·½¸ ·- °®±°±®¬·±²¿´ ¬± ¬¸» º´±©ò ×¬ ·- ³»¿-«®»¼ ¾§ ¬¸» ·²¼«½¬·ª» ¬®¿²-¼«½»® øÔ÷ ¿²¼ ¬¸» ½±·´ øÍ÷ ·- ¿¬ ¬¸» ±«¬°«¬ ±º ¬¸» ·²¼«½¬·ª» ½±·´ ó ïìèè ´ñ³·²òÌ¸» ®»-«´¬·²¹ ¬·³» ±º ¬¸» °·-¬±² ³±ª»³»²¬ ·- --³¿´´»® ¬¸¿² ðòððî -ò

ß°°´·½¿¬·±²

Ì¸» ®»¿´·¦¿¬·±² ±º ¬¸» Œ±© ¯«¿²¬·¬§ ·- ±¾¬¿·²»¼ ·²¼»° ó°®»--«®» ¸§¼®¿«´·½-ò

Ó±«²¬·²¹ ©·¬¸ ¬¸» ½±²²»½¬·±² ¾´±½µ °»®³·¬- ¿ ½±³°¿½¬ ³»¿-«®»³»²¬ ±º ºô Ì ¿²¼ Ïò É·¬¸ ¬¸» ·²¬»¹®¿¬»¼ ¬»³°»®¿¬«®» ¬®¿²-¼«½»® ©·¬¸ ³»¿-«®»³»²¬ ±º °®»--«®» ·² ¬¸» ÍÝÏ ·²¬»¹®¿¬»¼ ·²¬± ¬¸» ÍÝÏ ·²¬¸» hydraulics is achieved. The rugged construction enables use ¬±½±²¬·²«±«- ³»¿-«®»³»²¬ «²¼»® -»ª»®» »²ª·®±²³»²¬¿´ ½±²¼·¬·±²-ô ¿¬ ¸·¹¸ °®»--«®» ·²½´«¼·²¹ °®»--«®» °»¿µ-ò

×º ¬¸» ´±¿¼ ·² ¬¸» ¸§¼®¿«´·½ -§-¬»³ ·- ·²½®»¿-»¼ ¬¸» ÍÝÏ ·- ¬¸» ·³°´»³»²¬»¼ò Î¿°·¼ ´±¿¼ ½¸¿²¹»-ô ©¸·½¸ can cause damage to valves or pumps, can be safely ½¿°¬«®»¼ò Þ»½¿«-» ±º ·¬- «² ³»¿-«®·²¹ °®·²½·°´»ô ¬¸» ÍÝÏ ·- ¿´-± ·² °±-·¬·±² ¬± ½¿°¬«®» ª·-½±-·¬§- ·²¼»°»²¼»²¬·±²-ò

	ÍÝÏóðêð	ÍÝÏóïëð
³»¿-«®»³»²¬ ®¿²¹» Ï₀	óêðòòòõêð ´ñ³·²	óïëðòòòõïëð ´ñ³·²
Ï₃¿¨	óêêòòòõêê ´ñ³·²	óïêëòòòõïêë ´ñ³·²
³»¼·¿ ½±²²»½¬·±²	Óîì øÒÙïð÷	Óìî øÒÙïê÷
©»·¹¸¬ ø¹÷	êéð	ïðëð

ß½½«®¿½§	
½¸¿®¿½¬»®·-¬·½½«®ª» ¼»ª·¿¬·±²	o î û ÚÍ à ìê½Í¬ò
®»-°±²-» ¬·³»	î ³ -
¬¸»®³¿´ ¼®·º¬	o ðôðë û ÚÍñpÝ
®»°»¿¬ ¿½½«®¿½§	o ðôë û ÚÍ
Ð®»--«®» ®»-·-¬¿²½»	
°®»--«®» ®¿²¹»	í•ìîð ¾¿®
©±®µ·²¹ °®»--«®» Ð₀	íïë ¾¿®
±ª»®´±¿¼ °®»--«®» Ð₃¿¨	ìîð ¾¿®
°®»--«®» ¼®±° Δ Ð ø¾¿®÷ à øÚÍ÷	-»» ¼·¿¹®¿³-
Ó¿¬»®·¿´	
¸±«-·²¹	-¬»»´
-»¿´·²¹	ÒÞÎ
°¿®¬- ·² ½±²¬¿½¬ ©·¬¸ ³»¼·¿	-¬»»´ôÒÞÎ
Û²ª·®±²³»²¬¿´ ½±²¼·¬·±²-	
©±®µ·²¹ ¬»³°»®¿¬«®»	õïð•õêð pÝ
-¬±®¿¹» ¬»³°»®¿¬«®»	óîð•èð pÝ
Ì³¿¨ Œ«·¼	õèð pÝ
•´«¿¬·±²	îë k³
ª·-½±-·¬§ ®¿²¹»	ïë•ïðð ½Í¬ò
°®±¬»½¬·±² ½´¿--	×Ðêé Ü×Ò ÛÒ êðëîç
Û´»½¬®·½¿´ ½±²²»½¬·±²-	
°´«¹ó·² ½±²²»½¬±®	Óïî¨ïå ìó°±´»
-«°°´§ ª±´¬¿¹»	õïè•õíð ÊÜÝ
½«®®»²¬ ½±²-«³°¬·±²	ìð ³ ß
±«¬°«¬	ð•îð ³ß ã óÚÍ•õÚÍ øïð ³ß ã ð ´ñ³·²÷
©±®µ·²¹ ®»-·-¬¿²½»	≤ ïëðΩ
-·¹²¿´ ²±·-»	ä ë ³ Ê
ÛÓ Ý ½±³°¿¬·¾·´·¬§	
·²¬»®º»®»²½» »³·--·±²-	ÛÒ êïððððóêóí
·²¬»®º»®»²½» ®»-·-¬¿²½»	ÛÒ êïððððóêóî

Ð·² ¼»-·¹²¿¬·±²
Óïî °´«¹ó·² ½±²²»½¬·±²

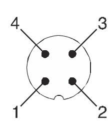

Ð×Ò	ðòòòîð ³ ß íó©·®»
ï	õËᵦ
î	Ï -·¹²¿´
í	ð ÊñÙÒÜ
ì	›

ÍÝÏóðêð -½®»©ó·² ¸±´» ¿²¼ °®»--«®» ¼®±° ½«®ª»

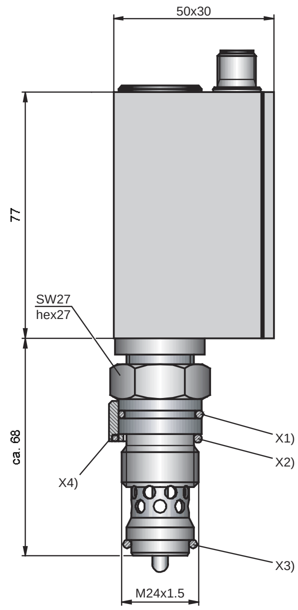

Ì·¹¸¬»²·²¹ ¬±®¯«» îð Ò³

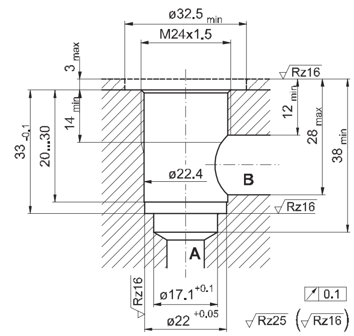

¨ï÷ Ñó®·²¹ îïôçë¨ïôéè
¨î÷ Ñó®·²¹ îðôîç¨îôî
¨í÷ Ñó®·²¹ ïëôëì¨îôêî
¨ì÷ Ýó®·²¹

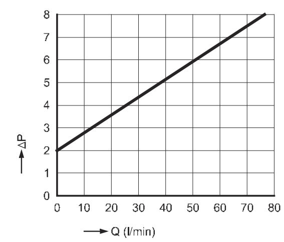

ÍÝÏóïëð -½®»©ó·² ¸±´» ¿²¼ °®»--«®» ¼®±° ½«®ª»

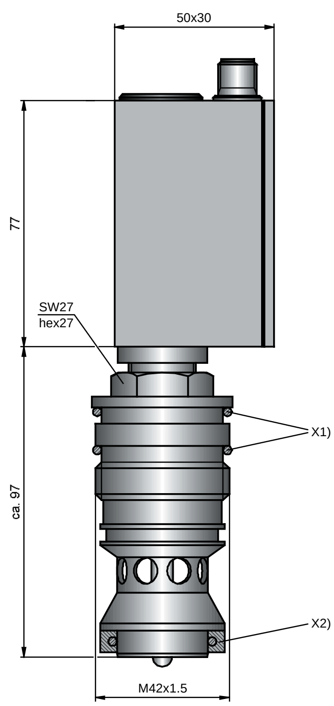

Ì·¹¸¬»²·²¹ ¬±®¯«» íð Ò³

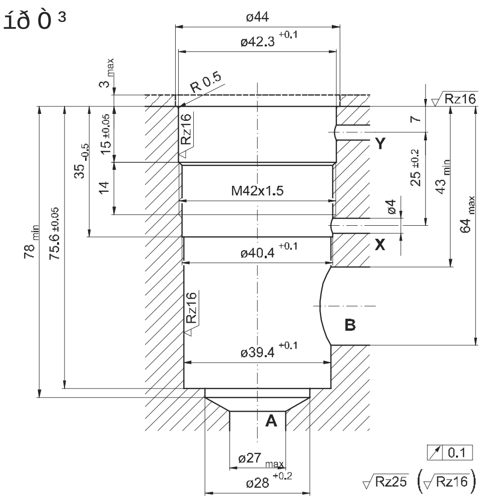

¨ï÷ Ñó®·²¹ íêôïé¨îôêî
¨î÷ ÐÌÚÛ ©·¬¸ Ñó®·²¹ îôêì¨îôêî

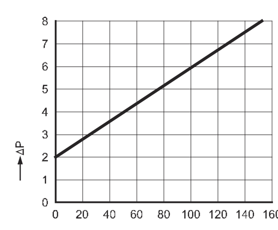

ÍÝßÏóðêð

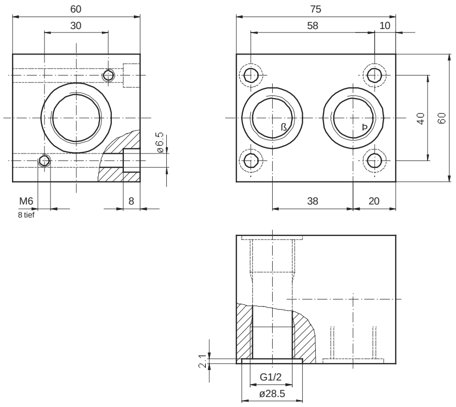

ÍÝßÏóÙ×óÎïñî

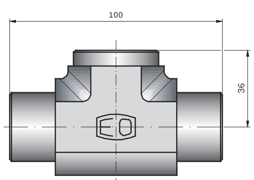

ÍÝßÏóïëð

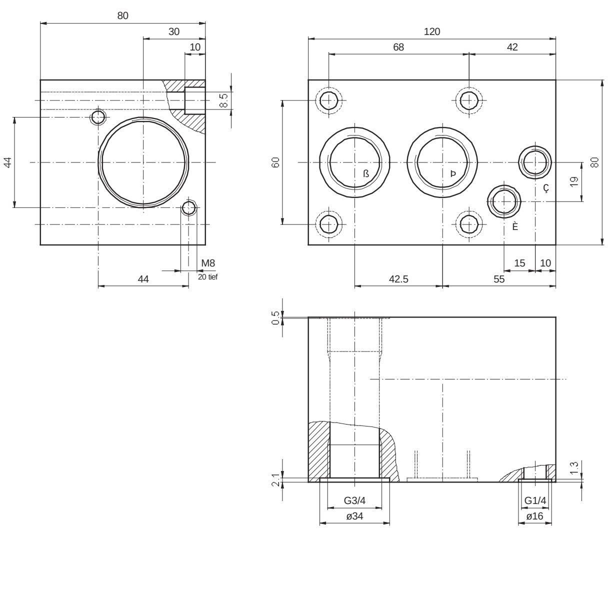

Ñ®¼»® ½±¼»

ÍÝÏóðêð øóêðàààõêð ´ñ³·²÷ ÍÝÏóðêðóïðóðé

Óïî¨ïô ìó°±´»å °´«¹·² ½±²²»½¬±®å ×Ðêé

ðàààîð ³ßå óêðàààõêð ´ñ³·² ø·²½´«·ª» ®·²¹÷

ÍÝÏóðêð ¿½½»±®·»æ

·²ó·²» ¿¼¿°¬±® ÍÝßÏóÙ×óÎïñîßìÝÈ

Ùïñî ÞÍÐÐ ·²¬»®²¿´ øßóÞ÷ «²¼ Óïî ·²¬»®²¿´

©·¬¸ ´±½µ·²¹ ½®»©æ

Óïî »¨¬»®²¿´ øÍÝÏóÓîìÈïôêóÛÜ÷

½±²²»½¬·²¹ ¾´±½µ ÍÝßÏóðêð

Ùïñî ÞÍÐÐ ·²¬»®²¿´ øßóÞ÷ ¿²¼ Óïî ·²¬»®²¿´

©·¬¸ ´±½µ·²¹ ½®»©æ

Óïî »¨¬»®²¿´ øÍÝÏóÓîìÈïôêóÛÜ÷

Ùïñî ÞÍÐÐ »¨¬»®²¿´ øßóÞ÷ øÍÝÏóÎïñîóÛÜ÷

ÍÝÏóïëð øóïëðàààõïëð ´ñ³·²÷ ÍÝÏóïëðóïðóðé

Óïî¨ïô ìó°±´»å °´«¹·² ½±²²»½¬±®å ×Ðêé

ðàààîð ³ßå óïëðàààõïëð ´ñ³·²

ÍÝÏóïëð ¿½½»±®·»æ

½±²²»½¬·²¹ ¾´±½µ ÍÝßÏóïëð

Ùíñì ÞÍÐÐ ·²¬»®²¿´ øßóÞ÷ ¿²¼ Óïì ·²¬»®²¿´

©·¬¸ ´±½µ·²¹ ½®»©

Óïì »¨¬»®²¿´ øÍÝÏóÓîìÈïôëóÛÜ÷

Ùíñì ÞÍÐÐ »¨¬»®²¿´ øßóÞ÷ øÍÝÏóÎíñìóÛÜ÷

Í°¿®» °¿®¬æ

¼·¬¿²½» ®·²¹ º±® ÍÝÏóðêð ÍÝóçïð

»¿´ »¬ º±® ÍÝÏóðêð ÍÝóçïï

»¿´ »¬ º±® ÍÝÏóïëð ÍÝóçïî

Ý±²²»½¬·²¹ ½¿¾´» ¿²¼ Í»°¿®¿¬» °´«¹

½±²²»½¬·²¹ ½¿¾´» ©·¬¸ ³¿¼» «° ÍÝÕóìðð¨¨ó¨¨

ø±°»² ½¿¾´» »²¼÷

½¿¾´» ´»²¹¬¸ ·² ³

ðî î ³

ðë ë ³

ïð ïð ³

°´«¹·² ½±²²»½¬±®

ìë Óïî ½¿¾´» »²¼»¼ ¬®¿·¹¸¬

ëë Óïî ½¿¾´» »²¼»¼ ¿²¹´»¼

Í»°¿®¿¬» °´«¹

Óïî ½¿¾´» »²¼»¼ ¬®¿·¹¸¬ ÍÝÕóïìë

Óïî ½¿¾´» »²¼»¼ ¿²¹´»¼ ÍÝÕóïëë

MOOG

D631 Series
Servo Control Valves
ISO 4401 Size 05

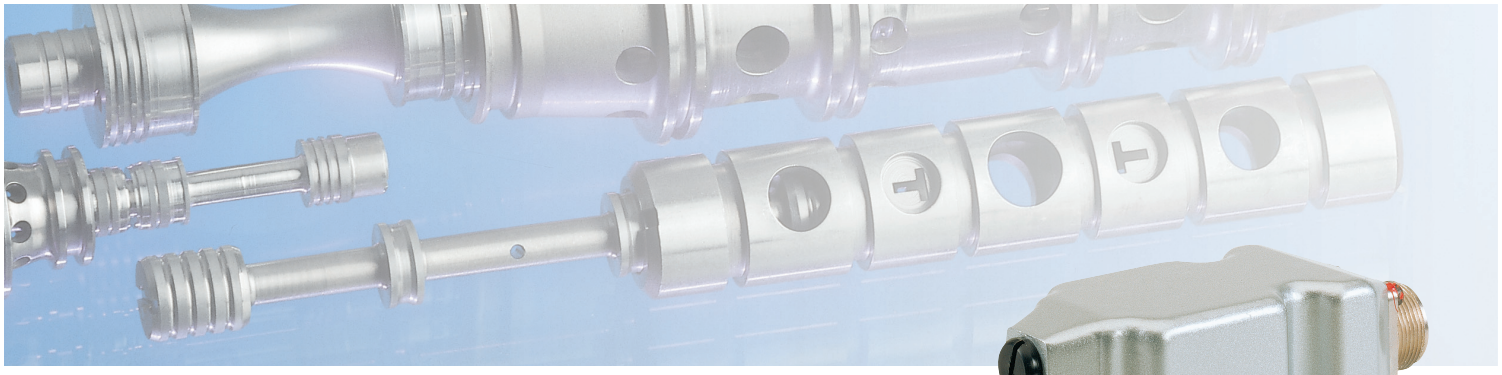

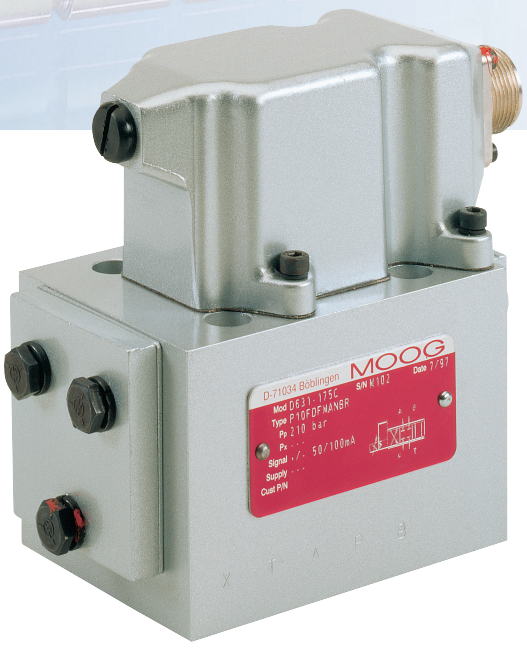

MOOG SERVO- AND PROPORTIONAL CONTROL VALVES

For over 50 years Moog has manufactured proportional control valves with integrated electronics. During this time more than 200,000 valves have been delivered. These servo control valves have been proven to provide reliable control including injection and blow molding equipment, die casting machines, presses, heavy industry equipment, paper and lumber processing and other applications.

D631 SERIES SERVO VALVE

The servo control valves D631 Series are throttle valves for 3- and preferably 4-way applications. According to the requirements of the application, the user can select either the standard version (P) or the high response version (H). The main features of the high response valves are short stroke related improved dynamics and a more precise axis null cut.

DESCRIPTION

The proportional valves D631 Series consist of an electromechanical transformer (torque motor), a hydraulic amplifier (nozzle/flapper principle), a spool in a bushing and a cantilever feedback spring. The torque motor contains coils, pole pieces, permanent magnets and an armature. The armature is connected to a flexible tube which allows a limited rotation of the armature and at the same time seals the electromagnetic components against the hydraulic fluid.
The hydraulic amplifier is a full bridge arrangement with two upstream fixed orifices and two downstream variable orifices created by two nozzles and a flapper between them. The flapper is connected at its upper end to the centre of the armature and extends downward through the flexure tube to the nozzles. A deflection of the flapper between the nozzles changes the size of the variable orifices in opposite sense.
The 4-way spool controls fluid flow from pressure port to one of the load ports and also from the other load port to return. Deflection of the feedback spring due to spool displacement produces a torque which is fed back to the torquemotor.

Valves available with intrinsically protection to EN 50.020 class EEx ia IIc T6. Special data sheet on request.

NOTICE

- ❒ Before installation of the valve into the system the complete hydraulic system must be flushed.

Our quality management system conforms to DIN EN ISO 9001.

BENEFTITS OF SERVO VALVES

Operational features

- ❒ 2-stage version with dry torque motor
- ❒ Low friction double nozzle pilot stage
- ❒ High spool control forces
- ❒ Mechanical feedback
- ❒ Protection filter easy to replace

SERVO CONTROL VALVE OPERATING PRINCIPLE

An electrical current (command or input signal) is applied to the coils of the torquemotor and produces depending on the current polarity a clockwise or counter clockwise torque to the armature. The thereby deflected nozzle flapper system creates a pressure difference across the drive areas of the spool and effects its movement. The feedback spring connected to the armature engages with its lower end into a bore of the spool and is thus deflected by spool displacement. The motion of the spool stops when feedback torque and electromagnetic torque are in equilibrium. Then the flapper is again in hydraulic centre position (approximately). Thus the position of the spool is proportional to the electrical command signal.

D631 Series
two stage servo control valves

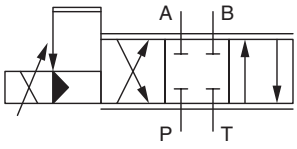

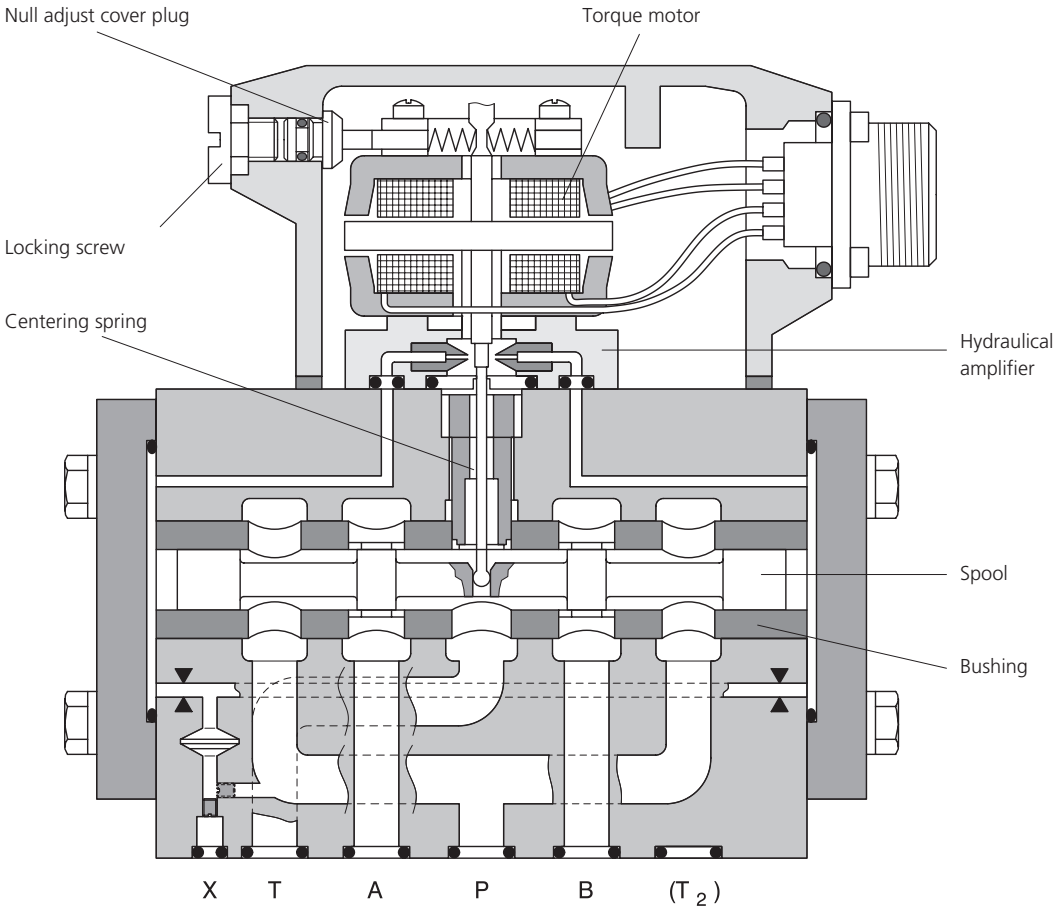

PERFORMANCE SPECIFICATIONS FOR STANDARD MODELS

Operating pressure range	
Main stage:	
ports P, A and B	up to 315 bar (4500 psi)
port T	20% of pilot pressure, max. 100 bar (1450 psi)
Pilot stage: regular version	15 to 210 bar (200 to 3000 psi)
with dropping orifice	25 to 315 bar (350 to 4500 psi)
Temperature range	
Ambient	–20 °C to +80 °C (-4 °F to +170 °F)
Fluid	–20 °C to +80 °C (-4 °F to +170 °F)
Seal material	NBR, FPM, others on request
Operating fluid	Mineral oil based hydraulic fluid (DIN 51524, part 1 to 3), other fluids on request
Viscosity, recommended	15 to 100 mm^2/s (cSt)

System filtration

High pressure filter (without bypass, but with dirt alarm) mounted in the main flow and if possible directly upstream of the valve.

Class of cleanliness

The cleanliness of the hydraulic fluid greatly effects the performance (spool positioning, high resolution) and wear (metering edges, pressure gain, leakage) of the valve.

Recommended cleanliness class	
for normal operation:	ISO 4406:1999 < 19/16 /13
for longer life:	ISO 4406:1999 < 17/14 /11
Filter rating recommended	
for normal operation:	$\beta_{15} \geq 75$ (15 µm absolute)
for longer life:	$\beta_{10} \geq 75$ (10 µm absolute)
Installation options	any position, fixed or movable
Vibration	30 g (0.7 lbs), 3 axes
Mass	2.2 kg (4.9 lbs)
Degree of protection	EN 60529: class IP 65, with mating connector mounted
Shipping plate	Delivered with an oil sealed shipping plate

4-WAY FUNCTION

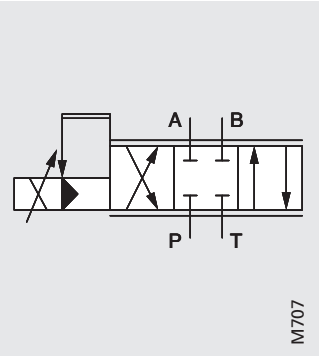

4-way version
optional X external

- ❒ Flow control (throttle valve) in port A and port B
- ❒ For 3-way fuction close port A or port B of the manifold
- ❒ Spools with exact axis cut, 1.5 to 3% or 10% overlap available

VALVE FLOW CALCULATIONS

The actual flow depends on the electrical command signal and the valve pressure drop, and may be calculated using the square root function for a sharp-edged orifice.

$$Q = Q_N \cdot \sqrt{\frac{\Delta p}{\Delta p_N}}$$

Q / l/min = calculated flow
Q_N / l/min = rated flow
Δp / bar = actual valve pressure drop
Δp_N / bar = rated valve pressure drop

If large flow rates with high valve pressure drops are required, an appropriate higher pilot pressure has to be chosen to overcome the flow forces. An approximate value can be calculated as follows:

$$p_X \geq 2{,}5 \cdot 10^{-2} \cdot \frac{Q}{A_K} \cdot \sqrt{\Delta p}$$

Q / l/min = max. flow
Δp / bar = valve pressure drop with Q
A_K / cm² = spool drive area
p_X / bar = pilot pressure

The pilot pressure p_X has to be at least 15 bar (200 psi), with throttle valve 25 bar (350 psi) above the return pressure of the pilot stage.

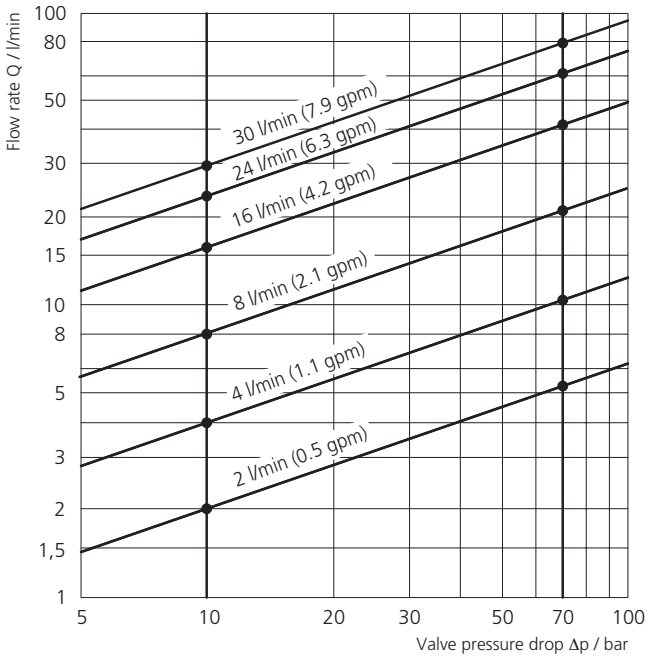

ELECTRICAL CONNECTION WITH 4-POLE CONNECTOR TO MIL C5015/14S-2

The torque motor has 2 coils. The leads of the coils are single connected to the pins. For operation in parallel, series or single coil mode the corresponding wiring must be done in the mating connector.
Optional two types of coils are available:
Coil R with 28 Ω per coil
Coil Q with 300 Ω per coil

Connector Mil C5015/14S-2	Parallel wiring		Series wiring		Single coils	
	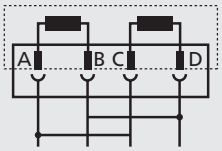		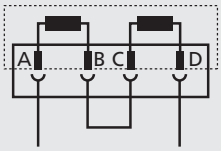		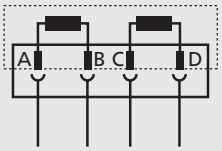	
Coil type	R	Q	R	Q	R	Q
Input resistance (at 25°C)[1] / Ω	14	150	56	600	28	300
Rated current / mA	± 100	± 30	± 50	± 15	± 100	± 30
Inductance (at 60 Hz) / H	0.2	1.8	0.8	7.0	0.25	2.0
Electrical power / W	0.14	0.14	0.14	0.14	0.28	0.27
Connections for valve opening P ⬧B, A ⬧T	A and C (+) B and D (–)		A (+), D (–) B and C connected		A (+), B (–) or C (+), D (–)	

ELECTRICAL CONNECTION WITH CONNECTOR TO DIN 43650

The torque motor has 2 coils. The coils are connected in parallel inside the valve.
Two types of coils are available:
Coil R with 28 Ω
Coil Q with 300 Ω

Connector DIN 43650	Parallel wiring	
	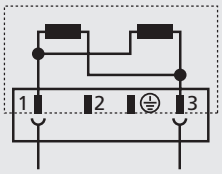	
Coil type	R	Q
Input resistance (at 25°C)[1] / Ω	14	150
Rated current / mA	± 100	± 30
Inductance (at 60 Hz) / H	0.2	1.8
Electrical power / W	0.14	0.14
Connections for valve opening P ⬧B, A ⬧T	1 (+) and 3 (–)	

[1] 65 °F

PERFORMANCE SPECIFICATIONS FOR STANDARD MODELS

Model ... Type			D631-... P...	D631-... H...
Mounting pattern			ISO 4401-05-05-0-94	
Valve body version			4-way, 2-stage with bushing-spool assembly	
Pilot stage	Nozzle / flapper		Standard	Highresponse
Pilot connection	optional, internal or external		X	X
Rated flow (± 10%)	at Δp_N= 5 bar per land	l/min	2 / 4 / 8 / 16 / 24 / 30	
	at Δp_N= 73 psi per land	gpm	0.5 / 1.1 / 2.1 / 4.2 / 6.3 / 7.9	
Response time[1)]		ms	25	13
Threshold[1)]		%	< 1	< 1
Hysteresis[1)]	without dither	%	< 5	< 3
Null shift	at ΔT = 55 K	%	< 5	< 4
Null leakage flow[1)]	total, max.	l/min (gpm)	< 2.5 to 4.2 (0.7 to 1.1)	< 2.5 to 4.2 (0.7 to 1.1)
Pilot leakage flow[1)]	Tare	l/min (gpm)	1.4 (0.4)	1.7 (0.5)
Pilot flow[1)] max.,	for 100% step input	l/min (gpm)	depending on hydraulic bridge 0.5 to 1 (0.1 to 0.3)	
Spool stroke		mm (inch)	± 2.54 (0.1)	± 1.3 (0.05)
Spool drive area		cm^2 ($inch^2$)	0.75 (0.3)	0.75 (0.3)

[1)] measured at 210 bar (3045 psi) pilot or operating pressure, respectively, fluid viscosity of 32 mm^2/s (0.05 in^2/s) and fluid temperature of 40 °C (104 °F)

TYPICAL CHARACTERISTIC CURVES MEASURED WITHOUT DROPPING ORIFICE
measured at 210 bar (3045 psi) pilot or operating pressure, respectively,
fluid viscosity of 32 mm²/s (0.05 in²/s) and fluid temperature of 40 °C (104 °F)

Step response standard valve

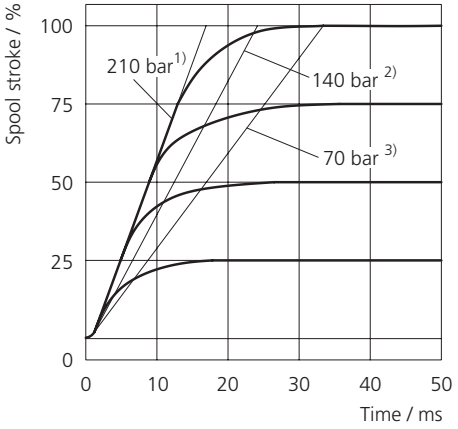

Step response high response valve

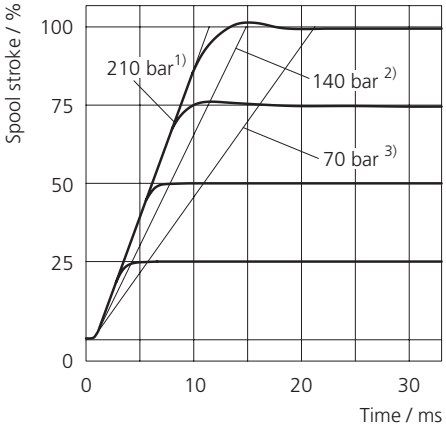

Frequency response standard valve

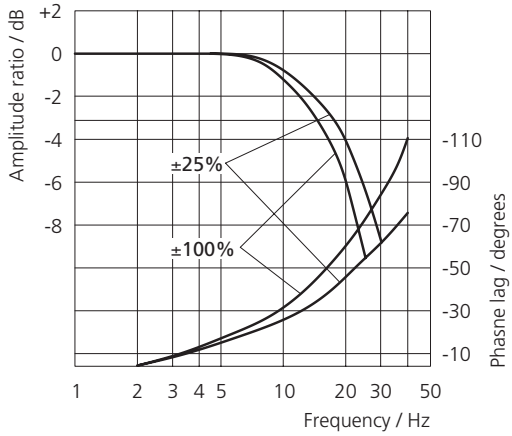

Frequency response high response valve

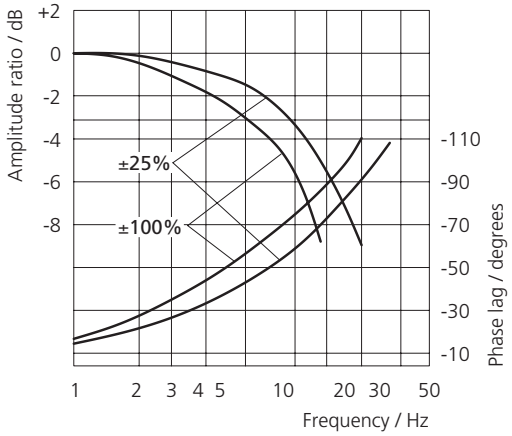

1) 210 bar = 3045 psi
2) 140 bar = 2030 psi
3) 70 bar = 1015 psi

INSTALLATION DRAWING

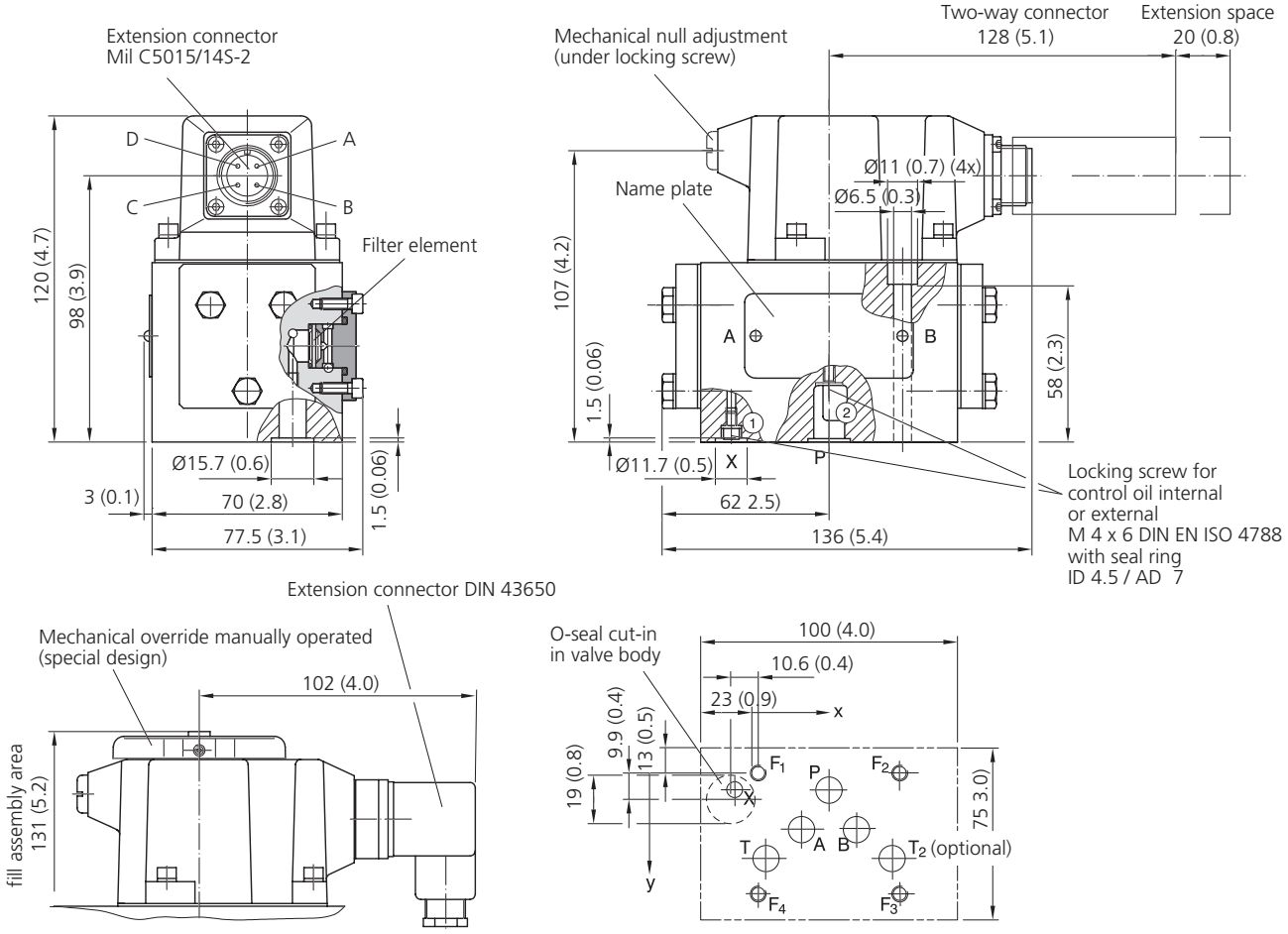

Mounting pattern
ISO 4401-05-05-0-94, without X-Connection

mm

	P	A	B	T	X[1)]	F_1	F_2	F_3	F_4
	Ø11.5	**Ø11.5**	**Ø11.5**	**Ø11.5**	Ø 6.3	M6	M6	M6	M6
x	27	16.7	37.3	3.2	-9	0	54	54	0
y	6.3	21.4	21.4	32.5	6.3	0	0	46	46

inch

	P	A	B	T	X[1)]	F_1	F_2	F_3	F_4
	Ø0.45	**Ø0.45**	**Ø0.45**	**Ø0.45**	Ø0.25	M6	M6	M6	M6
x	1.07	0.66	1.47	0.13	-0.36	0	2.13	2.13	0
y	0.25	0.85	0.85	1.28	0.25	0	0	1.82	1.82

The mounting manifold must conform to ISO 4401-05-05-0-94 [1)].

[1)] Note: Location of X port in valve body does not correspond to ISO standards.
Mounting surface needs to be flat within 0.02 mm (0.0008 inch).
Average surface finish value, Ra, better than 0.8 µm.

SPARE PARTS AND ACCESSORIES

O-rings (included in delivery)			NBR 85 Shore	FPM 85 Shore
for P, T, T_2, A, B	5 pieces	ID 12 x Ø 2 (ID 0.47 x Ø 0.08)	-66117-012-020	A25163-012-020
for X	1 piece	ID 8 x Ø 2 (ID 0.31 x Ø 0.08)	-66117-008-020	A25163-008-020
Mating connector, waterproof IP 65 (not included in delivery)		for cable dia		
4-pole Mil C50515/14S-2S		min. Ø 6,5 mm, max. Ø 9,5 mm min. Ø 0.25 in, max. Ø 0.37 in		B46744-004
Flushing plate		for P, A, B, T, T_2, X, Y B67728-001	for P, T, T_2, X, Y B67728-002	for P, T, T_2, und X, Y B67728-003
Mounting manifolds	see special data sheet			
Mounting bolts (not included in delivery)				
M 6 x 70 DIN EN ISO 4762-10.9	4 pieces	required torque 13 Nm (115 lb in)	A03665-060-070	
Replaceable filter		100 µm nominal	A67999 100 [1)]	
O-rings for filter replacement			NBR 85 Shore	FPM 85 Shore
for filter	1 piece	ID 13 x Ø 1,5 (ID 0.51 x Ø 0.06)	-66117-013-015	A25163-013-015
for filter cover	1 piece	ID 17 x Ø 2 (ID 0.67 x Ø 0.08)	-66117-017-020	A25163-017-020
Screw plug port X	1 piece	M 4 x 6 DIN EN ISO 4762-8.8	-66098-040-006	
Seal for screw plug	1 piece	ID 4,5 / AD 7 (ID 0.18 / AD 0.28)	A25528-040	

[1)] For standard models, others on request

ORDERING INFORMATION

Model number: **D631** . . . . . .

Type designation: . . . . . .

Specification status	
–	Series specification
E	Preseries specification
Z	Special specification
K	Intrinsically safe valve

Model designation	
	assigned at the factory

Factory identification	
	assigned at the factory

Valve version	
P	Standard valve
H	High response valve

Rated flow	Δp_N = 5 bar per land (Δp_N = 73 psi per land)	Q_N / l/min bei Δp_N = 35 bar (Q_N / gpm at Δp_N = 500 psi)
05	2 (0.5)	5 (1.3)
10	4 (1.1)	10 (2.6)
20	8 (2.1)	20 (5.3)
40	16 (4.2)	40 (10.6)
60	24 (6.3)	60 (15.8)
80	30 (7.9)	75 (19.8)

Maximum operating pressure		
F	210 bar	At $p_X \leq$ 210 bar (3045 psi) (X external) operating pressure in port P, A and B up to 315 bar possible 315 bar (4566 psi)
J	315 bar	(with dropping orifice)

Bushing spool type	
0	Axis cut, linear characteristic
D	± 10% overlap, linear characteristic
X	others on request

Special equipment	
	no
M	Mechanical override

Signals for 100% spool stroke	Command	for rated flow Q_N Valve Typ P	Valve Typ H
Q	±15 mA Series	05 to 80	05 to 60
	± 22,5 mA Series	–	80
R	± 50 mA Series	05 to 80	05 to 60
	± 75 mA Series	–	80
Y	others on request		

Valve connector	
B	Mil C5015/14S-2P
G	DIN 43650

Seal material	
N	NBR (Buna)
V	FPM (Viton)
X	others on request

Pilot connections and pressure		
A	15 to 210 bar (217 to 3045 psi)	internal supply
C	15 to 210 bar (217 to 3045 psi)	external supply
E	25 to 315 bar (363 to 4565 psi)	internal supply
G	25 to 315 bar (363 to 4565 psi)	external supply

Spool position without electrical signal P[1)]	
A	P ◗ B, A ◗ T
B	P ◗ A, B ◗ T
M	Mid position

Pilot stage	
F	Standard response for valve version "P"
G	Highresponse for valve version "H"

[1)] Control pressure

Preferred configurations are highlighted.
All combinations may not be available.
Options may increase price.
Technical changes are reserved.

Argentina
Australia
Austria
Brazil
China
Finland
France
Germany
India

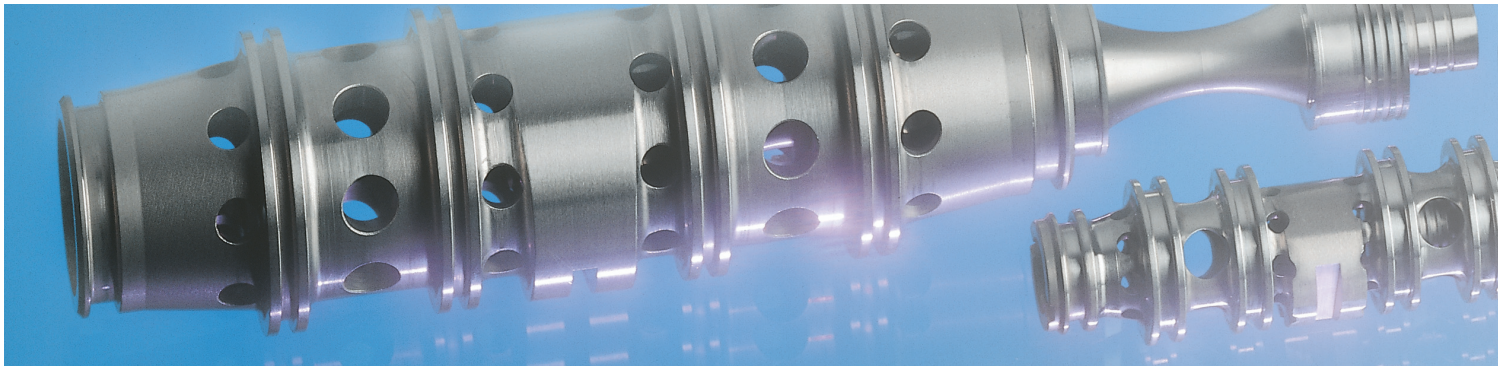

Ireland
Italy
Japan
Korea
Luxembourg
Norway
Philippines
Russia
Singapore
Spain
Sweden
United Kingdom
USA

MOOG

Moog GmbH
Hanns-Klemm-Straße 28
71034 Böblingen
email: sales@moog.de
www.moog.de
Telefon (0 70 31) 622-0
Telefax (0 70 31) 622-191

D631.en.09.02

Ksis / Wacker / 1000

National Semiconductor

May 1996

LM675 Power Operational Amplifier

General Description

The LM675 is a monolithic power operational amplifier featuring wide bandwidth and low input offset voltage, making it equally suitable for AC and DC applications.

The LM675 is capable of delivering output currents in excess of 3 amps, operating at supply voltages of up to 60V. The device overload protection consists of both internal current limiting and thermal shutdown. The amplifier is also internally compensated for gains of 10 or greater.

Features

- 3A current capability
- A_{VO} typicaly 90 dB
- 5.5 MHz gain bandwidth product
- 8 V/μs slew rate
- Wide power bandwidth 70 kHz
- 1 mV typical offset voltage
- Short circuit protection
- Thermal protection with parole circuit (100% tested)
- 16V–60V supply range
- Wide common mode range
- Internal output protection diodes
- 90 dB ripple rejection
- Plastic power package TO-220

Applications

- High performance power op amp
- Bridge amplifiers
- Motor speed controls
- Servo amplifiers
- Instrument systems

Connection Diagram

TO-220 Power Package (T)

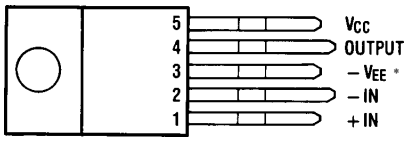

TL/H/6739–1

Front View

Order Number LM675T
See NS Package T05D

*The tab is internally connected to pin 3 ($-V_{EE}$)

Typical Applications

Non-Inverting Amplifier

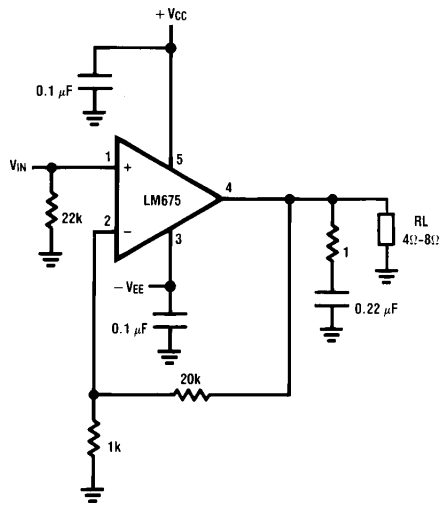

TL/H/6739–2

Absolute Maximum Ratings

If Military/Aerospace specified devices are required, please contact the National Semiconductor Sales Office/Distributors for availability and specifications.

Supply Voltage	±30V
Input Voltage	$-V_{EE}$ to V_{CC}
Operating Temperature	0°C to +70°C
Storage Temperature	−65°C to +150°C
Junction Temperature	150°C
Power Dissipation (Note 1)	30W
Lead Temperature (Soldering, 10 seconds)	260°C

ESD rating to be determined.

Electrical Characteristics $V_S = \pm 25V$, $T_A = 25°C$ unless otherwise specified.

Parameter	Conditions	Typical	Tested Limit	Units
Supply Current	$P_{OUT} = 0W$	18	50 (max)	mA
Input Offset Voltage	$V_{CM} = 0V$	1	10 (max)	mV
Input Bias Current	$V_{CM} = 0V$	0.2	2 (max)	μA
Input Offset Current	$V_{CM} = 0V$	50	500 (max)	nA
Open Loop Gain	$R_L = \infty\Omega$	90	70 (min)	dB
PSRR	$\Delta V_S = \pm 5V$	90	70 (min)	dB
CMRR	$V_{IN} = \pm 20V$	90	70 (min)	dB
Output Voltage Swing	$R_L = 8\Omega$	±21	±18 (min)	V
Offset Voltage Drift Versus Temperature	$R_S < 100\ k\Omega$	25		μV/°C
Offset Voltage Drift Versus Output Power		25		μV/W
Output Power	THD = 1%, $f_O = 1$ kHz, $R_L = 8\Omega$	25	20	W
Gain Bandwidth Product	$f_O = 20$ kHz, $A_{VCL} = 1000$	5.5		MHz
Max Slew Rate		8		V/μs
Input Common Mode Range		±22	±20 (min)	V

Note 1: Assumes T_A equal to 70°C. For operation at higher tab temperatures, the LM675 must be derated based on a maximum junction temperature of 150°C.

Typical Applications (Continued)

Generating a Split Supply From a Single Supply

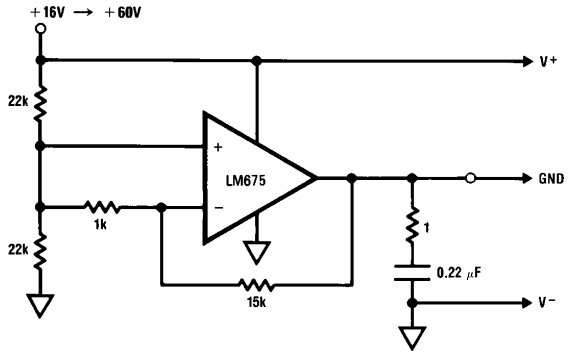

$V_S = \pm 8V \rightarrow \pm 30V$

TL/H/6739–3

Typical Performance Characteristics

THD vs Power Output

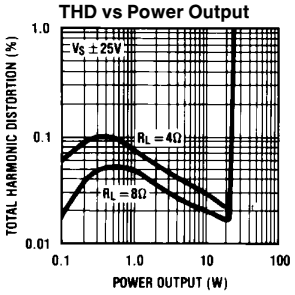

Input Common Mode Range vs Supply Voltage

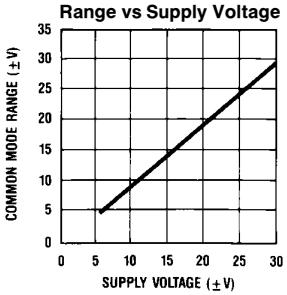

Supply Current vs Supply Voltage

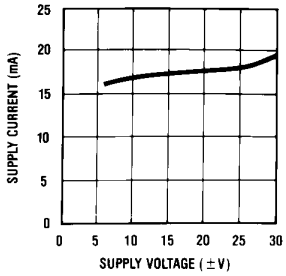

PSRR vs Frequency

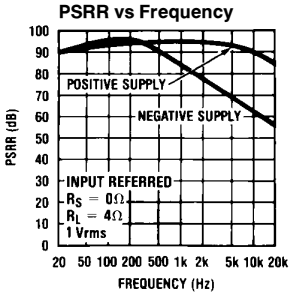

Device Dissipation vs Ambient Temperature†

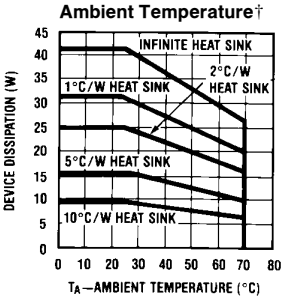

†θ INTERFACE = 1° C/W.
See Application Hints.

Current Limit vs Output Voltage*

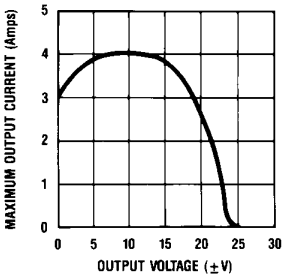

*V_S = ±25V

I_B vs Supply Voltage

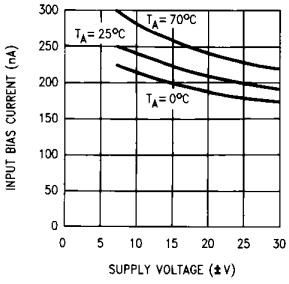

Output Voltage Swing vs Supply Voltage

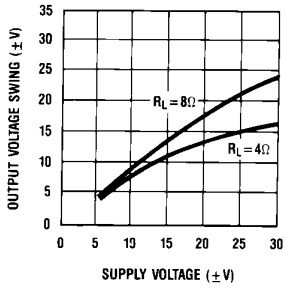

TL/H/6739–4

Schematic Diagram

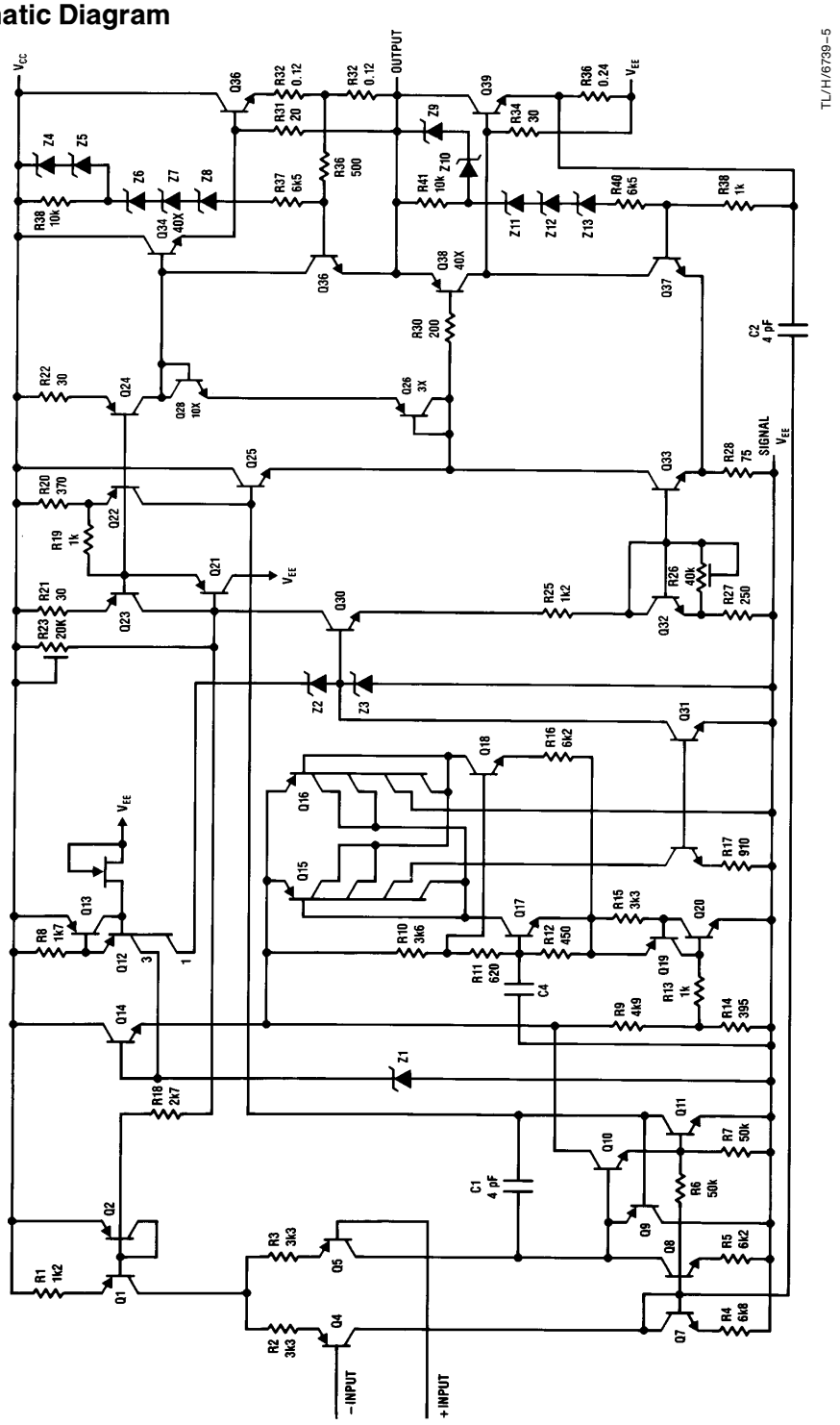

Application Hints

STABILITY

The LM675 is designed to be stable when operated at a closed-loop gain of 10 or greater, but, as with any other high-current amplifier, the LM675 can be made to oscillate under certain conditions. These usually involve printed circuit board layout or output/input coupling.

When designing a printed circuit board layout, it is important to return the load ground, the output compensation ground, and the low level (feedback and input) grounds to the circuit board ground point through separate paths. Otherwise, large currents flowing along a ground conductor will generate voltages on the conductor which can effectively act as signals at the input, resulting in high frequency oscillation or excessive distortion. It is advisable to keep the output compensation components and the 0.1 μF supply decoupling capacitors as close as possible to the LM675 to reduce the effects of PCB trace resistance and inductance. For the same reason, the ground return paths for these components should be as short as possible.

Occasionally, current in the output leads (which function as antennas) can be coupled through the air to the amplifier input, resulting in high-frequency oscillation. This normally happens when the source impedance is high or the input leads are long. The problem can be eliminated by placing a small capacitor (on the order of 50 pF to 500 pF) across the circuit input.

Most power amplifiers do not drive highly capacitive loads well, and the LM675 is no exception. If the output of the LM675 is connected directly to a capacitor with no series resistance, the square wave response will exhibit ringing if the capacitance is greater than about 0.1 μF. The amplifier can typically drive load capacitances up to 2 μF or so without oscillating, but this is not recommended. If highly capacitive loads are expected, a resistor (at least 1Ω) should be placed in series with the output of the LM675. A method commonly employed to protect amplifiers from low impedances at high frequencies is to couple to the load through a 10Ω resistor in parallel with a 5 μH inductor.

CURRENT LIMIT AND SAFE OPERATING AREA (SOA) PROTECTION

A power amplifier's output transistors can be damaged by excessive applied voltage, current flow, or power dissipation. The voltage applied to the amplifier is limited by the design of the external power supply, while the maximum current passed by the output devices is usually limited by internal circuitry to some fixed value. Short-term power dissipation is usually not limited in monolithic operational power amplifiers, and this can be a problem when driving reactive loads, which may draw large currents while high voltages appear on the output transistors. The LM675 not only limits current to around 4A, but also reduces the value of the limit current when an output transistor has a high voltage across it.

When driving nonlinear reactive loads such as motors or loudspeakers with built-in protection relays, there is a possibility that an amplifier output will be connected to a load whose terminal voltage may attempt to swing beyond the power supply voltages applied to the amplifier. This can cause degradation of the output transistors or catastrophic failure of the whole circuit. The standard protection for this type of failure mechanism is a pair of diodes connected between the output of the amplifier and the supply rails. These are part of the internal circuitry of the LM675, and needn't be added externally when standard reactive loads are driven.

THERMAL PROTECTION

The LM675 has a sophisticated thermal protection scheme to prevent long-term thermal stress to the device. When the temperature on the die reaches 170°C, the LM675 shuts down. It starts operating again when the die temperature drops to about 145°C, but if the temperature again begins to rise, shutdown will occur at only 150°C. Therefore, the device is allowed to heat up to a relatively high temperature if the fault condition is temporary, but a sustained fault will limit the maximum die temperature to a lower value. This greatly reduces the stresses imposed on the IC by thermal cycling, which in turn improves its reliability under sustained fault conditions. This circuitry is 100% tested without a heat sink.

Since the die temperature is directly dependent upon the heat sink, the heat sink should be chosen for thermal resistance low enough that thermal shutdown will not be reached during normal operaton. Using the best heat sink possible within the cost and space constraints of the system will improve the long-term reliability of any power semiconductor.

POWER DISSIPATION AND HEAT SINKING

The LM675 should always be operated with a heat sink, even though at idle worst case power dissipation will be only 1.8W (30 mA $\times$ 60V) which corresponds to a rise in die temperature of 97°C above ambient assuming θ_{jA} = 54°C/W for a TO-220 package. This in itself will not cause the thermal protection circuitry to shut down the amplifier when operating at room temperature, but a mere 0.9W of additional power dissipation will shut the amplifier down since T_J will then increase from 122°C (97°C + 25°C) to 170°C.

In order to determine the appropriate heat sink for a given application, the power dissipation of the LM675 in that application must be known. When the load is resistive, the maximum average power that the IC will be required to dissipate is approximately:

$$P_{D\,(MAX)} \approx \frac{V_S^2}{2\pi^2 R_L} + P_Q$$

where V_S is the total power supply voltage across the LM675, R_L is the load resistance and P_Q is the quiescent power dissipation of the amplifier. The above equation is only an approximation which assumes an ''ideal'' class B output stage and constant power dissipation in all other parts of the circuit. As an example, if the LM675 is operated on a 50V power supply with a resistive load of 8Ω, it can develop up to 19W of internal power dissipation. If the die temperature is to remain below 150°C for ambient temperatures up to 70°C, the total junction-to-ambient thermal resistance must be less than

$$\frac{150°C - 70°C}{19W} = 4.2°C/W.$$

Using θ_{JC} = 2°C/W, the sum of the case-to-heat sink interface thermal resistance and the heat-sink-to-ambient

Application Hints (Continued)

thermal resistance must be less than 2.2°C/W. The case-to-heat-sink thermal resistance of the TO-220 package varies with the mounting method used. A metal-to-metal interface will be about 1°C/W if lubricated, and about 1.2°C/W if dry. If a mica insulator is used, the thermal resistance will be about 1.6°C/W lubricated and 3.4°C/W dry. For this example, we assume a lubricated mica insulator between the LM675 and the heat sink. The heat sink thermal resistance must then be less than

$$4.2°C/W - 2°C/W - 1.6°C/W = 0.6°C/W.$$

This is a rather large heat sink and may not be practical in some applications. If a smaller heat sink is required for reasons of size or cost, there are two alternatives. The maximum ambient operating temperature can be restricted to 50°C (122°F), resulting in a 1.6°C/W heat sink, or the heat sink can be isolated from the chassis so the mica washer is not needed. This will change the required heat sink to a 1.2°C/W unit if the case-to-heat-sink interface is lubricated.

The thermal requirements can become more difficult when an amplifier is driving a reactive load. For a given magnitude of load impedance, a higher degree of reactance will cause a higher level of power dissipation within the amplifier. As a general rule, the power dissipation of an amplifier driving a 60° reactive load will be roughly that of the same amplifier driving the resistive part of that load. For example, some reactive loads may at some frequency have an impedance with a magnitude of 8Ω and a phase angle of 60°. The real part of this load will then be 8Ω × cos 60° or 4Ω, and the amplifier power dissipation will roughly follow the curve of power dissipation with a 4Ω load.

Typical Applications (Continued)

Non-Inverting Unity Gain Operation

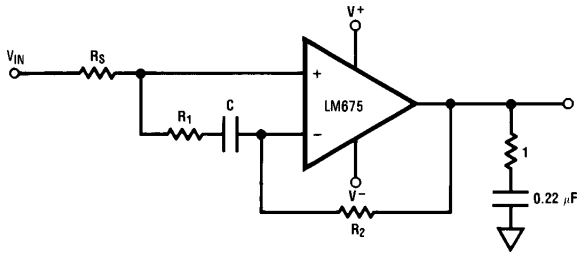

TL/H/6739–6

$$R_1C \geq \frac{1}{2\pi 500\ kHz}$$

$$R_1 \leq \frac{R_S + R_2}{10}$$

$$A_{V(DC)} = 1$$

UNITY GAIN BANDWIDTH ≅ 50 kHz

Inverting Unity Gain Operation

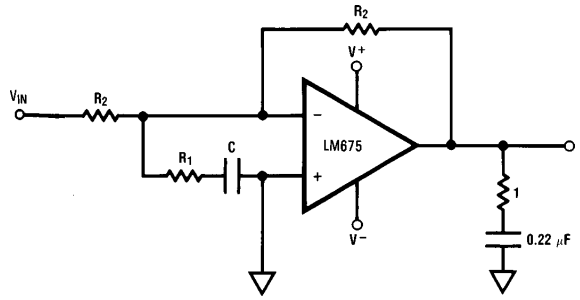

TL/H/6739–7

$$R_1C \geq \frac{1}{2\pi 500\ kHz}$$

$$R_1 \leq \frac{R_2}{10}$$

$$A_{V(DC)} = -1$$

UNITY GAIN BANDWIDTH ≅ 50 kHz

Typical Applications (Continued)

Servo Motor Control

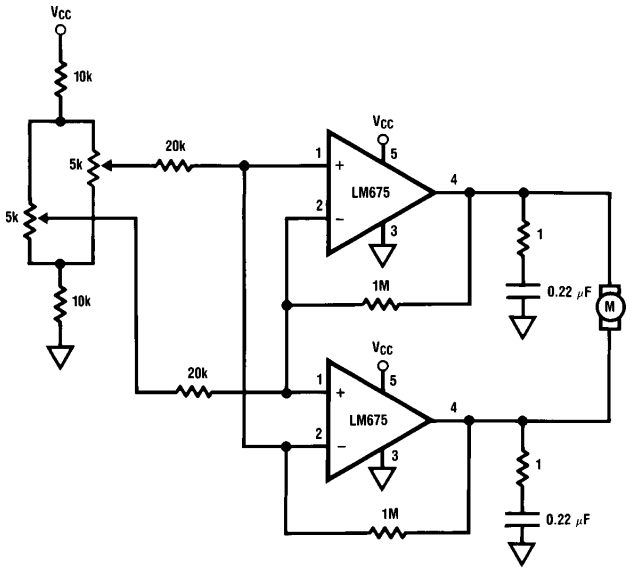

TL/H/6739–8

High Current Source/Sink

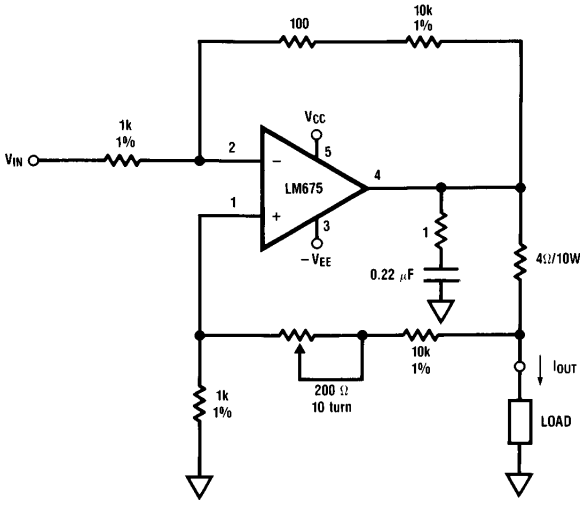

TL/H/6739–9

$I_{OUT} = V_{IN} \times 2.5$ amps/volt
i.e. $I_{OUT} = 1A$ when $V_{IN} = 400$ mV
Trim pot for max R_{OUT}

Physical Dimensions inches (millimeters) unless otherwise noted

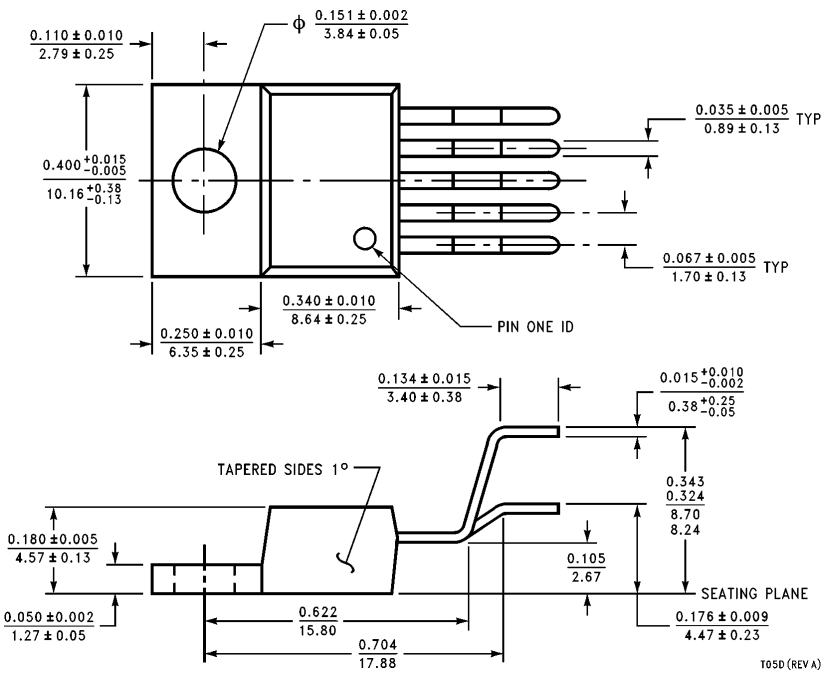

TO-220 Power Package (T)
Order Number LM675T
NS Package T05D

LIFE SUPPORT POLICY

NATIONAL'S PRODUCTS ARE NOT AUTHORIZED FOR USE AS CRITICAL COMPONENTS IN LIFE SUPPORT DEVICES OR SYSTEMS WITHOUT THE EXPRESS WRITTEN APPROVAL OF THE PRESIDENT OF NATIONAL SEMICONDUCTOR CORPORATION. As used herein:

1. Life support devices or systems are devices or systems which, (a) are intended for surgical implant into the body, or (b) support or sustain life, and whose failure to perform, when properly used in accordance with instructions for use provided in the labeling, can be reasonably expected to result in a significant injury to the user.
2. A critical component is any component of a life support device or system whose failure to perform can be reasonably expected to cause the failure of the life support device or system, or to affect its safety or effectiveness.

National Semiconductor Corporation
1111 West Bardin Road
Arlington, TX 76017
Tel: 1(800) 272-9959
Fax: 1(800) 737-7018

http://www.national.com

National Semiconductor Europe
Fax: +49 (0) 180-530 85 86
Email: europe.support@nsc.com
Deutsch Tel: +49 (0) 180-530 85 85
English Tel: +49 (0) 180-532 78 32
Français Tel: +49 (0) 180-532 93 58
Italiano Tel: +49 (0) 180-534 16 80

National Semiconductor Hong Kong Ltd.
13th Floor, Straight Block,
Ocean Centre, 5 Canton Rd.
Tsimshatsui, Kowloon
Hong Kong
Tel: (852) 2737-1600
Fax: (852) 2736-9960

National Semiconductor Japan Ltd.
Tel: 81-043-299-2308
Fax: 81-043-299-2408

- ✓ Í¬¿·²´»-- -¬»»´ ½»´´
- ✓ Í³¿´´ ½±²-¬®«½¬·±²
- ✓ Ø·¹¸ ¾«®-¬ °®»--«®»
- ✓ Î»-·-¬¿²¬ ¬± °®»--«®» °»¿µ-
- ✓ Í¸±½µ ¿²¼ ª·¾®¿¬·±²Ó°®±±º
- ✓ É·¼» ³»¼·¿ ®»-·-¬¿²½»
- ✓ Ø·¹¸ ´·²»¿®·¬§
- ✓ Ô±²¹Ó¬»®³ -¬¿¾·´·¬§

Ì¸» Ó·²·ÓÍÝÐ °®»--«®» -»²-±® ©¿- ¼»-·¹²»¼ º±® ·²¼«-¬®·¿´ ¿°°´·½¿¬·±² ®»¯«·®»³»²¬- ¿²¼ ·-«·¼»¼ ·²½±®°±®¿¬»-ô®»¹«´¿¬·±² ¿²¼ ³±²·¬±®·²¹ ¬¿-µ- ·² -§-¬»³- © ¸»®» ®¿°·¼ °®»--«®»ó½¸»½µ- ¿²¼ ¿¼¿°¬¿¬·±² ¬± ¬¸» ²»»¼»¼ò

Ì¸» ÍÝÐó·²· °®»--«®» -»²-±® ·- ±«¬-¬¿²¼·²¹ ¾»½¿«-» ±º ·¬- ½±³°¿½¬ ½±²-¬®«½¬·±²ô ¸·¹¸ ´·²»¿®·¬§ ¿²¼ »¨½»´´»²¬ ¬»³°»®¿¬«®» ®»-°±²-»ò

Ý±²-¬®«½¬·±²

Ì¸» ÍÝÐÓÓ·²· ·²½´«¼»- ¿ °®»© ·®»¼ ·²¬»¹®¿¬»¼ ½±²²»½¬±® º±® »¿-§ ½±²²»½¬·±² ¬± ¬¸» -»²-±® ¿²¼ »´»½¬®±²·½- º±® -·¹²¿´ ¿³°´·º·½¿¬·±²ò ßÍ×Ý ¿²¼ ½±²¬®±´´»® -©·¬½¸ ò

Ì¸» ßÍ×Ý ·- ¿ °®±¹®¿³³¿¾´» ®»½»·ª·²¹ ÝÓÑÍóßÍ×Ý ©·¬¸ ÛÛÐÎÑÓ ¼¿¬¿ ³»³±®§ ¿²¼ ¿´´±©- ¬¸» ½¿´·¾®¿¬·±² ô ¬¸» ½±³°»²-¿¬·±² ¿²¼ ´·²»¿®·¦¿¬·±² ±º ¬¸» »´»½¬®·½¿´ -·¹²¿´ ª¿®·¿¬·±²ò

Ð»½«´·¿® ¬± »´»½¬®±²·½ -»²-±®- ©·¬¸ ¸·¹¸ ¿½½«®¿½§ ¿²¼ ´±²¹Ó¬»®³ -¬¿¾·´·¬§ ¿®» ¬¸» ½¿°¿¾·´·¬§ ¬± ©·¬¸-¬¿²¼ ¸·¹¸ °®»--«®» °»¿µ-ò Ì¸» »´»½¬®±²·½- ¿®» ¿´-± °®±¬»½¬»¼ ¿¹¿·²-¬ ª·¾®¿¬·±²-ò

Ð®»--«®» ·-½¸¿®¹»¼ ¬± ¬¸» ¬®¿²-¼«½»® ¾§ ¿ ¦·®½±²·«³ ±¨·¼» ½»®¿³·½ -»²-±® ¬¸¿¬ ·- ¿´´ ¬¸» ³±®» ·³°®»--·ª»òThe hermetically welded stainless steel membrane is

ª¿½««³ ¬·¹¸¬ ¿²¼ ¸·¹¸ ´§ ®»-·-¬¿²¬ ¬± ¾«®-¬·²¹ò

Ì¸» -¬¿²¼¿®¼ ·-»¼ Ûïñì ÞÍÐÐ ½±®®±-·±²ó®»-·-¬¿²¬ -¬¿²¼¿²¼ ´»-- -¬»»´ °®±½»-- ½±²²»½¬·±² ·² -»ª»®¿´ ª»®-·±²- ¬·¹¸¬ -¬¿·²´»-- -¬»»´ ô ¹«¿®¿²¬»»- ©·¼»ó®¿²¹» ·¬ ©·¬¸ ³»¼·¿ ®»-·-¬¿²½»ò

ß°°´·½¿¬·±²-

Ð®»-§ ±º »´»½¬®±²·½ ±«¬°«¬ -·¹²¿´- ¿²¼ °®±½»-- ½±²²»½¬·±²- ®»½±³³»²¼»¼ ¿ ©·¼» -°»½¬®«³ ±º ¿°°´·½¿¬·±²-ò

Ì¸» -»²-±® ·- ³¿·²´§ «-»¼ ·² ¬¸» ³±¾·´» ¸§¼®¿«´·½ ¿²¼ ·²¼«-¬®·¿´ ¿°°´·½¿¬·±²-ô ¬¸¿¬ ·-ô ·² ¬»-¬ ¾»²½¸»-ô ³¿½¸·²» ¬±±´- ¿²¼ ¬¸» ¸§¼®¿«´·½ -§-¬»³- ¿²¼ ®»´¿¬»¼ ¿°°´·½¿¬·±²ò

ÍÝÐ Ó·²·	ðði	ððê	ðïð	ðïê	ðîë	ðìð	ðêð	ïðð	ïêð	îëð	ìðð	êðð
°®»--«®» ®¿²¹» ö Ðò Ø¾¿®÷	ðòòòì	ðòòòê	ðòòòïð	ðòòòïê	ðòòòîë	ðòòòìð	ðòòòêð	ðòòòïðð	ðòòòïêð	ðòòòîëð	ðòòòìðð	ðòòòêðð
±ª»®´±¿¼ °®»--«®» Ð¸¿¨ Ø¾¿®÷	î ¬·³»-											
¾«®-¬ °®»--«®» Ðþ«®-¬ Ø¾¿®÷	íó ¬·³»-											îôëó¬·³»-

Ð®»--«®» ½±²²»½¬·±²	
°®»--«®» ½±²²»½¬·±²	Ùïñìß ÞÍÐÐ
	Ü×Ò íèëî Ìïïô °±®³ Û
»®±-·±² ¾±®»	ðôê ³³
	ÛÜó-»¿´ ÚÕÓ
Ó¿¬»®·¿´	
°¿®¬- ·² ½±²¬¿½¬ ©·¬¸ ³»¼·¿	ÚÕÓå -¬¿·²´»-- -¬»»´ ïòìëìîôïòìëìïôïòìëéïå ïéóìÐØ
¸±«-·²¹	-¬¿·²´»-- -¬»»´ ïòìíðï
°®±¬»½¬·±² ½¿°	×Ðêé Ü×Ò ÛÒ êðëîç ø©·¬¸ Ü×Ò ïéëíðïóèðí °±®³ ß °´«¹ ×Ðêë÷
Ð´«¹ó·² ½±²²»½¬·±²	
ìó°±´»å Óïî ¨ ïå ×Ðêé	
ìó°±´»å Ü×Ò ÛÒ ïéëíðïóèðí °±®³ ßå ×Ðêë	
Û´»½¬®·½¿´ ½±²²»½¬·±²	
-¸·»´¼»¼ ½¿¾´»ô °»®³¿²»²¬ ½±²²»½¬»¼ô °»®³¿²»²¬ ½±²²»½¬»¼ô ½¿¾´» í	
ß½½«®¿½§	
½¿´½«´¿¬»¼ ·² ¿½½±®¼¿²½» ¬± Ü×Ò ÛÒ êðééð	ÿ ðôë û ÚÍ -¬¿²¼¿®¼ ¬±´»®¿²½»
Ù»²»®¿´	
®»-°±²-» ¬·³»	≤ ï ³-
´±²¹ó¬»®³ -¬¿¾·´·¬§	ä ðôï û ÚÍñ¿
©»·¹¸¬	½¿ò èð ¹
´±¿¼ ®»ª»®-¿´-	≥ îð Ó·±ò

Û²ª·®±²³»²¬¿´ ½±²¼·¬·±²-	
»²ª·®±²³»²¬¿´ ¬»³°»®¿¬«®» ®¿²¹»	óìðòòòõèë þÝ
³»¼·¿ ¬»³°»®¿¬«®» ®¿²¹»	óìðòòòõïîë þÝ
½±³°»²-¿¬»¼ ®¿²¹»	óîðòòòõèë þÝ
-¬±®¿¹» ¬»³°»®¿¬«®»	óìðòòòõïîë þÝ
¬»³°»®¿¬«®» ½±»ºº·½·»²¬	≤ ÿ ðôî û ÚÍñïð Õ
ª·¾®¿¬·±² ®»-·-¬¿²½»	×ÛÝ êðððèóîóêå ÿ ë ³³ å ïð Ø¦òòòïí Ø¦ îðð ³ñ-å íï Ø¦òòòî µØ¦
-¸±½µ ®»-·-¬¿²½»	×ÛÝ êðððèóîóîçæ ëðð ³ñ-å ïï ³- ×ÛÝ êðððèóîóîéæ ï ³ øº®»» º¿´´ ±²¬± ½±²½®»¬»÷
Û´»½¬®±³¿¹²»¬·½ ½±³°¿¬·¾·´·¬§	
·²¬»®º»®»²½» »³·--·±²	Ü×Ò ÛÒ êïðððóêóí
·²¬»®º»®»²½» ®»-·-¬¿²½»	Ü×Ò ÛÒ êïðððóêóî

Ñ«¬°«¬ -·¹²¿´	ðóîð ³ß ïó½±²¼«½¬±®	ìóîð ³ß îó½±²¼«½¬±®	ìóîð ³ß íó½±²¼«½¬±®	ðòòòïð Ê íó½±²¼«½¬±®
¿«¨·´·¿®§ »²»®¹§ õË¾ Œ Ë ÙÒÜ ÷	çòòòíð Ê	çòòòíð Ê	ïîòòòíð Ê	ïîòòòíð Ê
©±®µ·²¹ ®»-·-¬¿²½» ³¿¨ ò	Œ ¾ óç Ê÷ñîð ³ß	Œ ¾ óç Ê÷ñîð ³ß	Œ ¾ óïî Ê÷ñîð ³ß	ïë µΩ

ö ·»» °¿¹» èîô êðí

Ü×Ò ÛÒ ïéëíðïóèðí º±®³ ß øº±®³»®´§ Ü×Ò ìíêëð÷
°´«¹·² ½±²²»½¬±®

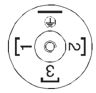

Ð×Ò	ðòòòïð ³ ß íó½±®»	ìòòòîð ³ ß íó½±®»	ìòòòîð ³ ß îó ½±®»	ðòòòïð Ê íó ½±®»
ï	Ð -·¹²¿´	Ð -·¹²¿´	Ð -·¹²¿´	Ð -·¹²¿´
î	ð Ê øÙÒÜ÷	ð Ê øÙÒÜ÷	²ò½ò	ð Ê øÙÒÜ÷
í	õË	õË	õË	õË
⏚	¹®±«²¼·²¹ ½±²²»½¬±® ½±²²»½¬»¼ ¬± ø²±¬ ½±²²»½¬»¼ ³«-¬ ²±¬ ¾» «-»¼÷			

Óïî °´«¹·² ½±²²»½¬±®

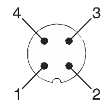

Ð×Ò	ðòòòïð ³ ß íó ½±®»	ìòòòîð ³ ß íó ½±®»	ìòòòîð ³ ß îó ½±®»	ðòòòïð Ê íó ½±®»
ï	õË	õË	õË	õË
î	Ð -·¹²¿´	Ð -·¹²¿´	Ð -·¹²¿´	Ð -·¹²¿´
í	ð Ê øÙÒÜ÷	ð Ê øÙÒÜ÷	²	ð Ê øÙÒÜ÷
ì	²	²	²	²

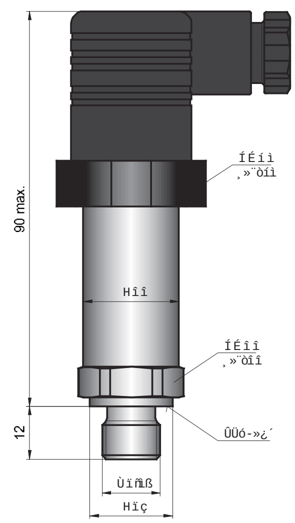

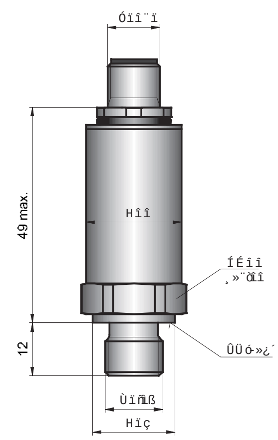

Ñ®¼»® ½±¼»-

Ð®»--«®» ®¿²¹» ö
ðòìå ðòêå ïòðå ïòêå îòëå
ìòðå êòðå ïðòðå ïêòðå
ìðòðå êðò ¾¿®

Ü×Ò ÛÒ ïéëíðïóèðí º±®³ ßô
Ùïñì ÞÍÐÐô ½´¿-- ðòë û

ðòòòïð ³ßå íó½±®»	ÍÝÐÓ¨¨¨óïìïóðê
ìòòòîð ³ßå íó½±®»	ÍÝÐÓ¨¨¨óîìïóðê
ìòòòîð ³ßå îó½±®»	ÍÝÐÓ¨¨¨óíìïóðê
ðòòòïð Êå íó½±®»	ÍÝÐÓ¨¨¨óìïóðê

Óïî °´«¹·² ½±²²»½¬±®ô
Ùïñì ÞÍÐÐô ½´¿-- ðòë û

ðòòòïð ³ßå íó½±®»	ÍÝÐÓ¨¨¨óïìïóðé
ìòòòîð ³ßå íó½±®»	ÍÝÐÓ¨¨¨óîìïóðé
ìòòòîð ³ßå îó½±®»	ÍÝÐÓ¨¨¨óíìïóðé
ðòòòïð Êå íó½±®»	ÍÝÐÓ¨¨¨óìïóðé

ö -»» °¿¹» èîô èí

Ý±²²»½¬·²¹ ½¿¾´»- ¿²¼ -»°¿®¿¬» °´«¹-

Ý±²²»½¬·²¹ ½¿¾´»ô ³¿¼» «° ÍÝÕóïðîó¨¨ó¨¨
ø±°»² »²¼»¼÷

Ý¿¾´» ´»²¹¬¸ ·² ³
ðî î ³
ðë ë ³
ïð ïð ³

Ð´«¹·² ½±²²»½¬±®
ìë Óïî ½¿¾´» -±½µ»¬ -¬®¿·¹¸¬
ëë Óïî ½¿¾´» -±½µ»¬ ¿²¹´»¼
ëê Ü×Ò ÛÒ ïéëíðïóèðí º±®³ ß °´«¹ ½±²²»½¬±®
ø¬»®³»®´§ Ü×Ò ìíêëð÷

Í»°¿®¿¬» °´«¹-

Óïî ½¿¾´» -±½µ»¬ -¬®¿·¹¸¬	ÍÝÕóïìë
Óïî ½¿¾´» -±½µ»¬ ¿²¹´»¼	ÍÝÕóïëë
Ü×Ò ÛÒ ïéëíðïóèðí º±®³ ß °´«¹ ½±²²»½¬±® ø¬»®³»®´§ Ü×Ò ìíêëð÷	ÍÝÕóðêê

Hydraulic Bladder Accumulator Standard

1. DESCRIPTION

1.1. FUNCTION

Fluids are practically incompressible and cannot therefore store pressure energy.

The compressibility of a gas is utilised in hydraulic accumulators for storing fluids. HYDAC bladder accumulators are based on this principle, using nitrogen as the compressible medium.

A bladder accumulator consists of a fluid section and a gas section with the bladder acting as the gas-proof screen.
The fluid around the bladder is connected to the hydraulic circuit so that the bladder accumulator draws in fluid when the pressure increases and the gas is compressed.
When the pressure drops, the compressed gas expands and forces the stored fluid into the circuit.

HYDAC bladder accumulators can be used in a wide variety of applications, some of which are listed below:

- energy storage
- emergency operation
- force equilibrium
- leakage compensation
- volume compensation
- shock absorption
- vehicle suspension
- pulsation damping

See catalogue section:

- Hydraulic Dampers
  No. 3.701

1.2. DESIGN

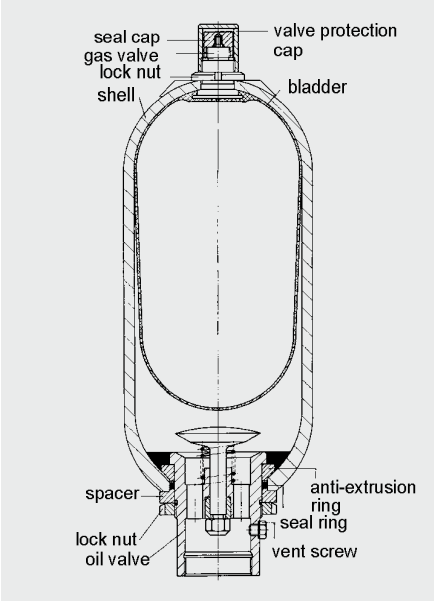

1.2.1 Design

- Standard Bladder Accumulator
  SB330/400/500/550
  HYDAC standard bladder accumulators consist of the pressure vessel, the flexible bladder with gas valve and the hydraulic connecction with check valve. The pressure vessel is seamless and manufactured from high tensile steel.
- Bladder accumulator
  SB330N
  The flow optimised design of the standard oil valve enables the maximum possible operating fluid flow rate to increase to 25 l/s on this accumulator type.
- High Flow bladder accumulator
  SB330H
  HYDAC high flow bladder accumulators, type SB330H, are high performance accumulators with a flow rate of up to 30 l/s. The fluid connection is enlarged to allow higher flow rates.

1.2.2 Bladder material

The following elastomers are available as standard:

- NBR (acrylonitrile butadiene rubber, Perbunan),
- IIR (butyl rubber),
- FKM (fluoro rubber, Viton®),
- ECO (ethylene oxide epichlorohydrin rubber).

The material must be selected according to the particular operating fluid and temperature.

When choosing the elastomer, allowances must be made for the fact that the gas can cool down to below the permitted elastomer temperature if there are adverse discharge conditions (high pressure ratio p_2/p_0, high discharging velocity). This can cause cold cracking in the elastomer.
The gas temperature can be calculated using the HYDAC Accumulator Simulation Program ASP.

1.2.3 Corrosion protection

For operation with chemically aggressive media, the accumulator shell can be supplied with corrosion protection, such as plastic coating on the inside or chemical nickel-plating. If this is insufficient, then stainless steel accumulators must be used.

1.3. MOUNTING POSITION

HYDAC bladder accumulators can be installed vertically, horizontally and at a slant. When installing vertically or at a slant, the oil valve must be at the bottom. On certain applications listed below, particular positions are preferable:

- Energy storage:
  vertical,
- Pulsation damping:
  any position from horizontal to vertical,
- Maintaining constant pressure:
  any position from horizontal to vertical,
- Volume compensation:
  vertical.

If the mounting position is horizontal or at a slant, the effective volume and the maximum permitted flow rate of the operating fluid are reduced.

1.4. TYPE OF MOUNTING

By using an appropriate adapter, HYDAC accumulators, up to size 1 l, can be mounted directly inline.

For strong vibrations and volumes above 1 l, we recommend the use of HYDAC accumulator supports or the HYDAC accumulator mounting set.

See catalogue sections:

- Supports for Hydraulic Accumulators
  No. 3.502
- ACCUSET SB
  No. 3.503

2. TECHNICAL SPECIFICATIONS

2.1. EXPLANATORY NOTES

2.1.1 Operating pressure

See tables
(may differ from nominal pressure for foreign test certificates)

2.1.2 Nominal volume

See tables

2.1.3 Effective gas volume

See tables
based on nominal dimensions, this differs slightly from the nominal volume and must be used when calculating the effective volume.

2.1.4 Effective volume

Volume of fluid which is available between the operating pressures p_2 and p_1.

2.1.5 **Max. flow rate of operating fluid**

In order to achieve the max. flow rate given in the tables, the accumulator must be mounted vertically. It must be remembered that a residual fluid volume of approx. 10% of the effective gas volume remains in the accumulator.

2.1.6 Fluids

The following sealing and bladder materials are suitable for the fluids listed below.

Material	Fluids
NBR20	Mineral oils (HL, HLP, HFA, HFB, HFC), water
ECO	Mineral oil
IIR	Phosphate ester
FKM	Chlorinated hydro-carbons, petrol

2.1.7 Permitted operating temperature

The permitted operating temperatures are dependent on the application limits of the metallic materials and the bladders.

The standard valve bodies, gas valves and accumulator shells are suitable for temperatures from -10 °C ... +80 °C.

Outside these temperatures, special material combinations must be used.
The following table shows the correlation between bladder material and application temperature.

Material	Temperature ranges
NBR20	-15 °C ... + 80 °C
NBR21	-50 °C ... + 80 °C
NBR22	-30 °C ... + 80 °C
ECO	-30 °C ... +120 °C
IIR	-40 °C ... +100 °C
FKM	-10 °C ... +150 °C

2.1.8 Gas charging

Always only charge with nitrogen class 4.5, filtered to < 3 µm.
If other gases are to be used, please contact HYDAC for advice.

Hydraulic accumulators must only be charged with nitrogen.
Never use other gases.
Risk of explosion!

2.1.9 Limits for gas pre-charge pressure

$p_0 \leq 0.9 \bullet p1$

with a permitted pressure ratio of:

$p_2 : p_0 \leq 4 : 1$

p_2 = max. operating pressure
p_0 = gas pre-charge pressure

2.1.10 **Certificate codes**

China	A9
EU member states	U [1)]
Japan	P
Canada	S1 [2)]
Switzerland	U
USA	S
others on request	

[1)] Alternative certificates possible

[2)] Approval required in the individual provinces

On no account must any welding, soldering or mechanical work be carried out on the accumulator shell. After the hydraulic line has been connected it must be completely vented.

Work on systems with hydraulic accumulators (repairs, connecting pressure gauges etc) must only be carried out once the pressure and the fluid have been released.

Please read the operating manual!
No. 3.201.CE

Note:
Application examples, accumulator sizing and extracts from approvals regulations on hydraulic accumulators can be found in the following catalogue section:

- Accumulators
  No. 3.000

2.2. MODEL CODE
(also order example)

SB330 H – 32 A 1 / 112 U – 330 A 050

Series

Type
H = high flow
N = increased flow, standard oil valve dimensions
A = shock absorber
P = pulsation damper
S = suction flow stabiliser
B = bladder top-repairable
Combinations possible, e.g. HB - High flow with a top-repairable bladder
PH - pulsation damper with high flow rate.
No details = standard

Nominal volume [l]

Fluid connection
A = standard connection, thread with internal seal face
F = flange connection
C = valve mounting with screws on underside
E = sealing surfaces on front interface (e.g. on thread M50x1.5 - valve)
G = male thread
S = special connection, to customer specification

Gas side
1 = standard model [4]
2 = back-up model
3 = gas valve 7/8-14UNF with M8 female thread
4 = 5/8" gas valve
5 = gas valve M50x1.5 in accumulators smaller than 50 l
6 = 7/8-14UNF gas valve
7 = M28x1.5 gas valve
8 = M16x1.5 gas valve
9 = special gas valve, to customer specification

Material code [1]
Standard model = 112 for mineral oil
Depending on operating fluid
others on request

Fluid connection
1 = carbon steel
2 = high tensile steel
3 = stainless steel [3]
6 = low temperature steel

Accumulator shell
0 = plastic coated (internally)
1 = carbon steel
2 = chemically nickel-plated (internal coating)
4 = stainless steel [3]
6 = low temperature steel

Accumulator bladder [2]
2 = NBR20
3 = ECO
4 = IIR (butyl)
5 = NBR21 (low temperature)
6 = FKM
7 = other
9 = NBR22

Certification code
U = PED 97/23/EC

Permitted operating pressure [bar]

Connection
Thread, codes for fluid connections: A, C, E, G
A = Thread to ISO 228 (BSP)
B = Thread to DIN 13 or ISO 965/1 (metric)
C = Thread to ANSI B1.1 (UN..-2B seal SAE J 514)
D = Thread to ANSI B1.20.1 (NPT)
S = special thread, to customer specification

Flange, codes for fluid connection: F
A = DIN flange
B = flange ANSI B16.5
C = SAE flange 3000 psi
D = SAE flange 6000 psi
S = special flange, to customer specification

Pre-charge pressure p_0 [bar] at 20 °C must be stated separately, if required!

[1] Not all combinations are possible
[2] When ordering spare bladders, please state smallest bladder connection port size
[3] Depending on type and pressure rating
[4] Gas valve type in SB < 50 l = 7/8 - 14 UNF, in SB ≥ 50 l = M50x1.5

3. DIMENSIONS AND SPARE PARTS

3.1. DIMENSIONS

Nominal volumes [l]	Valve	Max. operating pressure (PED 97/23/EC) [bar]	Effective gas volume [l]	Weight [kg]	A max. [mm]	B [mm]	C [mm]	Ø D max. [mm]	J thread ISO 228	Ø E [mm]	SW [mm]	Q [1] [l/s]
0.5	standard	400	0.5	2.8	270	57	33.5	95.5	G 3/4	50	32	4
1		330	1.0	4.5	302		58	118				
		550		8.5	334	68		121	G 1	67	45	
2.5		330	2.4	10	531	63		118	G 1 1/4		50	10
		550	2.5	13.5	539	68		121	G 1		45	4
4		330	3.7	11.5	419	63		173	G 1 1/4		50	10
		400		15.5								
5		550	4.9	23	867	68		121	G 1		45	4
6		330	5.7	15	531	63		173	G 1 1/4		50	10
10 [2]		330	9.3	25	728				G 1 1/4			
10	standard	330	9.3	31.5	568	103	58	229	G 2	103	70	15
	N											25
	H		9	34.5	603	138			G 2 1/2	125	90	30
	standard	400	9.3	37.5	572	103		233	G 2	100	70	15
		500	8.8	41	585	77	68	241				
13	standard	330	12	43	660	103	58	229	G 2	100	70	15
	N											25
	H			46	695	138			G 2 1/2	125	90	30
	standard	400		49	666	103		233	G 2	100	70	15
20	standard	330	18.4	50.5	896	103	58	229	G 2	100	70	15
	N											25
	H		17.5	53.5	931	138			G 2 1/2	125	90	30
	standard	400	18.4	63.5	896	103		233	G 2	100	70	15
		500	17	75.5	901	77	68	241		110	75	
24	standard	330	23.6	69.0	1062	103	58	229	G 2	100	70	15
	N											25
	H		24	72	1097	138			G 2 1/2	125	90	30
32	standard	330	33.9	87	1411	103	58	229	G 2	100	70	15
	N											25
	H		32.5	90	1446	138			G 2 1/2	125	90	30
	standard	400	33.9	104.5	1411	103		233	G 2	100	70	15
		500	33.5	127	1446	77	68	241		110	75	
50		330	47.5	117.5	1931	103	68	229	G 2	100	70	15
	N											25
	H			120.5	1966	138			G 2 1/2	125	90	30
	standard	400		142	1931	103		233	G 2	100	70	15
		500	48.3	169	1951	77		241			75	
60	standard	330	60	182	1156	138	68	356	G 2 1/2	125	90	30
80			85	221	1406							
100			105	255	1656							
130			133	305	1976							
160			170	396	2006			406				
200			201	485	2306							

[1] Q = max. flow rate of pressure fluid
[2] slimline version, for confined spaces

Dimensions

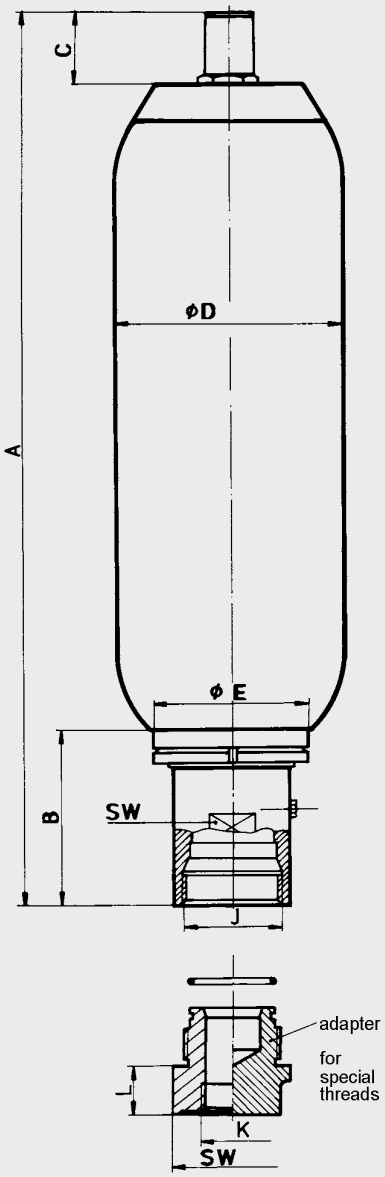

3.2. SPARE PARTS

SB330/400/440/500/550
SB330H / SB330N

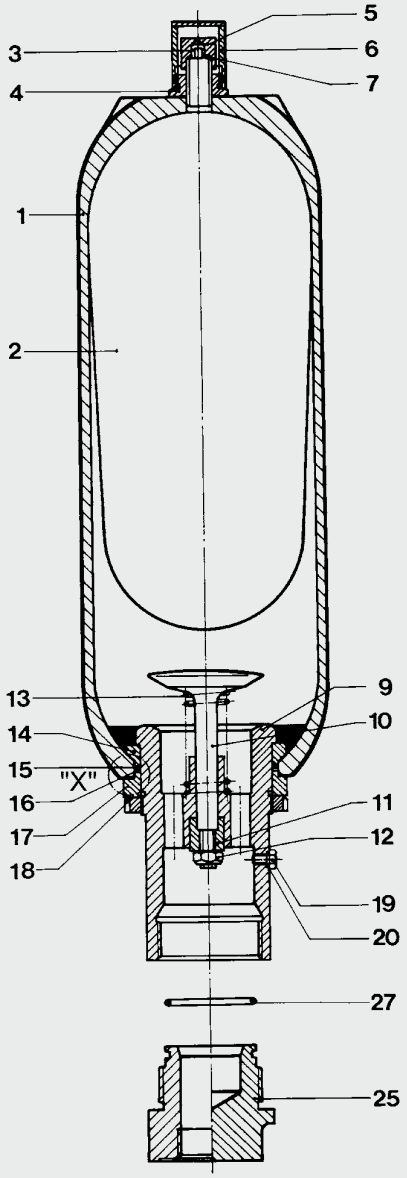

Detail "X"
SB330/400 – 0.5 ... 6 l

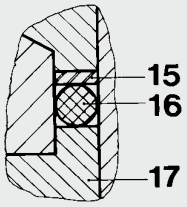

SB330/400/500 – 10 ... 200 l and
SB330H – 10 ... 200 l
SB550 – 1 ... 5 l

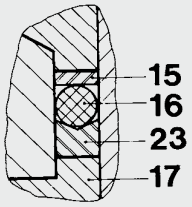

Description	Item
Bladder kit consisting of:	
Bladder	2
Gas valve insert*	3
Lock nut	4
Seal cap	5
Valve protection cap	6
O-ring	7
Seal kit consisting of:	
O-ring	7
Washer	15
O-ring	16
Vent screw	19
Support ring	23
O-ring	27
Repair kit [1] consisting of:	
Bladder kit (see above)	
Seal kit (see above)	
Anti-extrusion ring	14
Oil valve assembly consisting of:	
Valve assembly (items 9-13)	9
Anti-extrusion ring	14
Washer	15
O-ring	16
Spacer	17
Lock nut	18
Vent screw	19
Support ring	23

* available separately
[1] When ordering please state smallest bladder connection port size.
Item 1 not available as a spare part.
Item 19 for NBR/Carbon steel:
seal ring (item 20) included
Item 25 must be ordered as an accessory (see Point 4).

3.3. REPAIR KITS

NBR, carbon steel
Nom. volume: 0.5 ... 200 litres
Standard gas valve

Nom. volume [l]	Part no.
0.5	02128169
1	02106261
2.5	02106200
4	02106204
5	02106208
6	02112100
10 *)	03117512
10	02106212
13	02106216
20	02106220
24	02106224
32	02106228
50	02106252
60	03117513
80	03117514
100	03117515
130	03117516
160	03117517
200	03117558

*) slimline version for confined spaces others on request

4. ACCESSORIES FOR BLADDER ACCUMULATORS

4.1. ADAPTERS (GAS SIDE)

To monitor the accumulator pre-charge pressure, HYDAC offers a selection of gas side adapters.

These must be ordered separately

4.1.1 Pressure gauge model:

Gas side connection on the bladder accumulator for permanent monitoring of the pre-charge pressure

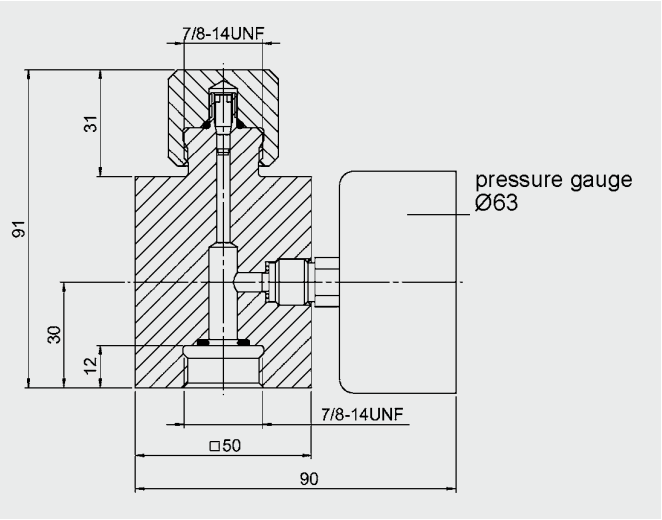

Gauge indication range	Gauge Part no.	Adapter body* Part no.	Adapter assembly Part no.
–	–	00239275	00366621
0 - 10 bar	00614420		02108416
0 - 60 bar	00606886		03093386
0 - 100 bar	00606887		02104778
0 - 160 bar	00606888		03032348
0 - 250 bar	00606889		02100217
0 - 400 bar	00606890		02102117

* p_{max} = 400 bar

4.1.2 Pressure gauge model with shut-off valve

Gas side connection on the bladder accumulator for permanent monitoring of the pre-charge pressure with shut-off option.

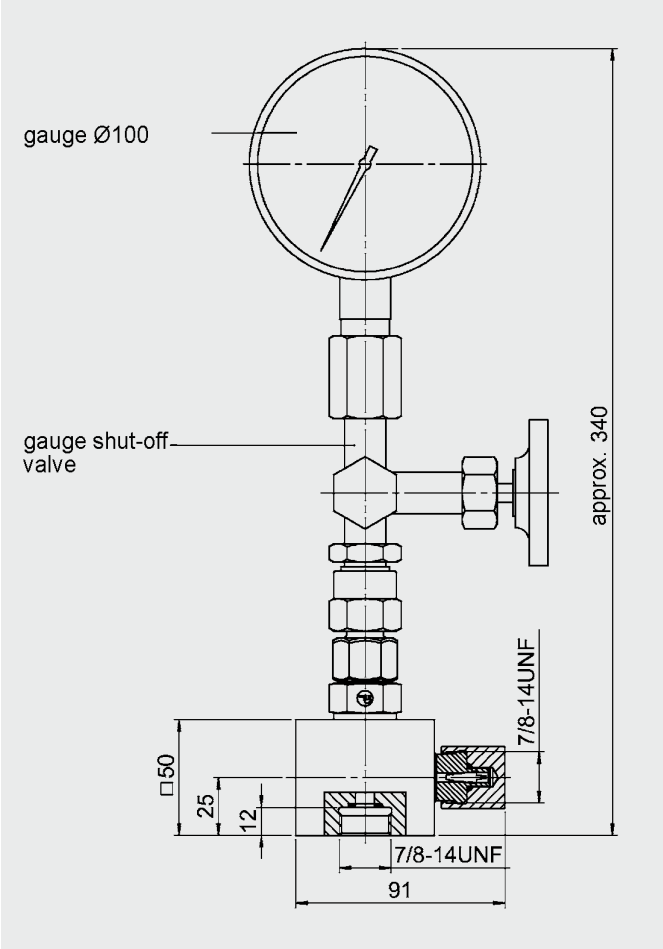

Gauge indication range	Gauge Part no.	Adapter body* Part no.	Adapter assembly Part no.
–	–	00363713	02103381
0 - 25 bar	00631380		02105216
0 - 60 bar	00606771		02110059
0 - 100 bar	00606772		03139314
0 - 160 bar	00606773		03202970
0 - 250 bar	00606774		03194154
0 - 400 bar	00606775		02103226

* p_{max} = 400 bar

4.1.3 Remote monitoring of the pre-charge pressure

To monitor the pre-charge pressure in hydraulic accumulators remotely, gas side adapters with pressure gauge and mounting holes are available.

In order to connect these adapters directly with the hydraulic accumulator using appropriate lines, accumulator adapters are also available for connection at the top (see diagram 1) or for side-connection (see diagram 2).

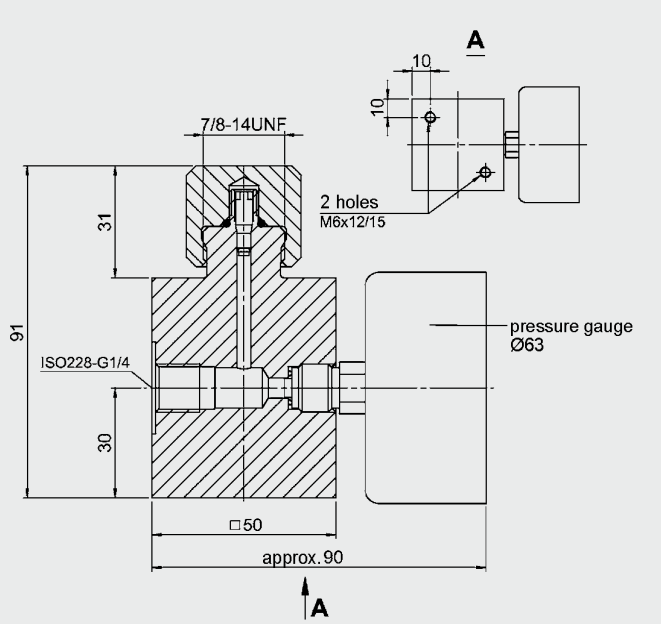

Gauge indication range	Gauge Part no.	Adapter body* Part no.	Adapter assembly Part no.
–	–	02116746	03037666
0 - 10 bar	00614420		03095818
0 - 60 bar	00606886		03095819
0 - 100 bar	00606887		03095820
0 - 160 bar	00606888		03095821
0 - 250 bar	00606889		03095822
0 - 400 bar	00606890		03095823

* p_{max} = 400 bar

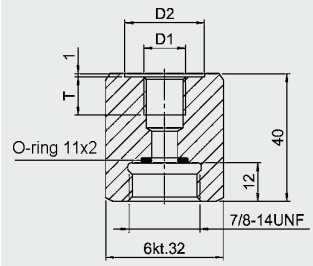

Diagram 1

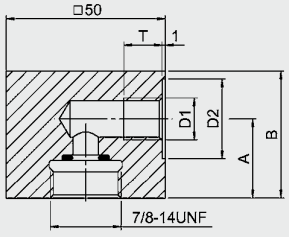

Diagram 2

D1 Threaded connection	D2 [mm]	T	Adapter body* Part no.	Adapter assembly Part no.	Diag.
ISO228- G 1/4	25	14	00238709	02109481	1
			00241740	02102042	2
ISO228- G 3/8	28		00355021	02109483	1
			03280414	00366607	2
ISO228- G 1/2	34	16	02110594	02110636	1
			00237884	00366608	2

* p_{max} = 400 bar

4.2. ADAPTERS FOR STANDARD BLADDER ACCUMULATORS (FLUID SIDE)

to connect the bladder accumulator to pipe fittings. These are available separately.

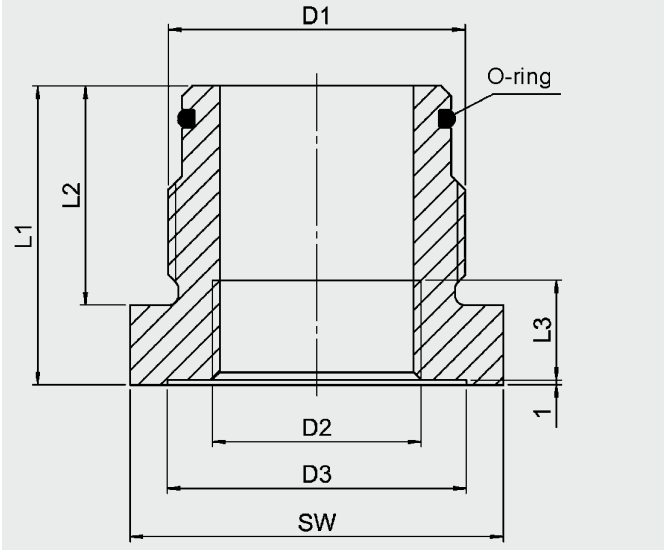

D1 Accum. conn.* (ISO228-BSP)	D2 [mm]	D3 [mm]	L1 [mm]	L2 [mm]	L3 [mm]	SW [mm]	O-ring [mm]	Part no. NBR/ Carbon steel
G 3/4	G 3/8	28	55	28	12	32	17x3	02104346
	G 1/2	28	60	28	14	36		02104348
G 1 1/4	G 3/8	28	50	37	12	46	30x3	02116345
	G 1/2	34	50	37	14	46		02105232
	G 3/4	44	50	37	16	46		02104384
	G 1	50	67	37	18	65		02110124
G 2	G 1/2	34	60	44	14	65	48x3	02104853
	G 3/4	44	60	44	16	65		02104849
	G 1 1/4	60	60	44	20	65		02107113
	G 1 1/2	68	80	44	22	70		02105905

* others on request

5. NOTE

The information in this brochure relates to the operating conditions and applications described. For applications and operating conditions not described, please contact the relevant technical department. Subject to technical modifications.

HYDAC Technology GmbH
Industriegebiet
D-66280 Sulzbach/Saar
Tel.: 0 68 97 / 509 - 01
Fax: 0 68 97 / 509 - 464
Internet: www.hydac.com
E-Mail: speichertechnik@hydac.com

E 3.201.25/04.09

emulator - target.vi
C:\Users\Johannes\Documents\000 master thesis\labview\emulator\emulator - target.vi
Last modified on 27.05.2010 at 12:08
Printed on 27.05.2010 at 15:26

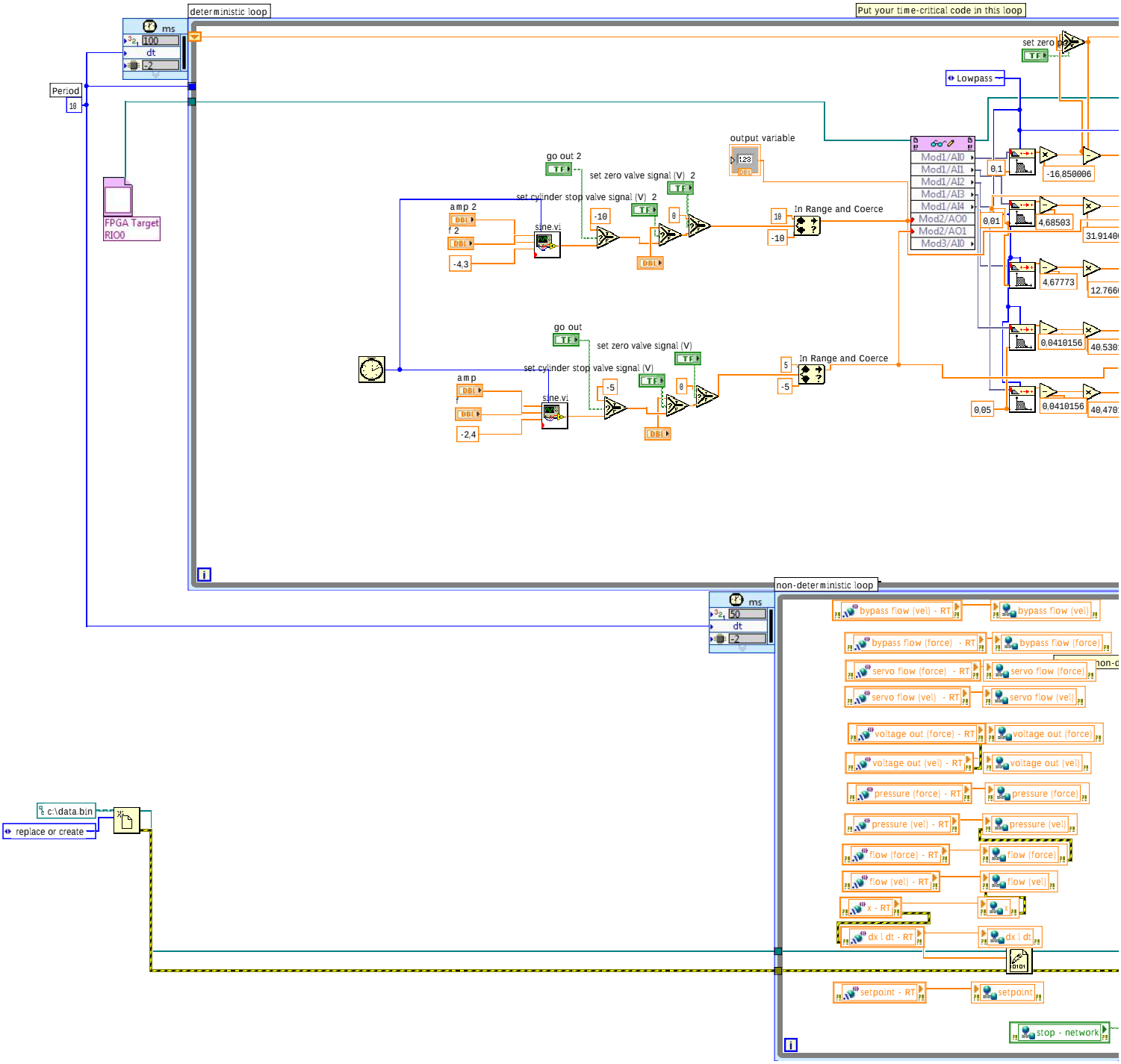

emulator - target.vi
C:\Users\Johannes\Documents\000 master thesis\labview\emulator\emulator - target.vi
Last modified on 27.05.2010 at 12:08
Printed on 27.05.2010 at 15:26